Communications on Hydraulic and Geotechnical Engineering
2012-02
ISSN 0169-6548

Wave overtopping simulator on a 1/15 slope protected by two local grass species

Yen Binh, Thach That, Ha Noi - June, 2012

Report of measurements and observations

Lê Hai Trung*

September, 2012

* PhD student, Section of Hydraulic Engineering, Faculty of Civil Engineering and Geosciences, Delft University of Technology, P.O. Box 5048, 3600 GA Delft, The Netherlands.
Tel. + 31 15 27 83348; Fax: +31 15 27 85124
e-mail: H.T.Le@tudelft.nl, trunglh@wru.vn

Faculty of Civil Engineering and Geosciences
Delft University of Technology

Communications on Hydraulic and Geotechnical Engineering 2012-02

ISSN 0169-6548

The communications on Hydraulic an Geotechnical Engineering have been published by the Department of Hydraulic Engineering at the Faculty of Civil Engineering of Delft University of Technology. In the first years mainly research reports were published, in the later years the main focus was republishing Ph.D.-theses from this Department. The function of the paper version of the Communications was to disseminate information mainly to other libraries and research institutes. (Note that not all Ph.D.-theses of the department were published in this series. For a full overview is referred to www.hydraulicengineering.tudelft.nl ⇛ research ⇛ dissertations).

At this moment this series is mainly used to disseminate background information related to other publications (e.g. data reports with data underlying journal papers and Ph.D. theses). Recent issues of the Communications are only available in digital format. A notification will be sent to interested readers when new issues are released. For placement on the notification list, please send an e-mail to h.j.verhagen@tudelft.nl.

Older versions (before 1986) were published as Communications on Hydraulic Engineering. A number of internal reports were not published in this series, but are available via this website.

Postal address for the Communications is: TU Delft, Faculty of Civil Engineering and Geosciences, department of Hydraulic Engineering, Stevinweg 1, 2628CN Delft, Netherlands. Permissions for republishing parts (figures, data), can be obtained from the responsible publisher, ir. H.J. Verhagen.

This publication has been produced in cooperation with the Water Resources University, Hanoi, Viet Nam.

This study was conducted within the research project "Super Sea Dike with high safety level and environmental friendly" financed by the Viet Nam Ministry of Agriculture and Rural Development. Tests were performed by the Faculty of Marine and Coastal Engineering, Water Resources University, Ha Noi, Viet Nam.

TU Delft, Section Hydraulic Engineering,
Water Resources University Hanoi,
Hai Trung Lê

Contents

Chapter 1

Introduction

1.1 Destructive tests

The four 'Wave Overtopping Simulator' tests were done within the framework of the Research project 'Super sea dike with high safety level and environmental friendly' funded by Viet Nam government. The main objective of these tests was to test the resistance of the gentle slope (steepness of 1/15) protected with local grass against wave overtopping with the Wave Overtopping Simulator. The super dike model was built up at the outdoor laboratory of the Viet Nam academy for water resources, in Yen Binh ward, Thach That district, Ha Noi. In June 2012, the super dike slope covered with one year grass mat was tested with the simulator. Figure 1.1 presents the original site where the super dike model was constructed and a water pond.

Figure 1.1: Site of constructing the super dike model and the water source.

The Wave Overtopping Simulator has been developed by van der Meer et al. [2006]. In 2007, 2008, 2009 and 2011, destructive tests have been performed at a number of dike stretches in the Netherlands and Belgium. Various slope characteristics were tested in order to investigate the effect of wave overtopping with the mean discharge of up to 125 l/s per m.

In Viet Nam, the pilot test with the simulator was carried out in Do Son, Hai Phong city in May 2009. The dike crest, upper part of the landward slope and the berm were reinforced with concrete while the lower part of the slope was protected with Vetiver grass which could withstand a mean overtopping discharge of up to 120 l/s per m [Le, 2011]. In January 2010, the second test was conducted on Thinh Long dike in Hai Hau, Nam Dinh province. The seaward slope covered with Bermuda grass was chosen to be tested with the Simulator. The dike slope failed at different mean discharge varying from section to section, e.g. 70 l/s per m at the first section and 20 l/s per m at the second section [Le, 2011]. At the end of 2010, in November and December, a mix of Bermuda grass and Vetiver grass on a 1:3 slope was tested at dike No. 07 in Thai Tho, Thai Thuy, Thai Binh province [Le, 2011]. Within 50 m of a dike stretch, three slope sections showed similar quality while

(a) Bermuda grass (b) Bermuda and Vetiver grass

Figure 1.2: Simulator tests on Bermuda grass slope at Thinh Long and on mixed grass at Thai Tho.

no damage could be observed with discharge less than 80 l/s per m (see Figure 1.2, right panel).

1.2 The wave overtopping simulator

The phenomenon of wave overtopping on sea dikes has been understood sufficiently, for example Eur. While the effects of overtopping waves on the structure has been not studied fully, mainly due to the fact that this issue can not be studied in a small wave flume as it is hardly to scale down either soil or grass. Therefore, the Wave Overtopping Simulator has been developed, see Van der Meer et al. (2006, 2007 and 2008).

Basically, the Simulator is a water tank which can be easily moved from place to place. The maximum volume is 5.5 m^3 per 1 m of width (22 m^3 for the Simulator of 4 m in width). The Simulator is continuously filled by one or more pumps with a certain discharge and is emptied at desired moments through two butterfly valves at the bottom in a way that simulate the overtopping tongues on the dike crest and then on the landward slope. Figure 1.3 illustrates the principle of the Simulator and its operation on site. As can be seen from the figure, as long as the flow velocity and the flow depth released from the Simulator are similar to those in reality on the dike crest, the flow characteristics on the landward slope will then automatically follow.

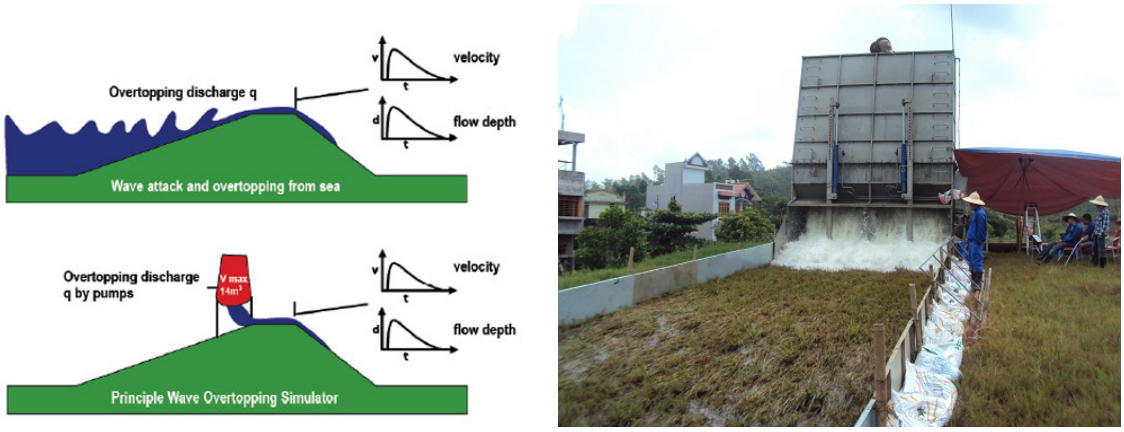

(a) Principle (b) Releasing flow

Figure 1.3: Principle of the Wave Overtopping Simulator and an overtopping flow is being generated.

Each test condition is represented by a mean overtopping discharge which is theoretically remained constant in 4 hours. Different values of applied discharge are 40, 60, 80 and 100 l/s per m. A test with full series of discharges at one location normally lasts one week including assembly and preparation. As the dike model is a super dike, tests can be extended as far as possible in order to reach maximum damages. Each test condition includes a distribution of overtopping volumes which is simulated, see EurOtop, . The distribution depends on wave condition at the toe of the structure: significant wave height and wave period. Two wave conditions were used for the four test points, a significant wave height of 1.5 m at YB1, YB2 and YB3, and 2 m at YB3 and YB4.

1.3 Failure mechanisms

Wave overtopping may cause damage to the crest and landward-side slope of a sea dike. In principle, two different failure mechanisms are distinguished. Overtopping flow can damage the surface of the crest and the landward slope, if initial damage or erosion occurs, it can extend to the underneath material layer that may lead to dike breaching. This mechanism is simulated by the Simulator: slope erosion.

The second mechanism mainly happens on steep slope (especially inclination between 1/1.5 and 1/2.0) due to water infiltration and sliding. These slide failures may directly cause dike collapse. However, they are not likely due to wave overtopping as such, but because of large infiltration quantities of water. This process may be aggravated by heavy rainfall. It is possible that these failures take place on slope which is gentler than 1:3. Simulator tests are not aimed to simulate these failure as slide failures need a dike section which is longer than 4 m as the cistern gate width, for example around 30 m. Figure 1.4 schematically gives impression of the two different failure mechanisms of the landward slope. Erosion is induced by fast wave overtopping (left panel) while sliding is caused by an increase in water pressure, water infiltration and decrease in the shear resistance in the slip circle (right panel).

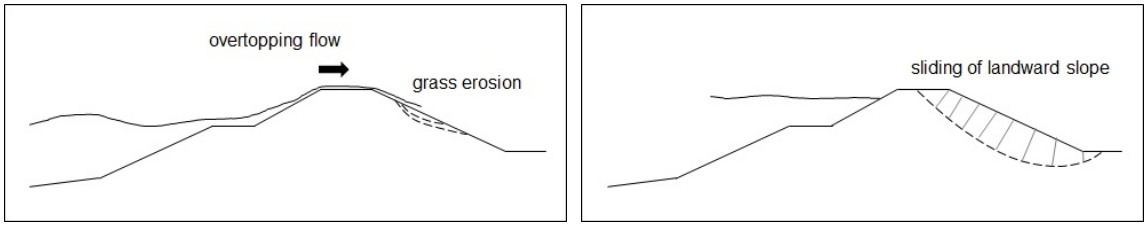

Figure 1.4: Failure mechanisms of landward slope. Left: erosion by wave overtopping. Right: macro instability.

The first mechanism, erosion of the landward-side slope was observed in previous simulator tests. The 1/15 slope would be damaged according to similar mechanism due to wave overtopping. On the gentle slope, flows are expected less intensive than on 1/3 slopes, which were the case of Thinh Long and Thai Tho dikes, therefore damages would be less considerable.

1.4 Measurements

On a dike slope with a inclination of 1/3, flow velocity can reach 6 to 7 m/s [Le, 2011] and the flow is highly turbulent with a lot of white bubble, as depicted in Figure 1.3 (right panel). Most of the laboratory devices are not designed for this kind of condition. In 2009, measurement devices and measurement methods were developed further in order to obtain reliable data. Then, flow depth was measured with a floating device which was a wooden board connected to a rotary encoder. The board can rotate around an axis when the flow runs over and pushed it up, the angle at the axis is recorded by the rotary encoder and then converted into the flow depth. The front velocity was estimated by using a digital camcorder capturing the flow from above or aside.

Figure 1.5 shows two images of the flow on the landward slope captured with the digital camcorder. A given distance was marked on the dike slope, based on the time lag between the two images and

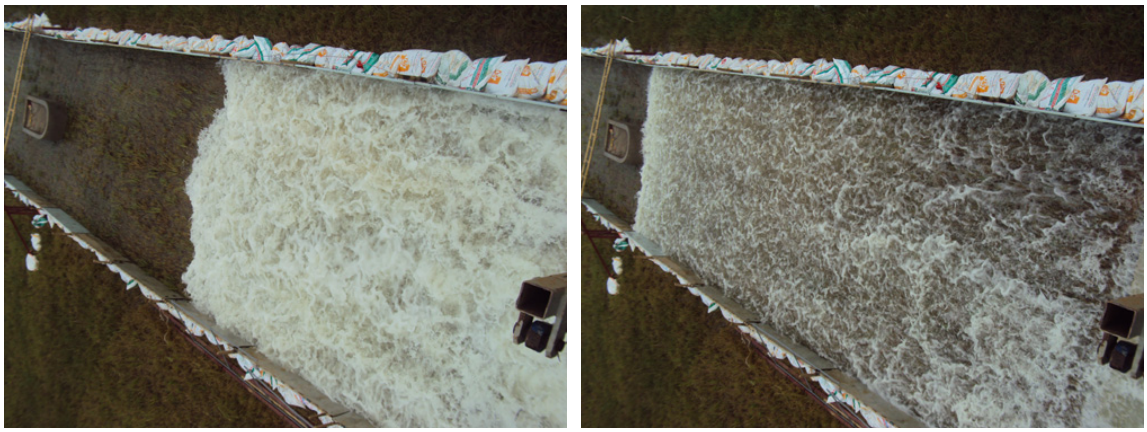

Figure 1.5: Flow induced by wave overtopping on the 1/15 slope.

the difference in position of the front part of the flow, the front velocity could be derived.

The simplest way to describe a grass slope under attack of wave overtopping is photographs. The slope surface was captured with photo camera before and during testing. A frame of 1 by 1 m^2 was used in taking picture of the grass slope. Unit images were then merged into larger one to illustrate the entire tested slope section. Besides, slope profiles were measured as well with density of 1 point/ (0.5 to 1.0) m in order to investigate the damage process induced by wave overtopping.

1.5 Report outline

This report presents measurement and observation results obtained during destructive tests with the Simulator on the super dike model. After the first chapter, chapter 2 describe the four test sections and test scenarios. The methods and results of front velocity measurements are given in chapter 3. Chapter 4 and chapter 5 present the cross-profiles and photographs of grass slopes. The formation and development of the damages induced by wave overtopping flows are discussed in chapter 6. Finally, chapter 7 recapitulates the main results of the experiments conducted on the super dike slope.

Data of the cross-profiles measured at all slope sections are presented in appendix A. Appendix B includes the photographs of the four sections during the simulator tests. A number of characteristics of the soil used to construct the super dike is presented in appendix C.

Chapter 2

Test sections and test scenarios

2.1 The super dike model

2.1.1 Geometry

The super dike model covered with local grass was built up on an area of about 2000 m^2. The construction was completed in June 2011. Next to the dike model, there is a pond supplying and discharging water for testing. The dike stretch is 30 long, 3 m high, and the crest is 5 m wide. The front slope has an inclination of 1/15 and is about 40 m long. Figure 2.1 illustrates the dike model and its main design parameters.

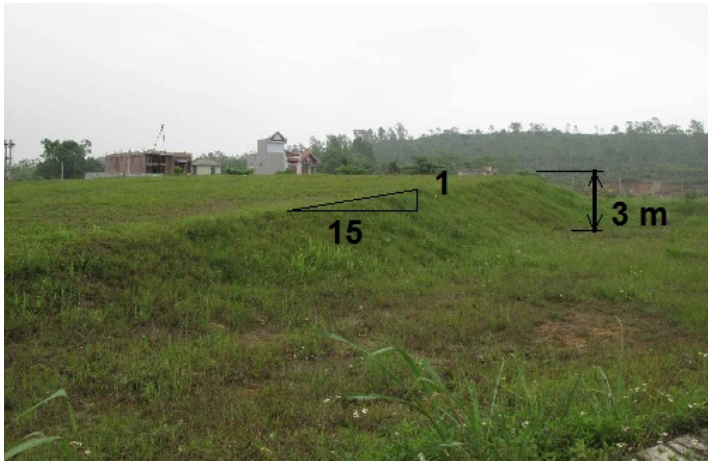

Figure 2.1: The super dike model with a slope of 1/15 and a height of 3 m.

The overtopping simulator was positioned on the dike crest to release water on the 1/15 slope; and a 55 kW pump was located close to the pond as shown in Figure 2.2.

On two halves of the 1/15 dike slope, respectively two local grass species were planted, Bermuda grass (*Cynodon dactylon*) and Carpet grass (*Axonopus compressus*). These species are popularly found in the north of Vietnam, on river dikes, sea dikes and meadow. Border between two parts of Bermuda and Mat grass can be recognised by the colour change from left to right in Figure 2.3.

2.1.2 Condition of grass cover

The condition of the grass cover was investigated during and after the simulator test in June 2012. On site, distribution of number of root in depth (root structure) was determined manually. A hollow steel cylinder with diameter of 3 cm was used to take samples of grass turf with a depth of at least 30 cm. Each sample was divided into shorter parts which were 3 cm long for each. The number of roots was counted and recorded with representative depth of every part (from surface to the middle of the

Figure 2.2: The super dike model with the simulator, pump and pipes.

Figure 2.3: The 1/15 dike slope is covered by Bermuda grass and Carpet grass.

part). About 12 samples of Bermuda grass and Carpet grass were taken giving distributions of roots in depth as shown in Figure 2.4 and 2.5. The grass cover condition was poor to average for Bermuda grass and average to good for Carpet grass according to Min [2006],

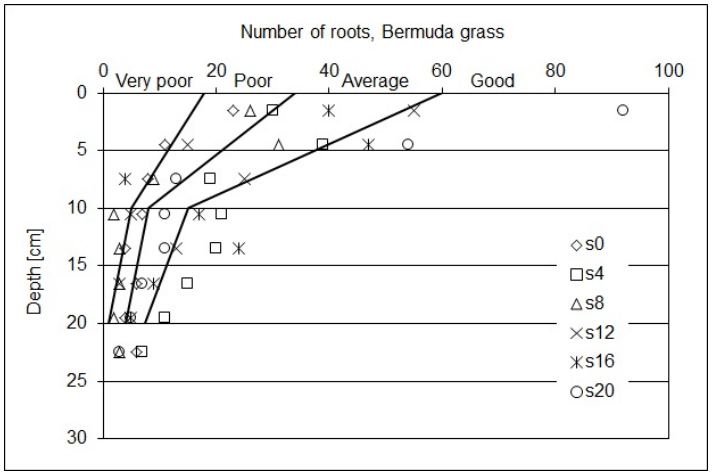

Figure 2.4: Root distribution in depth of Bermuda grass compared to Min [2006].

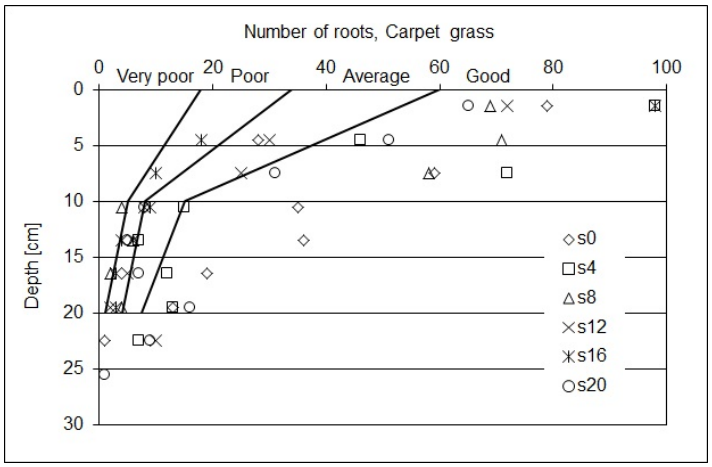

Figure 2.5: Root distribution in depth of Carpet grass compared to Min [2006].

In the above figures, different dot shapes present samples taken on the slope at different distances s from the dike crest, e.g., $s12$ is 12 m away from the crest. Main material characteristics of the soil underneath the grass turf are introduced in the next paragraph.

2.1.3 Soil properties

The dike body was constructed of local soil excavated from a hill nearby. The dike material was estimated homogeneous therefore only four soil samples were analysed to determine main properties such as grain size distribution, flow limit w_l, plasticity limit w_p and plasticity index I_p. These Atterberg limits measure the plastic properties of soil which are governed by the physical properties of the solids.

Analysis results indicated that the super dike body is constructed of clay with sand content of less than 40 %. According to the guidelines currently applied in Viet Nam [Vie], sand contents of grains with size smaller than 2 mm and larger than 0.005 mm. While sand grain sizes vary between 0.063 and 2 mm in TAW [1996]. Obtained values of w_l and I_p are plotted in the erosion-resistance category diagram given in TAW [1996]. Similar category remains an issue that needs to be established in Vietnamese condition. As can be seen in Figure C.5, the super dike soil is classified into clay with little erosion resistance. The analysed value points are close to the A-line, the limit between erosion resistance and little erosion resistance. However [TAW, 1996] does not describe clearly characteristics associated with these categories, for example, maximum flow velocity and corresponding applied duration.

More properties of the soil used to construct the dike model are given in Appendix C. Test sections are briefly described in the next section.

2.2 Test sections

The super dike slope was divided into four sections YB1, YB2, YB3 and YB4 to be tested with the simulator. In order to investigate effect of structures on the slope performance under attack of overtopping waves two obstacles were erected at YB1 and YB4. Specifications and test conditions of the four sections are described in Table 2.1.

As aforementioned, two local grass species Bermuda grass and Carpet grass were applied to protect the super dike slope. Figure 2.7 gives impressions to distinguishing Bermuda grass from Carpet grass. The grass mat was fertilised once and about 1 year old when being tested. Irregular and weak spots were randomly found to reflect the dike slopes in reality. More characteristics of these grass species are given in a separate report, Tuan [2012].

Figure 2.8 illustrates section YB1 that is covered with Bermuda grass and has a round head obstacle against overtopping flows. The obstacle is 1.2 m wide, 2.0 m long (in flow direction) and 0.8 m high. It can be seen that two side walls are symmetrical with respect to the obstacle.

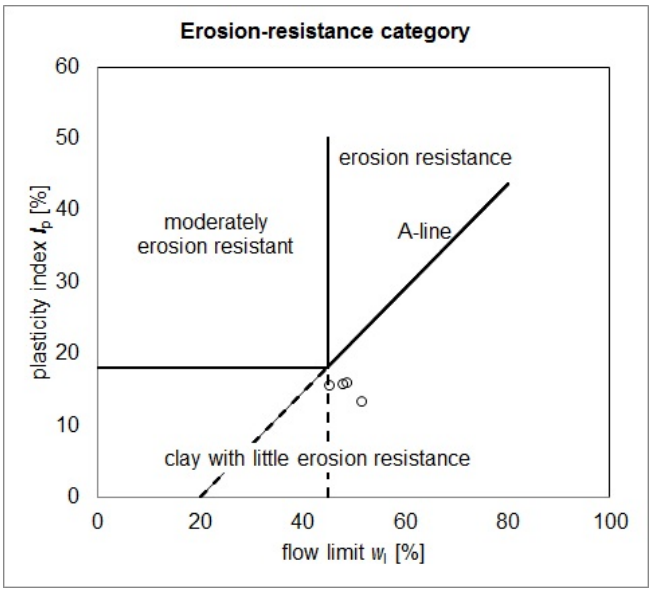

Figure 2.6: Erosion resistance category based on flow limit and plasticity [TAW, 1996], round dots are soil samples taken from the super dike body.

Table 2.1: Descriptions of the test sections

No.	Section	Grass	Obstacle	q_{max} [l/s per m]	H_s [m]
1	YB1	Bermuda grass	No	100	1.5
2	YB2	Bermuda grass	Round head	110	1.5
3	YB3	Carpet grass	No	100	1.5 and 2.0
4	YB4	Carpet grass	Square head	100	2.0

Figure 2.7: Two local grass species protect the 1/15 slope, Bermuda grass (left) and Mat grass (right).

The plain slope without obstacle of the section YB2 is shown in Figure 2.9.

Next to YB2, the section YB3 is regular without obstacle and covered with Carpet grass. Figure 2.10 presents the slope section from toe to crest.

The last section was YB4, a Carpet grass slope with a square head obstacle. This has the same

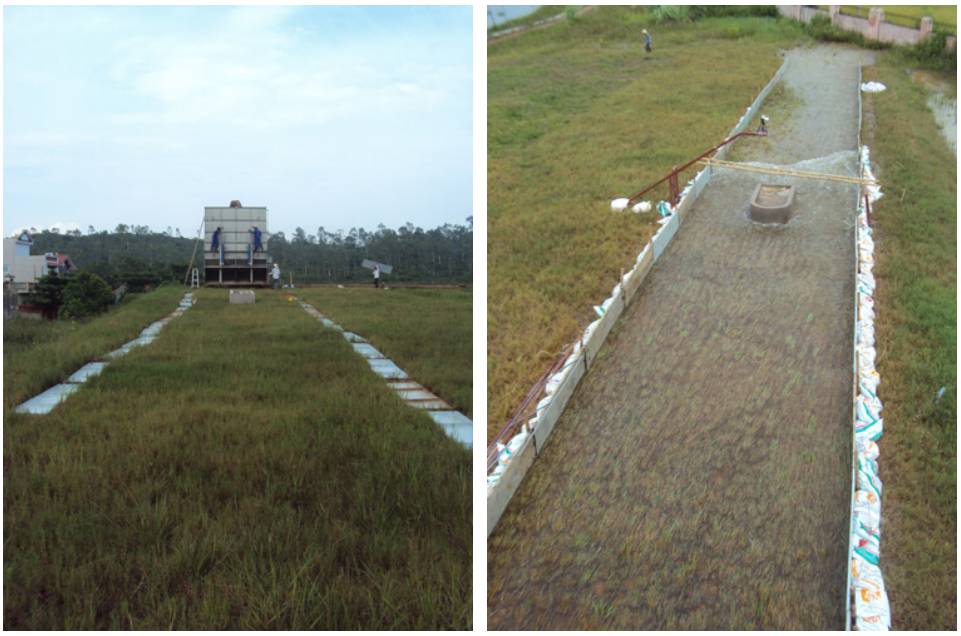

Figure 2.8: The first section YB1, Bermuda grass and round head obstacle.

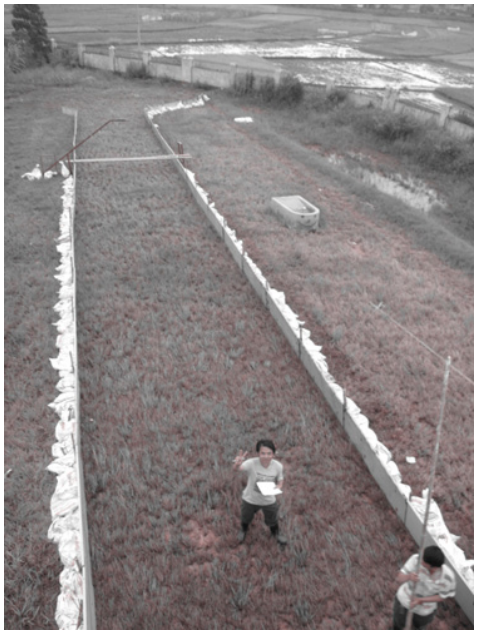

Figure 2.9: Section YB2, plain slope covered by Bermuda grass.

size as the round one. Toe to crest and crest to toe views of YB4 are given in Figure 2.11.

Wave conditions and test scenarios applied at each section are presented in the next part.

2.3 Test scenarios

The wave overtopping resistance of four grass covered slopes were tested with increasing mean overtopping discharge from small to large. Each mean discharge represents a simulated storm lasting about 6 hours which characterises storms in the north of Viet Nam. Tested discharges were divided into several levels such as 40; 80; 100 and 110 l/s per m, compared to 120 in Thai Tho and 70 in

Figure 2.10: Section YB3, plain slope covered by Mat grass.

Figure 2.11: The last section YB4, Mat grass and square head obstacle.

Thinh Long. Each simulated storm was divided into a number of 1 hour periods, during which the Wave Overtopping Simulator worked continuously (i.e., it was continuously supplied with a constant discharge). After every hour of testing, slope profiles were measured and slope surfaces were captured by photo-camera in order to determine erosion development in time under wave overtopping attack. All overtopping rates, applying durations and wave heights are given in Table 2.2.

Table 2.2: Unit discharges, durations and wave heights.

Section	Unit discharge [l/s per m]					H_s	Total duration
	40	60	80	100	110		
YB1	-	3 h	1 h	1 h	-	1.5 m	5 h
YB2	-	4 h	2 h	4 h	2	1.5 m	12 h
YB3	-	4 h	6 h	10 h	-	1.5 m	20 h
YB3	1	2 h	2 h	1 h	-	2.0 m	6 h
YB4	2	6 h	6 h	6 h	-	2.0 m	20 h

Each test condition is a distribution of overtopping volumes, see Eur. This distribution depends on wave boundary at the seaside such as a wave height, wave period and water depth. The same wave condition was used at YB1, YB2 and YB3 with a significant wave height of 1.5 m and a peak period of 6.0 s. It is assumed that the seaward slope is smooth and has a $\tan\alpha$ of 1:4. The wave height was increased to 2 m at YB3 due to the durable grass mat against overtopping flows. The simulator is capable of generating storm with a significant wave height of 2 m and a maximum discharge of 100 l/s per m. When a higher discharge is simulated, waves with overtopping volumes larger than 5.5 m^3/m can not be fully generated because the simulator tank is 22 m^3 in total for its length of 4 m. Waves with volumes V larger than 5.5 m^3/m are released two times, first with 5.5 m^3/m and second with the rest (V - 5.5).

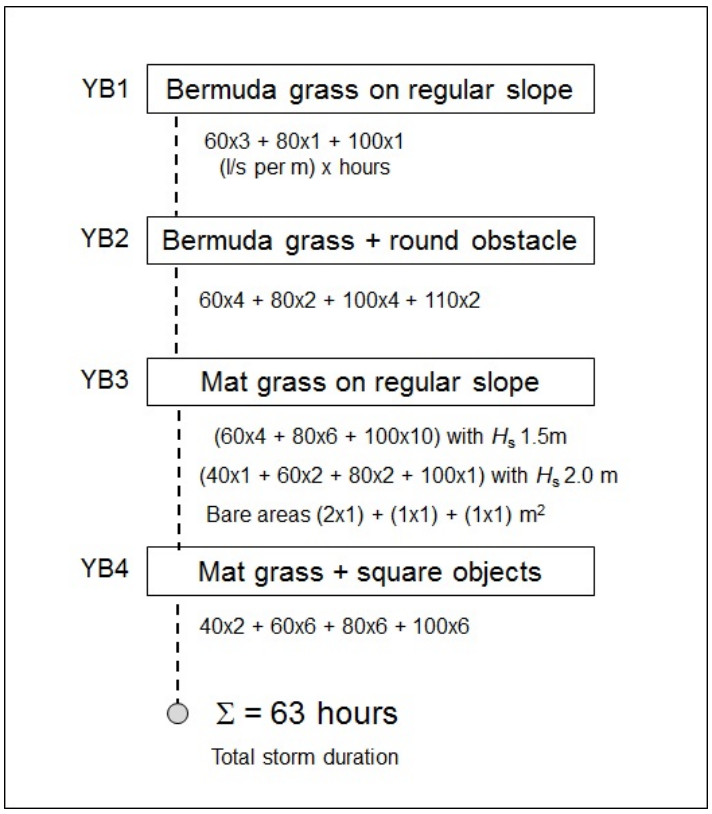

Figure 2.12: Test scenarios at the four sections.

Overtopping volume distributions of the 1.5 m wave height with different overtopping rates are graphically illustrated in Figure 2.13.

2.4 Experimental procedures

When assembly and calibration of devices and equipments were completed, destructive tests could be carried out according to a common procedure. The procedure was also adjusted during implementation to become more and more reasonable and effective. A sequence of alternative steps are described in Table 2.3.

The above table lists main steps of how to implement a test set, hydraulic measurement and profile measurement are described in separate parts of this report. In general, experimental procedures in Yen Binh were similar to Do Son, Thinh Long and Thai Thuy.

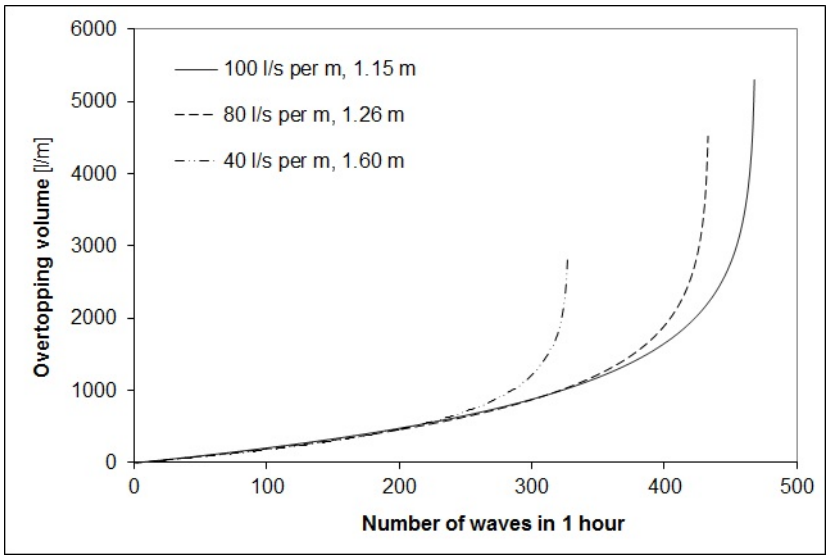

Figure 2.13: Wave overtopping volume distribution with different mean discharges generated by the Simulator in 1 hour. $H_s = 1.5$ m, $T_p = 6.0$ s and $\tan\alpha = 1/4$.

Table 2.3: Experimental procedure.

Step	Work	Duration [hours]	Manpower [men]	Note
1	prepare generator, pumps and the Simulator	0.1	3	at the same time
2	ignite generator and pumps, discharge calibration	0.3	3	
3	compute control tables	0.1	1	each control table is calculated for a certain discharge
4	perform test	1 - 2	3	each test lasts about 1 hour, can be shorter or longer depending on the real discharge of pumps
5	capture slope surface	1.0	2	with photo-camera
7	measure slope profiles	0.5	3	
	Total	$3 \sim 4$ hours		

2.5 Expected damages

Specifications of the four sections are described above. Main features are differences in grass species and configurations of obstacles. Damages are predicted to be initiated at the geometrical transitions and around obstacles. Here, damage is defined as part of the grass mat is eroded, even with a small area of some square centimetre. From the initial points, damage can be enlarged due to the effect of overtopping flow to a certain level that sufficiently large to threaten the stability of the slope section.

It is noted that the super dike slope is 1/15, which is much smaller than the popularly applied dike

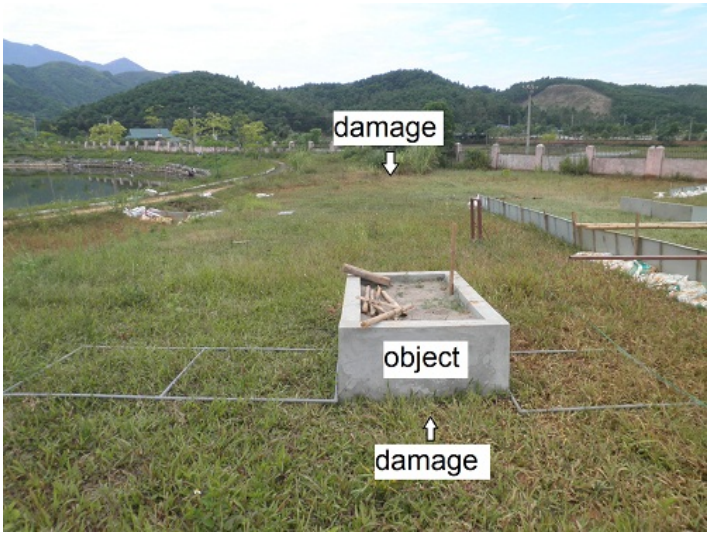

Figure 2.14: Expected damages on the super dike slope.

slopes in Viet Nam. Damages are expected to take place at the transition between the slope and the horizontal toe due to the impacts of hydraulic jumps. Damage might occur in front of the obstacles where flows are blocked and concentrated. While the areas behind the obstacles are not exposed to flows therefore remain intact. Damage around the square obstacle at YB4 can be more significant than the round one at YB1 because of the former is more effective in retaining flows. Figure 2.14 indicates potential points of damage on the super dike slope. Followings are detailed description of the measurements and results of the overtopping flows which are considered predominant factors inducing damage to the grass covered slopes.

Chapter 3

Front velocity

Phenomenon of wave overtopping generates water tongue on seaward slope, exceeding dike crest and then following on the landward slope. Crest and landward slope can be damaged due to these overtopping flows. It is therefore necessary to determine characteristics of overtopping flows such as flow depth and flow velocity on the dike crest and landward slope. In this chapter, devices and measurement methods of front velocity are introduced first, then main results are given.

3.1 Devices and measurement method

Flow released from the Simulator are very turbulent with high density of air bubbles which normally makes flow very white. Presently, there is no reliable device for this kind of flow. In previous simulator tests in Hai Phong, Nam Dinh and Thai Binh, digital camcorders were applied in determining front velocities on the dike slope. Based on the differences in positions of the front part of the overtopping flow between successive images, with a given distance and given time step, front velocity can be derived. Set-up of the first camcorder is shown in Figure 3.1. The camcorder was mounted on a steel frame to capture the flow over a distance of 10 m. The second camcorder was positioned aside to capture the flow as shown in Figure 3.2.

Figure 3.1: Set-up of the camcorder to capture overtopping flow on the dike slope

Theoretically flow velocity has to be measured for every wave generated by the Simulator during the entire simulated storm. That will result in a large amount of data to be analysed. A limited number of overtopping volumes were therefore selected to measure the front velocity such as 1, 2, 3, 4 and 5 m^3/m which were called representative volumes. Depending on the mean overtopping discharge 40, 60, 80 ...l/s per m, small or large overtopping volumes will be found in the wave volume distribution. For a mean discharge of 40 l/s per m, wave with volume of 2 m^3/m can be hardly found but small volumes as 0.5 or 1 m^3/m. In contrast, a mean overtopping discharge of 80 l/s per m may contents of waves with large volumes of up to 4 or even 5 m^3/m.

Figure 3.2: The flow captured by a camcorder positioned aside.

To perform hydraulic measurement a team of three staffs was required. One controlled the bottom valves and watched the water level in the Simulator. When the desired level was about reached, about $2 \sim 3$ seconds in advance, he signaled the other two to start recording with camcorders. A name card indicating volume and order of replication was hold in front of these two camcorders for a couple of seconds in order to document properly. The bottom valves were totally opened right when the desired volume was reached. Recording was stopped after the released volume had passed the measurement areas. The pumps discharge q_p had to be measured beforehand, then time for filling the representative volume could be calculated $\Delta t_f = V/q_p$. Normally next measurement would be prepared and carried out after the previous one that had been done while the 55 kW pump was kept working stably giving a constant discharge. Measurement of each volume was repeated three times.

The slope was about 40 m long, front velocities were observed at three areas, from $x_s = 5 \sim 8$ m, $8 \sim 11$ m (the first camcorder), and $11 \sim 15$ m (the second camcorder). In which x_s is the distance from crest edge. Measurement was performed at the YB3 section which was covered with Mat grass and had no obstacle.

3.1.1 Image processing

Data processing is basically done by analysing movies of the overtopping flows on dike slope corresponding to certain volumes. Using some programs which are capable of reading files in .avi or .mts format to watch the flow flow movies in a slow speed or in sequence of frames, for instance 25 frames/ second. It can be seen in Figure 3.3, the front part of the flow traveled from $x_s = 8$ m to 11 m within a time of $(t_2 - t_1$. The front velocity is then determined as the ratio of the distance and the time as:

$$u = \frac{\Delta s}{\Delta t} = \frac{s_2 - s_1}{t_2 - t_1} \tag{3.1}$$

Movies recorded by the second camcorder were analysed with similar method giving the front velocity from $x_s = 11$ to 15 m on the dike slope.

3.2 Results

Applying the above mentioned methods to process all recorded movies at YB3, value of the front velocity of different overtopping volumes were obtained. Figure 3.4, 3.5 and 3.6 illustrate the relationship between overtopping volume and front velocity. The horizontal axis gives the overtopping volumes and the vertical axis gives the corresponding values of the front velocities. Despite the small scattering of data in these figures, it is revealed that increasing volume gives increasing front velocity on the dike slope. Comparing these three figures indicates that along the slope, front velocities tend to increase slightly.

The estimated traveling times of different overtopping volumes are given in Table 3.1.

Figure 3.3: A series of two images in which the front part of overtopping flow traveled over a distance of 3 m within Δt seconds.

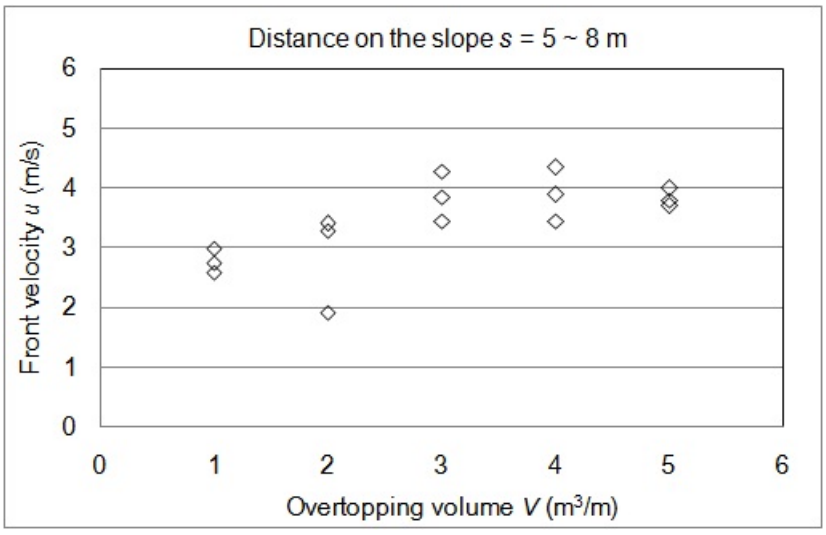

Figure 3.4: Front velocities of different overtopping volumes, distance from the dike crest 5 - 8 m.

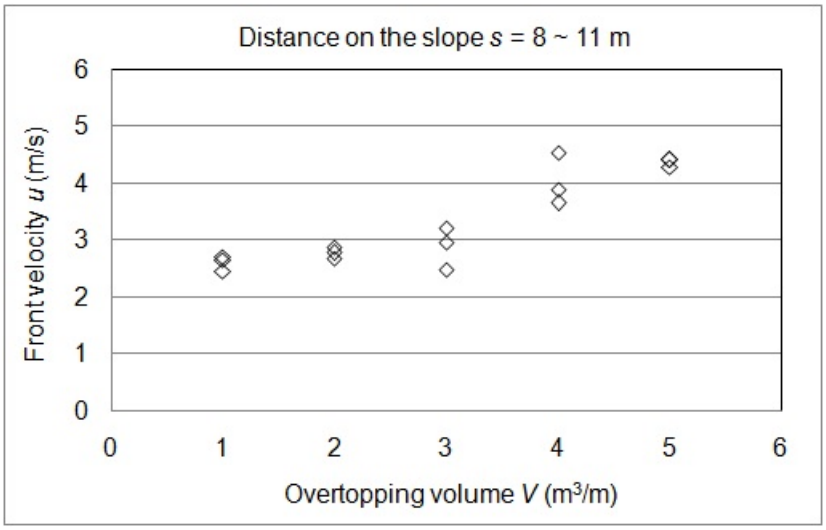

Figure 3.5: Front velocities of different overtopping volumes, distance from the dike crest 8 - 11 m.

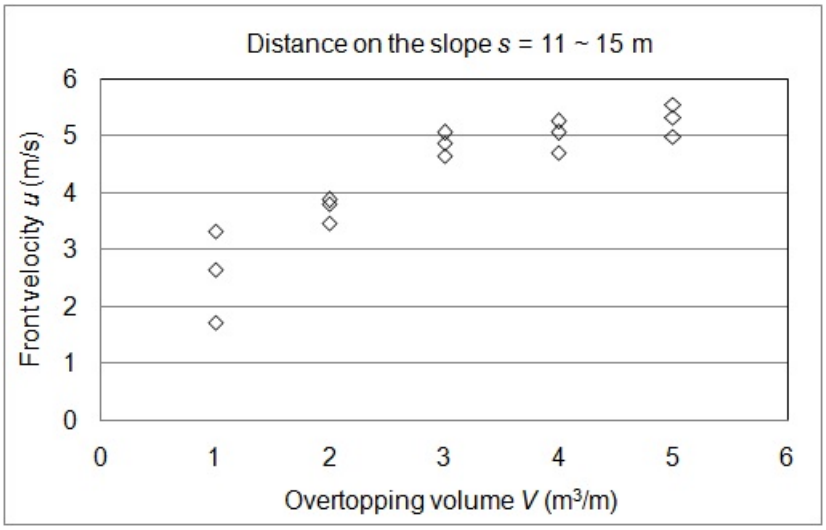

Figure 3.6: Front velocities of different overtopping volumes, distance from the dike crest 11 - 15 m.

Table 3.1: Estimated traveling time of the overtopping flows.

V [m^3/m]	Distance from the crest [m]					Front velocity [m/s]		
0.00	5.00	8.00	11.00	11.00	15.00	u_1	u_2	u_3
1.00	16.05	17.21	18.32	5.75	7.26	2.59	2.70	2.65
1.00	11.12	12.21	13.34	5.18	7.49	2.75	2.65	1.73
1.00	5.70	6.70	7.92	4.88	6.08	3.00	2.46	3.33
2.00	16.83	17.71	18.79	4.89	6.04	3.41	2.78	3.48
2.00	20.29	21.85	22.89	12.25	13.28	1.92	2.88	3.88
2.00	14.03	14.94	16.06	7.53	8.58	3.30	2.68	3.81
3.00	15.48	16.35	17.28	7.29	8.08	3.45	3.23	5.06
3.00	15.09	15.87	17.08	5.62	6.44	3.85	2.48	4.88
3.00	29.80	30.50	31.51	29.98	30.84	4.29	2.97	4.65
4.00	7.55	8.24	9.06	5.60	6.45	4.35	3.66	4.71
4.00	17.13	17.90	18.67	13.28	14.07	3.90	3.90	5.06
4.00	17.93	18.80	19.46	2.50	3.26	3.45	4.55	5.26
5.00	16.25	17.04	17.72	4.92	5.67	3.80	4.41	5.33
5.00	4.74	5.49	6.17	3.88	4.60	4.00	4.41	5.56
5.00	7.74	8.55	9.25	4.84	5.64	3.70	4.29	5.00

Chapter 4

Dike slope profiles

Under attack of overtopping flow released from the simulator, dike slope can be damaged resulting in the changes of slope profiles. These changes are recorded by measuring the slope profiles between consecutive test periods. The distance between the two side walls was 4 m as large as the width of the Simulator. Profiles were measured 1 m away from the side wall, both of the left one and the right one in order to minimise the side effects of experimental set-up.

4.1 Measurement method and data processing

To measure slope profile, a simple method with simple equipments were applied. A straight steel bar was placed on two sticks across two side walls at every 50 cm from the crest ($x_s = 0$) to the toe. The bar was marked at every 0.5 m from the left side wall to the right one giving a value - distance of the measured profile from the left side wall, min 0 and max 4 m. A pole was hold vertically at every 0.5 m along the steel bar (a coordinate) to measure the distance from the horizontal bar to the slope surface y_s. Coordinate set of one measured point consisted of $x_s(i)$, $a(i)$ and $y_s(i)$. Value of y_s was then converted to slope level. It took about 30 minutes to complete a slope profile measurement including not less than 100 points. A measurement performance on the super dike slope is illustrated in Figure 4.1.

Figure 4.1: Measurement of the dike slope profile.

It was guaranteed that the stick lengths remained constant, 70 cm, through all measurements. This was the distance from the horizontal bar to the slope surface outside the side walls. First, baseline profile has to be identified, later profiles are calculated w.r.t the baseline profile.

Baseline profile

The baseline profile is defined as imaginary line that has a starting coordinates $x_s = 0$ and $y_s = 70$ cm, and a ending coordinates $x_s = 370 * 15$ and $y_s = 0$ cm. The super dike was built with a slope of

1/15 and a crest height of 300 cm. The x_s and y_s coordinates are converted into x and y coordinates as follows:

$$\begin{cases} x = x_s \cos[\arctan(1/15)] \\ y = 370 - x/15 \end{cases} \tag{4.1}$$

Initial profile

The initial profile is measured before testing with $x_0(i)$ is the distance from the crest edge (on x_s axis) and $y_0(i)$ is the vertical distance between the horizontal bar and the slope surface. These values are converted into x and y coordinates as follows:

$$\begin{cases} x = x_0 \cos[\arctan(1/15)] \\ y = (370 - x/15) - y_0 \end{cases} \tag{4.2}$$

Present profiles during the tests

Between consecutive test periods (one-hour storm), if some damages can be apparently observed the dike prolies are measured with $x_p(i)$ is the distance from the crest edge (on x_s axis) and $y_p(i)$ is the vertical distance between the horizontal bar and the slope surface. These values are converted into x and y coordinates as follows:

$$\begin{cases} x = x_p \cos[\arctan(1/15)] \\ y = (370 - x/15) - y_p \end{cases} \tag{4.3}$$

As can be seen in Figure 4.2, these coordinates x_s, x_0 and x_p are the same and constant at each measured point. The coordinate y_s at each measured point is constant in all calculations.

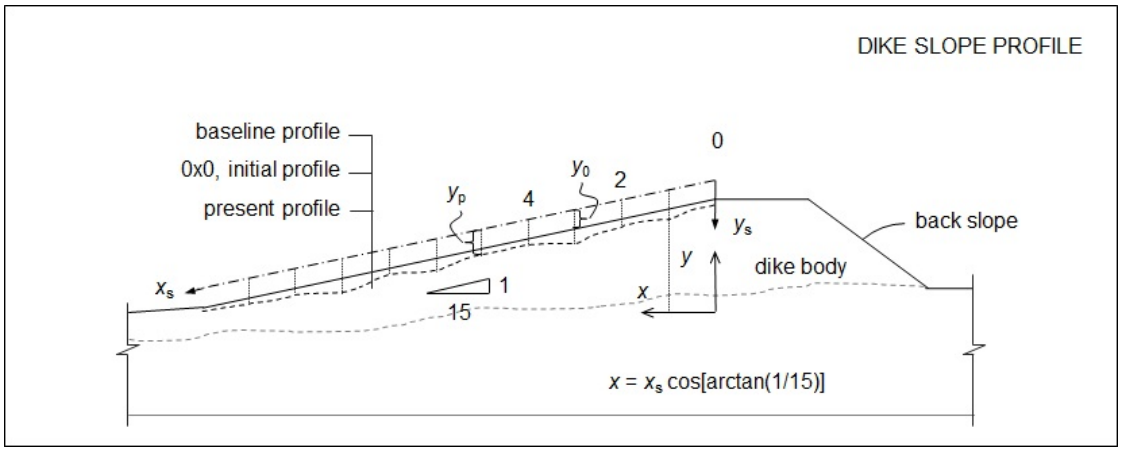

Figure 4.2: Baseline profile, initial profile and present profile of the dike slope.

In the followings, slope profiles are given in separate test sections. At each section, there are five profiles with increasing distance from the left side wall a = 1.0; 1.5; 2.0; 2.5 and 3.0 m. Due to the varying of characteristics at different sections, erosion developments in time were significantly different amongst those. Measurements were therefore performed in different sequences of moments. Legends in figures are denoted in order of mean overtopping rates that were applied at specific test section. For instance, 40x4 + 60x4 means profiles were measured after testing with 4 hours of 40 l/s per m and 4 hours of 60l/s per m. All initial profiles are labeled as 0x0. Data of slope profiles measured at 4 test sections are given in Appendix A.

4.2 Section YB1

At the section YB1, the slope was severely damaged next to the simulator gate due to the high energy flow after some hours testing. Figure A.1 and A.5 compare profiles with distance to the left side wall of 1 and 3 m, respectively, showing that the left erosion hole is deeper.

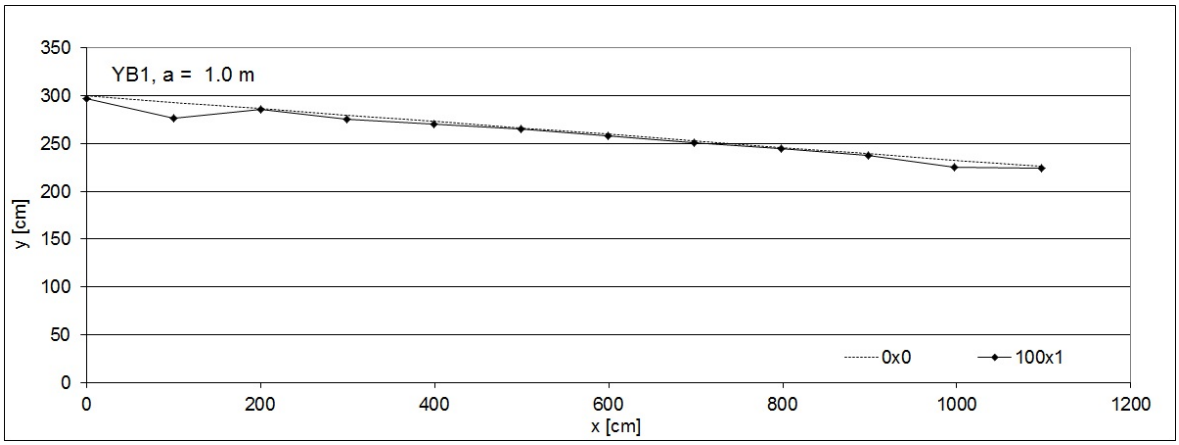

Figure 4.3: Changes of slope profile induced by wave overtopping, $a = 1.0$ m, YB1.

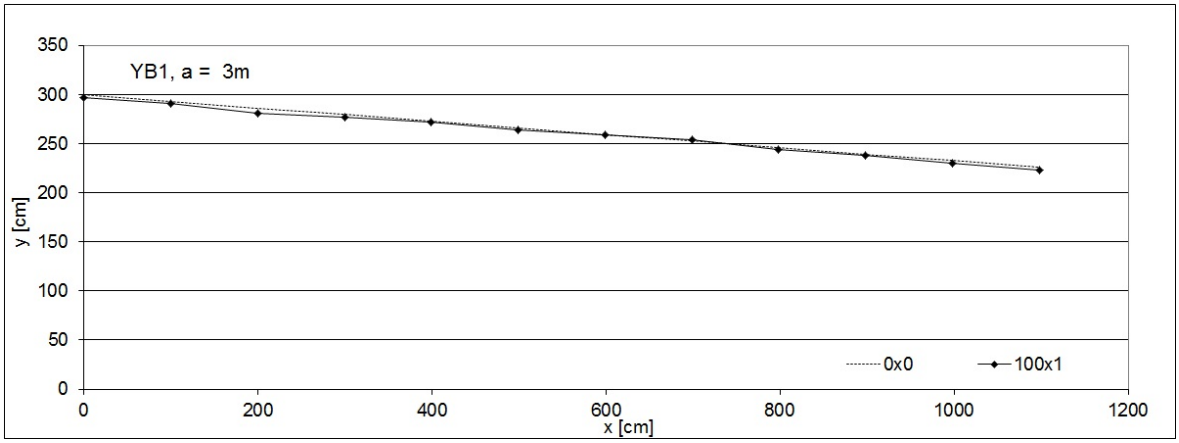

Figure 4.4: Changes of slope profile induced by wave overtopping, $a = 3.0$ m, YB1.

The transportation and assembly time at the section YB1 were much longer than planned therefore test scenario and measurement program was shortened. There are two profiles measured before testing and after 3 hours 60 + 1 hour 80 and 1 hour 100 l/s per m. The dike slope was damaged at a limited area near the crest, the lower part remained intact till the end of the test. Around the obstacle, damage was small and was not measured.

4.3 Section YB2

Similar to YB1, the slope was significantly damaged in front of the simulator gate after some hours. Figure A.6 and A.10 show that the left side was eroded about 50 cm while the right side was not affected.

Slope erosion in front of the simulator gate was unexpected and was not a study object. It can be explained by the gate position to the dike crest. Later on, steel plates were applied at the first meter after the gate to protect the grass slope from overtopping flow. Under discharges of 100 and 110 l/s per m, the left hole extended considerably as in (Figure A.6.

4.4 Section YB3

Before testing, the first meter of the slope was covered with steel plates to reduce the flow impact. After 4 hours of 60 l/s per m, the next 0.5 m was protected because the slope area underneath these

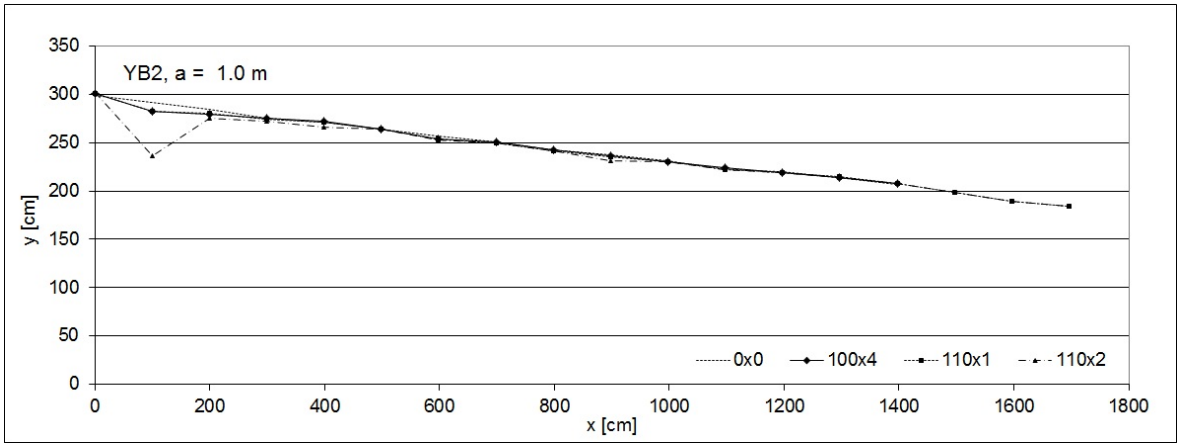

Figure 4.5: Changes of slope profile induced by wave overtopping, $a = 1.0$ m, YB2.

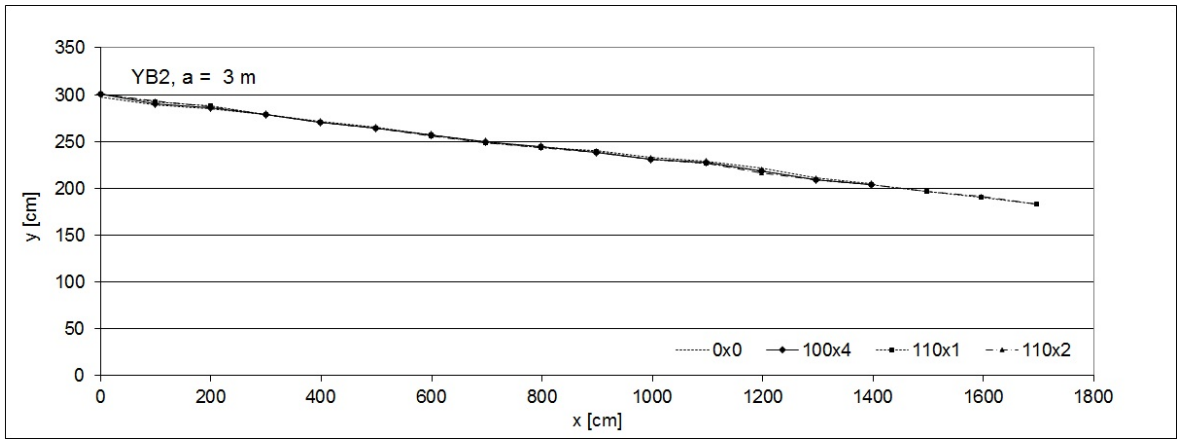

Figure 4.6: Changes of slope profile induced by wave overtopping, $a = 3.0$ m, YB2.

steel plates was damaged gradually. Two profiles with $a = 1$ and 2.5 m are plotted in Figure A.11 and A.14, data were measured at three moments.

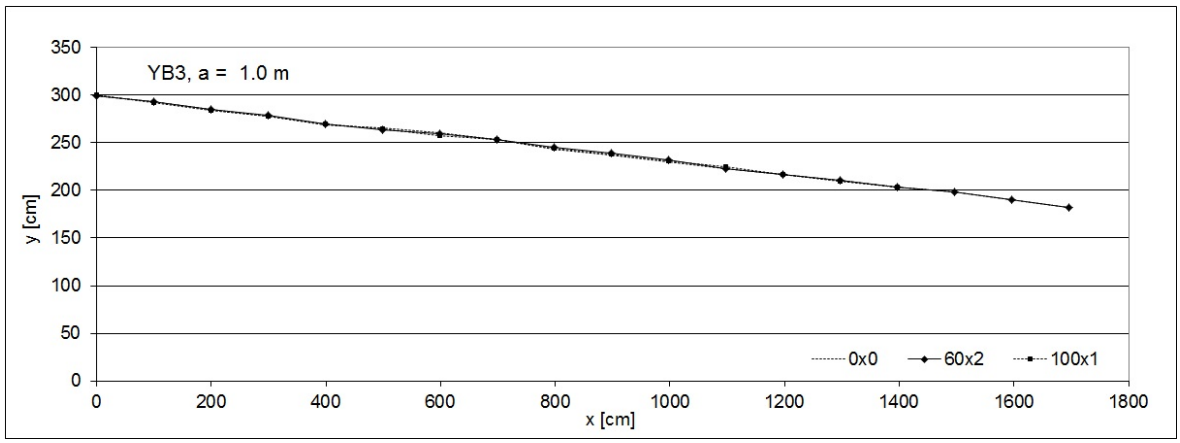

Figure 4.7: Changes of slope profile induced by wave overtopping, $a = 1.0$ m, YB3.

After testing 4 hours of 60 + 6 hours of 80 and 10 hours of 100 l/s per m with a significant wave height of 1.5 m, the Mat grass slope remained intact at YB3. A significant wave height was adapted to 2 m, and discharge was applied with increasingly values. After 1 hour of 40 l/s per m, damages

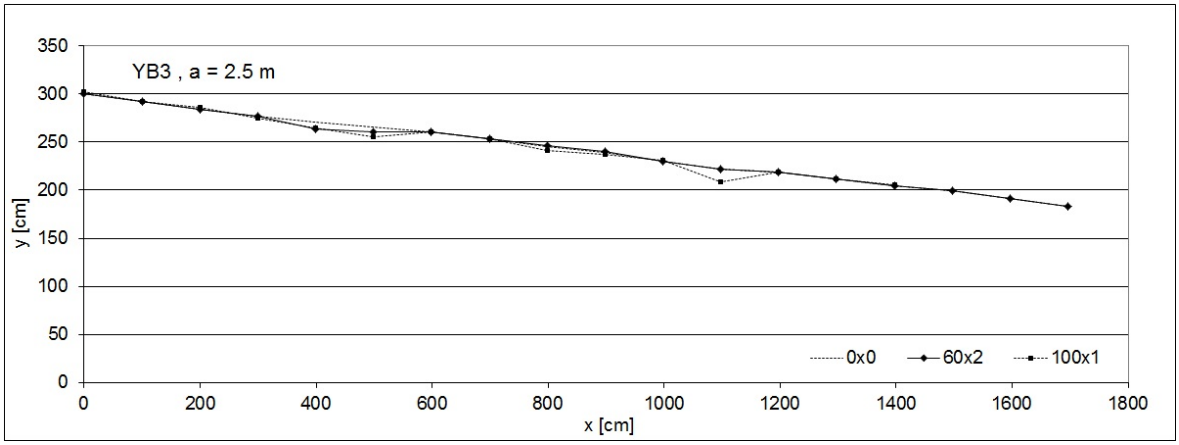

Figure 4.8: Changes of slope profile induced by wave overtopping, $a = 2.5$ m, YB3.

were created by removing 10 cm of the top soil layer including grass root at two positions. The first damage was 4 m from the dike crest and 2 m ^{2} in area, the second was 8 m from the dike crest and 1 m^2 in area. The profiles after (1 hour of 40 + 2 hours of 60 l/s per m) and after (1 hour of 40 + 2 hours of 60 + 2 hours of 80 + 1 hour of 100 l/s per m given in FigureA.14 show that even the top grass sod was removed, the damage did not extend further.

4.5 Section YB4

The first 1.5 m from the simulator gate was covered with steel plates as at YB2 and YB3. The damage started right after the protected area. Figure A.18, A.21 and A.22 give the dike profiles at $a = 1$, 2.5 and 3 m showing the damage distribution from left to right.

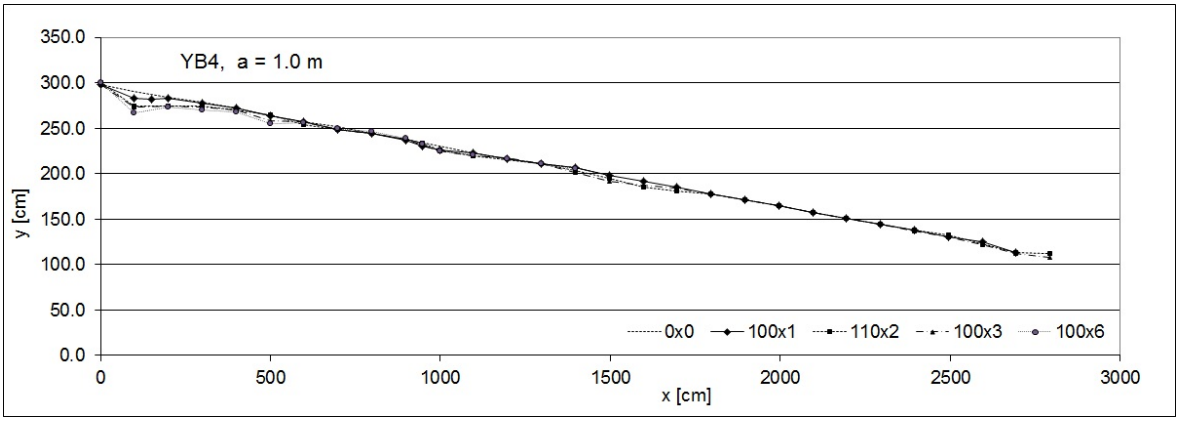

Figure 4.9: Changes of slope profile induced by wave overtopping, $a = 1.0$ m, YB4.

Slope profiles were measured times during the entire test at YB4 corresponding to five poly-lines. The dike slope was eroded on the left side with a hole depth of about 30 cm, see Figure A.18 and A.22. The grass mat was eroded slightly in front of the square obstacle which is not drawn in Figure A.21. Behind the obstacle, the slope was not damaged.

All data and slope profiles measured at YB1, YB2, YB3 and YB4 are given in Appendix A.

4.6 Discussion

The grass covered slope at four sections were eroded due to overtopping flows however the damage was not considerable that could threaten the slope stability. Discharge of 40 l/s per m could not

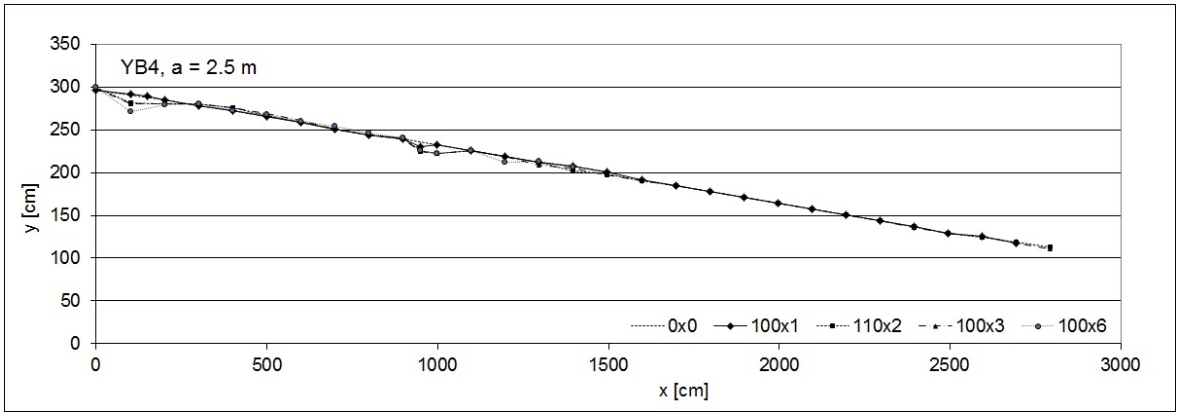

Figure 4.10: Changes of slope profile induced by wave overtopping, $a = 2.5$ m, YB4.

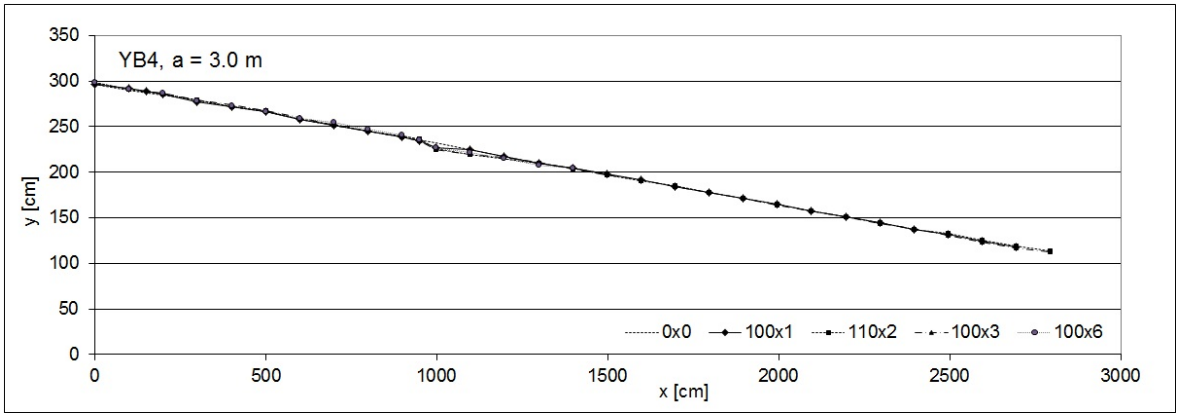

Figure 4.11: Changes of slope profile induced by wave overtopping, $a = 3.0$ m, YB4.

cause any damage to the grass cover. Damage was only initiated by sufficiently large discharges, 60 l/s per m at YB3, 100 at YB2 and YB4. Similar phenomena were observed in previous simulator tests both in Viet Nam and the Netherlands. For example, Steendam et al. [2008] concluded that a overtopping discharge below 30 l/s per m did not cause any grass covered slope, which was tested, to fail. The weakest slope section Thinh Long TL2 in Nam Dinh was first eroded by 10 l/s per m [Le, 2011]. The new test results confirm the hypothesis suggested in previous studies small overtopping discharges with small wave volumes have no damage effect but large discharges producing waves which are sufficiently energetic [van der Meer et al., 2009, 2010].

Chapter 5

Grass slope observations

5.1 Observation method and image processing

During the simulator tests, grass slopes were captured with a digital camera in order to examine the development of damages obviously such as geometric shape and dimensions. A frame with dimension of 1 by 1 m^2 was used in taking pictures of the slope surface according to a fixed sequence. The original images of this 1m-by-1m cell were cropped to a square shape which was considered as a unit image, Figure 5.1. These unit images were then merged into a larger one representing the entire tested section as wide as 4 m within the two side walls.

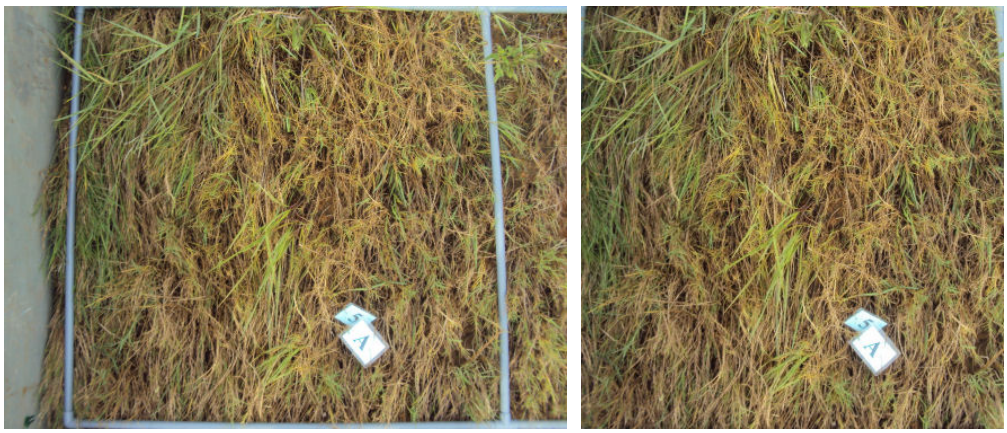

(a) Original (b) Cropped

Figure 5.1: Image of 1 m^2 grass slope, original compared to cropped.

In the followings, conditions of four slope sections before and after testing are compared. Wave conditions and test scenarios are given in Table 2.2, Chapter 2.

5.2 Section YB1

The grass mat was eroded considerably at the left area in front of the simulator gate with a depth of up to 30 cm. Figure 5.2 shows the plan view of this damage which is about 4 m long and 2 m wide.

There was a square obstacle on the YB1 slope with a distance of 12 m to the dike crest. Opposite the prediction in Chapter 2, damage did not really take place around the obstacle. The constraints of time and budget would not allow to extend scenarios at YB1, test was stopped after 5 hours of 60, 80 and 100 l/s per m.

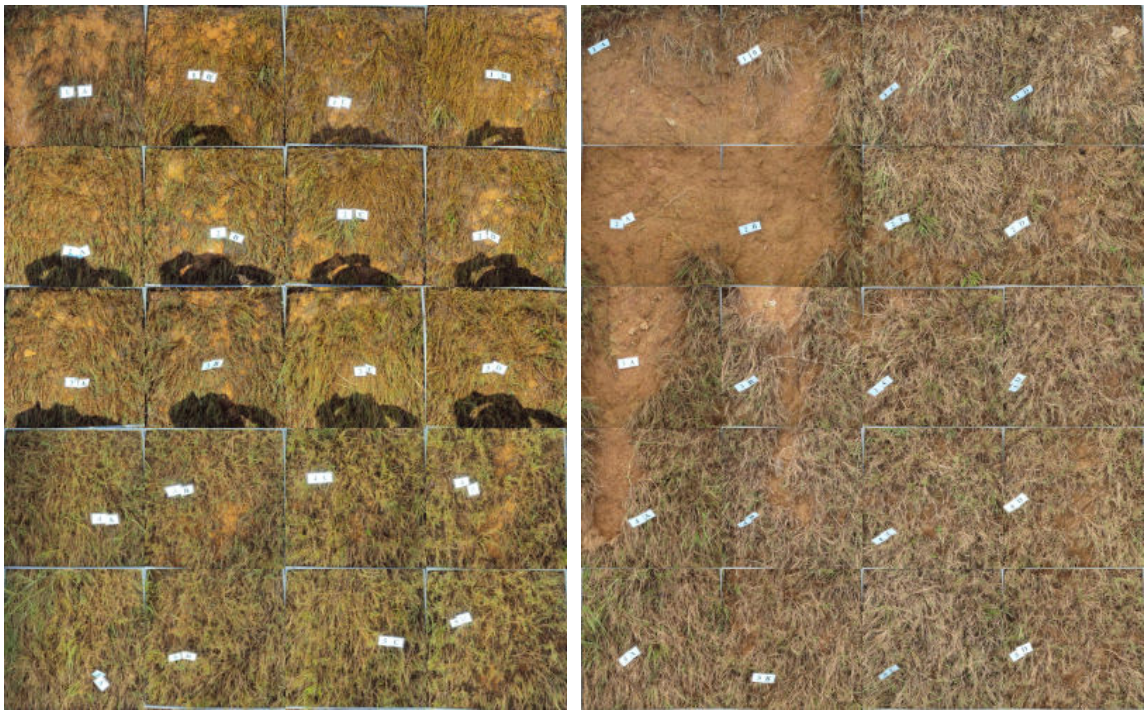

Figure 5.2: Section YB1, 0 to 5 m from the dike crest, after 60x1 (left) and after 60x3 + 80x1 + 100x1 (right).

5.3 Section YB2

Figure 5.3 compares the YB2 grass slope at initial (left) and final situation (right) after 4 hours 60 + 2 hours 80 + 4 hours 100 and 2 hours 110 l/s per m. Within the first 4 m from the gate, the top grass turf was swept away. Next to the left side wall, an erosion hole was about 50 cm deep. Flows released from the simulator were likely to focus energy upon this area. Testing duration at YB2 was much longer than YB1 therefore damages at YB2 were more considerable.

5.4 Section YB3

The first 5 m of the YB3 section from the crest is depicted in Figure 5.4 before testing and after (4 hours 60 + 6 hours 80 + 10 hours 100 l/s per m) with a wave height of 1.5 m and (1 hour 40 + 2 hours 60 + 2 hours 80 + 1 hour 100 l/s per m) with 2.0 m. It can be seen that the top part remained intact through the experiment.

After 1 hour of 40 l/s per m with 2.0 m, two damages were created by remove about 10 cm of the grass turf at two positions, 4 and 8 m from the crest, respectively. Figure 5.5 shows that the man-made damages extended lightly in the flow direction. While widths and depths were likely to maintain constant.

5.5 Section YB4

Similar to YB1 and YB2, the YB4 slope was mainly damaged on the left and close to the simulator. A wave height of 2.0 m was used resulting in more significant damages than at previous sections. For example, Figure 5.6 shows a damage of 6 m long compared to 4 m at YB2 (see Figure 5.3).

Damage around the square obstacle is depicted in Figure 5.7. The damage developed slowly and its dimensions were in order of some 10 cm. Behind the obstacle, the grass mat was not damaged as predicted in Chapter 2. Test at YB4 ended after 2 hours 40 + 6 hours 60 + 6 hours 80 and 6 hours 100 l/s per m, though damages did not reach maximum dimensions.

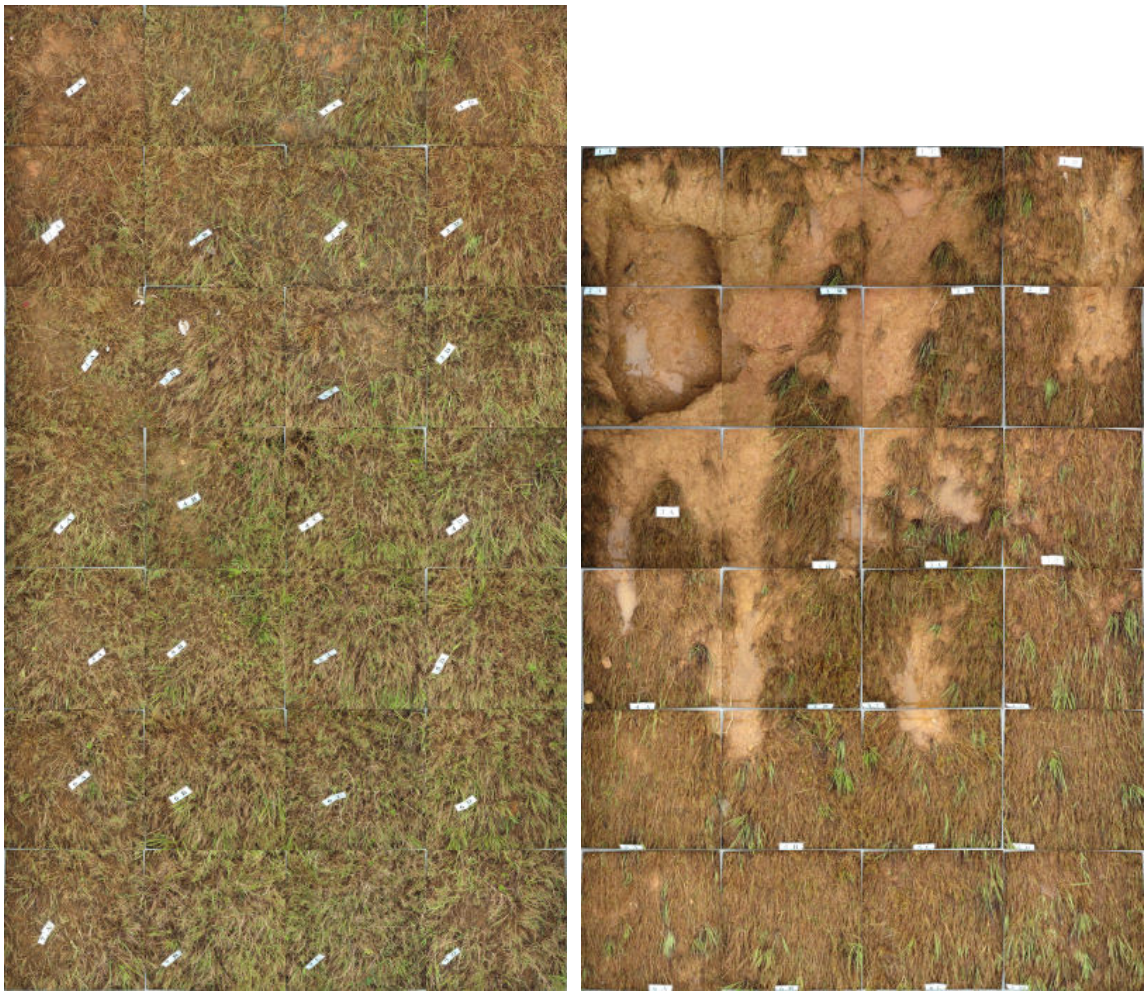

Figure 5.3: Section YB2, 0 to 7 m from the dike crest, initial condition (left) and after 60x4 + 80x2 + 100x4 + 110x2 (right).

Photographs of four sections at different moments during the simulator tests are fully collected in Appendix B. Chapter **??** discusses in more details about the formation and development of damage on grass slope induced by wave overtopping.

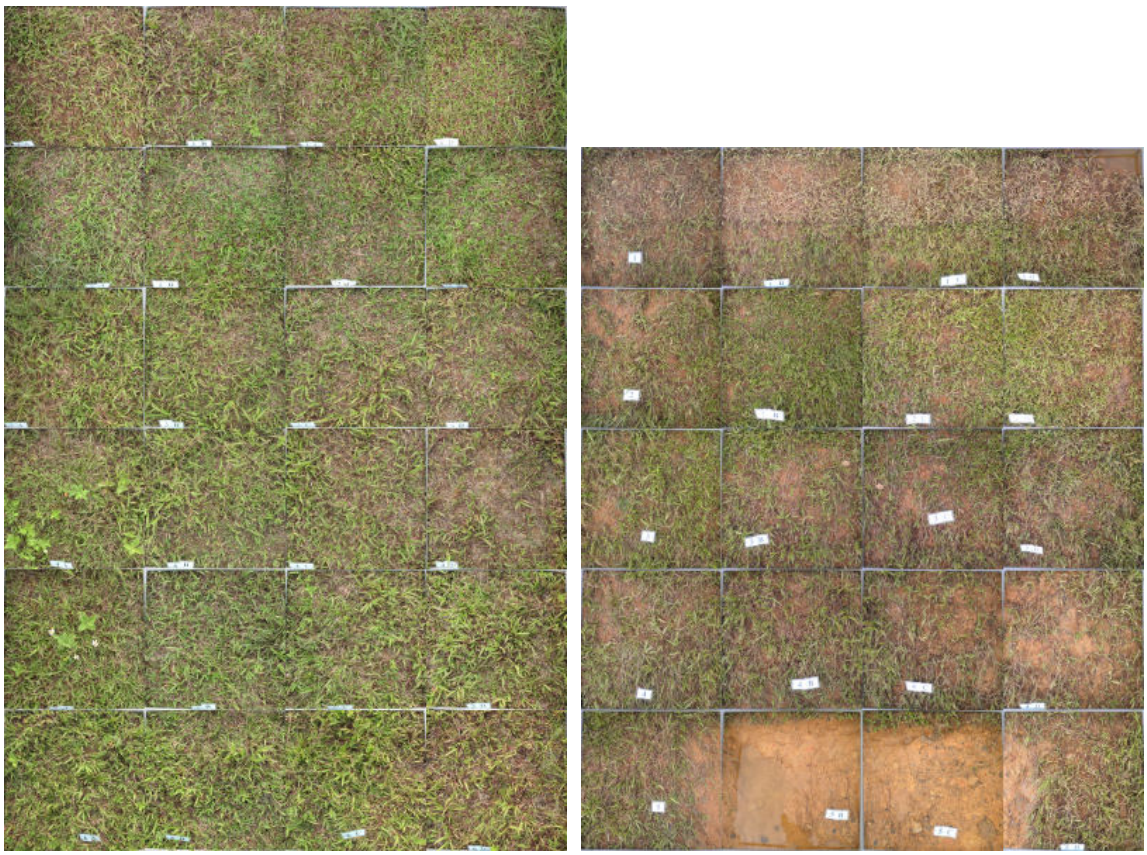

Figure 5.4: Section YB3, 0 to 7 from the dike crest. Left: initial condition. Right: after 60x4 + 80x6 + 100x10 with H_s 1.5 m and 40x1 + 60x2 + 80x2 + 100x1 with H_s 2.0 m.

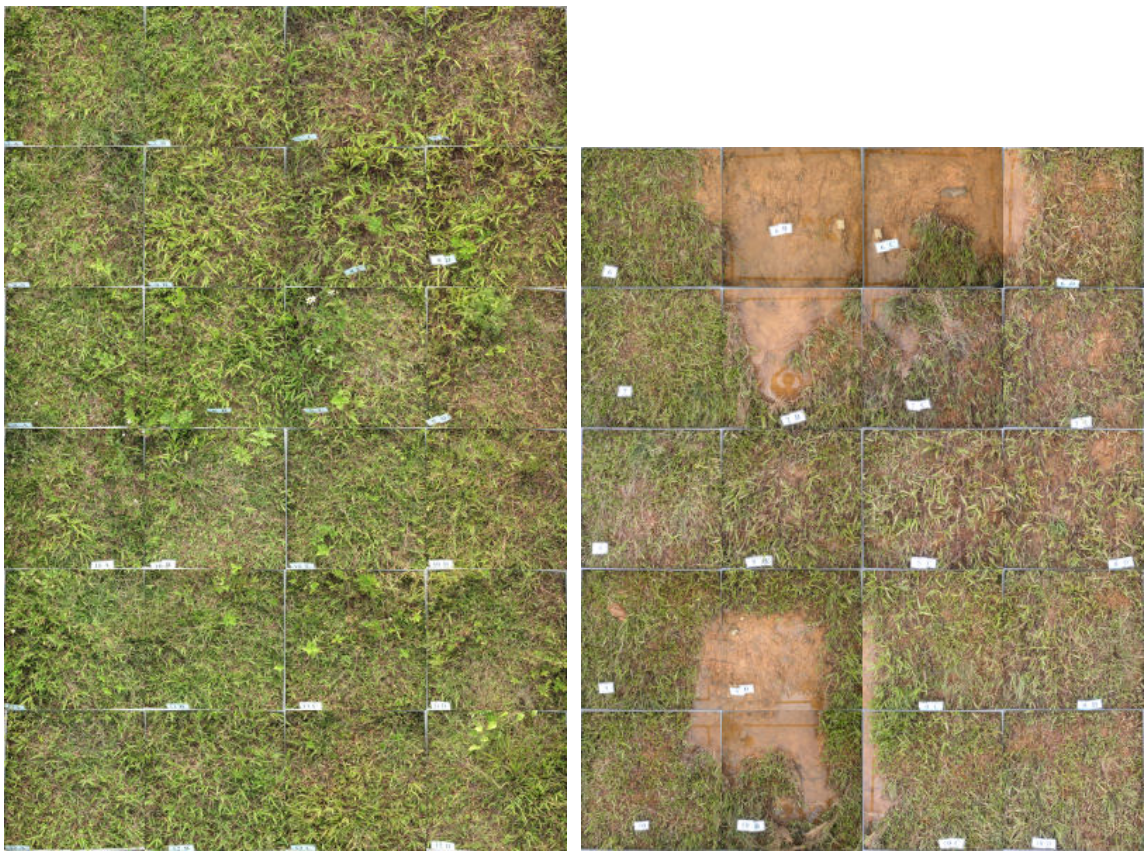

Figure 5.5: Section YB3, 7 to 12 from the dike crest. Left: initial condition. Right: after 60x4 + 80x6 + 100x10 with H_s 1.5 m and 40x1 + 60x2 + 80x2 + 100x1 with H_s 2.0 m.

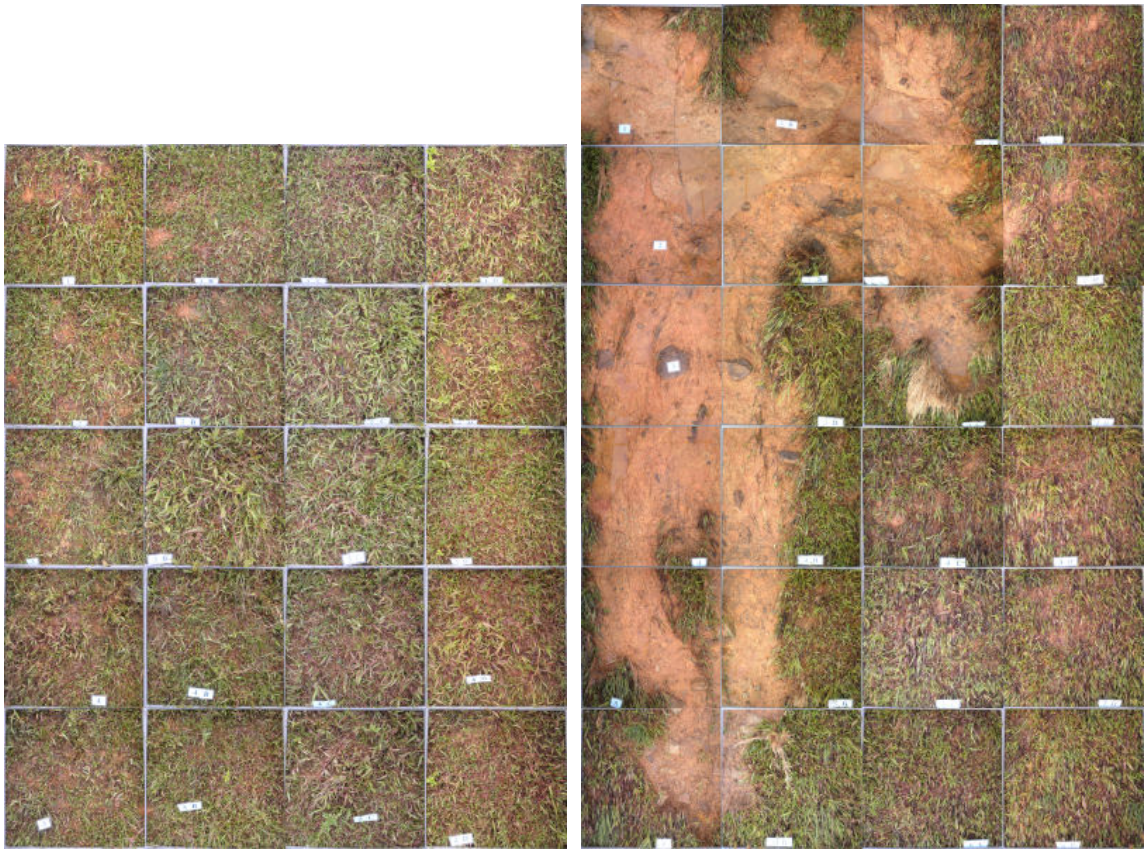

Figure 5.6: Section YB4, 1 to 5 m from the dike crest. Left: initial condition. Right: after 40x2 + 60x6 + 80x6 + 100x6.

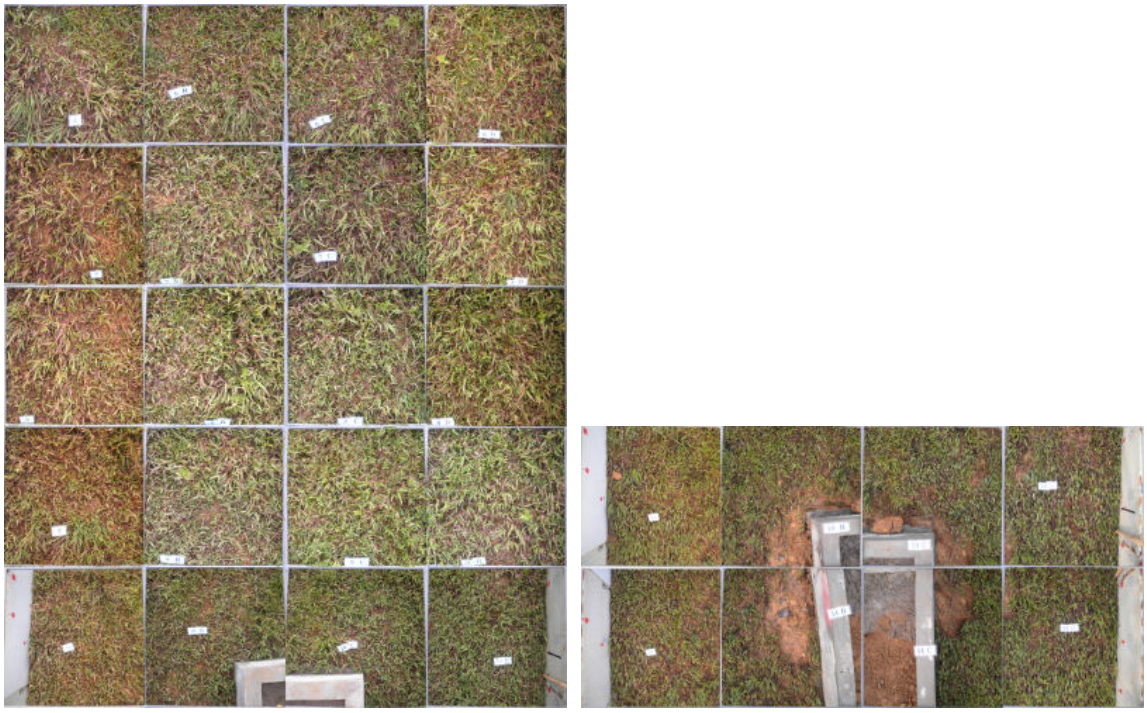

Figure 5.7: Section YB4, 6 to 10 m from the dike crest. Left: initial condition. Right: after 40x2 + 60x6 + 80x6 + 100x6.

Chapter 6

Damage on grass slopes

6.1 Geometry transition

In the simulator tank, water is first released vertically. The transition chute then guides water to flow horizontally on the dike crest. Getting out of the simulator gate, water starts flowing down on the dike slope. At the end of the slope, water turns to flow horizontally again on the dike toe. Damages were observed to take place at the geometric transitions, between dike crest and slope, and between slope and toe. The final situations of the top erosions at YB1 and YB2 are depicted in Figure 6.1, maximum discharges were 100 and 110 l/s per m, respectively.

(a) Section YB1 (b) Section YB2

Figure 6.1: Damages at the transition between dike crest and slope on Yen Binh dike.

Damage next to dike crest during simulator tests at YB2 and YB4 are depicted in Figure 6.2. YB2 slope was most severely damaged giving an erosion hole of 30 cm deep and some meters wide. At YB3 and YB4, steel plates were applied to protect partly the grass mat as shown in 6.2, right panel. Therefore, the magnitudes of damage were mitigated. Right at the simulator gate, the highly energetic flows attack directly the 1/15 grass covered slope as shown in Figure 6.3.

Velocities at the dike crest are sketched in Figure 6.4 with two slope angles. The flow released from the simulator is u_0 in horizontal orientation. At the edge crest, the flow changes to flow on the slope with a velocity of $u_0 \cos\beta$. With a smaller steepness (more gentle slope) the value of $u_0 \cos\beta$ is larger resulting in more destructive effects on the dike slope. This hypothesis might explain why there was no damage around the dike crest at Thinh Long and Thai Tho while the 1/15 slope at Yen Binh was seriously eroded.

At the end of the dike slope, a transition to the horizontal toe, grass sod was eroded and swept away at all four sections, for example see Figure 6.5. In general, the regime of the overtopping flow on the dike slope is critical or supercritical. Flow on the horizontal toe is in sub-critical regime. Hydraulic jump has to take place to dissipate a part of the flow energy when flow changes its regime.

(a) Section YB2 (b) Section YB4

Figure 6.2: Damages at the transition between dike crest and slope on Yen Binh dike.

Figure 6.3: Energetic flow at the simulator gate.

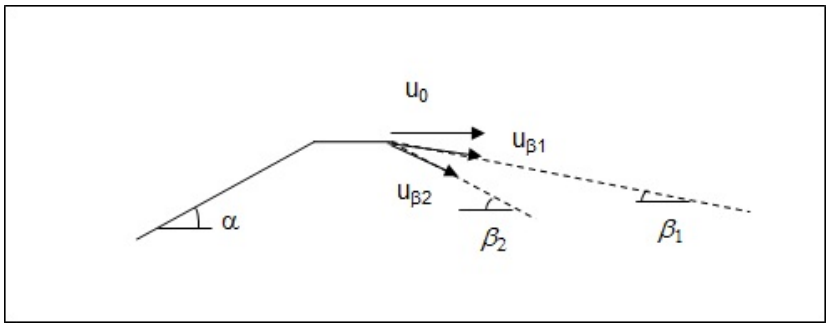

Figure 6.4: Flow velocity at the crest edge.

Also another part of the energy discrepancy between the two regimes causes damage of the dike toe which is actually the bed of flow.

In Figure 6.6, toe damage are shown at two conditions, after (2 hours 40 + 6 hours 60 + 4 hours 80 l/s per m) and after (2 hours 40 + 6 hours 60 + 6 hours 80 + 6 hours 100 l/s per m). On the left side, grass sod was eroded about 1 m downward. The mechanism is similar to what happens on the dike slope, about 5 to 10 cm of the top soil layer where grass roots concentrate is eroded and rolled up. The mechanism 'roll up' or 'turf set-off' was described in the work of Hewlett et al. [1987] and later was observed in the simulator tests in the Netherlands [van der Meer et al., 2009]. The 'roll up' mechanism is sketched in Figure 6.7 after Hewlett et al. [1987]. The grass turf was swept away to

Figure 6.5: Damage at the YB3 dike toe after 60x4 + 80x6 + 100x4.

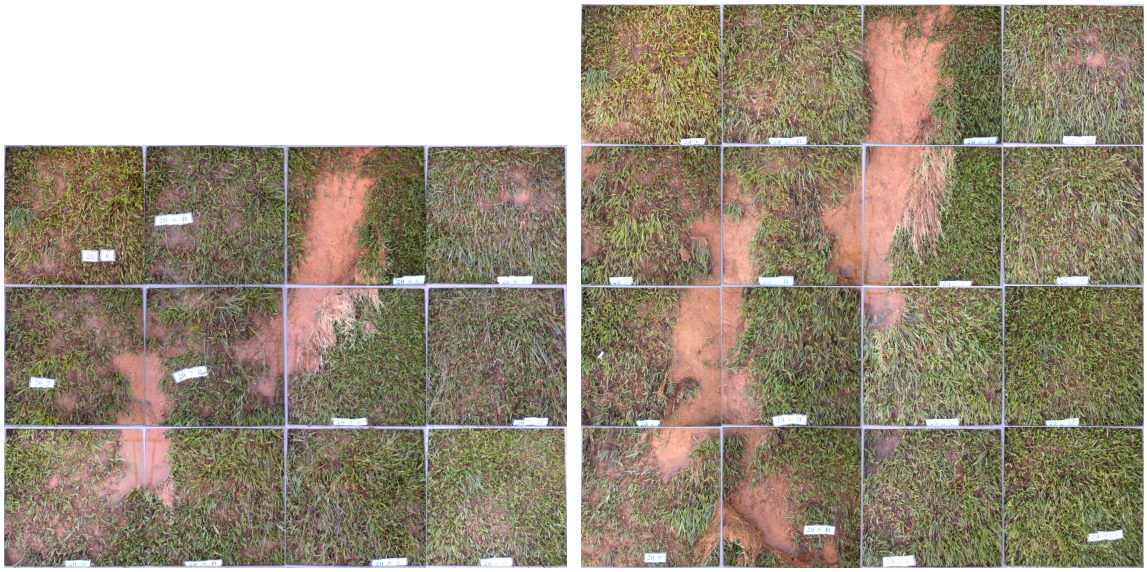

Figure 6.6: Damages at the YB4 dike toe after 40x2 + 60x6 + 80x4 (left) and after 40x2 + 60x6 + 80x6 + 100x6 (right).

expose the underneath soil body which classified hard clay.

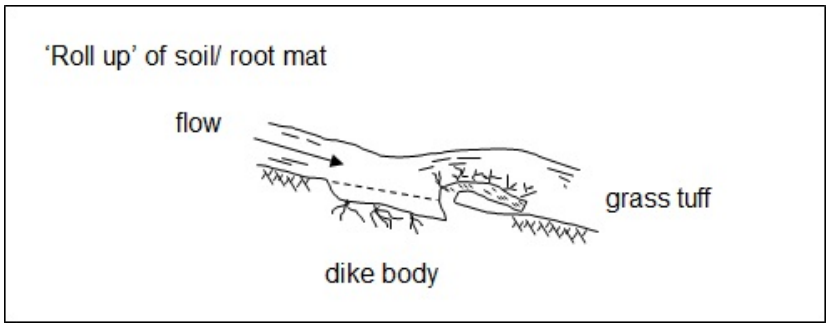

Figure 6.7: Mechanism 'roll up', grass mat is cut underneath and pushed up gradually.

Damage around the super dike toe is far different from what happened at Thinh Long TL1 section. Overtopping flows caused a hole of some 40 to 50 cm deep at the transition between slope and horizontal toe where grass cover was rather thin compared to other areas [Le, 2011]. The shallow erosion at the super dike toe is comparable to damage taking place at Boonweg dike, Friesland. Some hours of 75 l/s per m swept away the top layer of the grass turf to expose a hidden path constructed of brick stones [van der Meer et al., 2009].

6.2 Obstacles

At YB1 and YB4, two obstacles with round and square shapes were erected to investigate effects of structures on the dike slope performance under overtopping wave attacks. In Thinh Long simulator tests, a Casuarina tree with a trunk diameter of 7 cm blocked flows, thus resulting in more intensive force to erode the Bermuda grass slope [Le, 2011]. Figure 6.8 illustrates the flow pattern around the round head obstacle at YB1. Flows concentrated in front of the obstacle and caused a little erosion to the grass mat. Along and behind the obstacle, no damage was found. Load and duration applied at YB1 was limited, the grass mat was eroded slightly. Therefore it is not feasible to assess the influence of obstacle on the erosion resistance of the grass covered slope.

Figure 6.8: Left: flow around the round obstacle at YB1. Right: damage in front of the round obstacle.

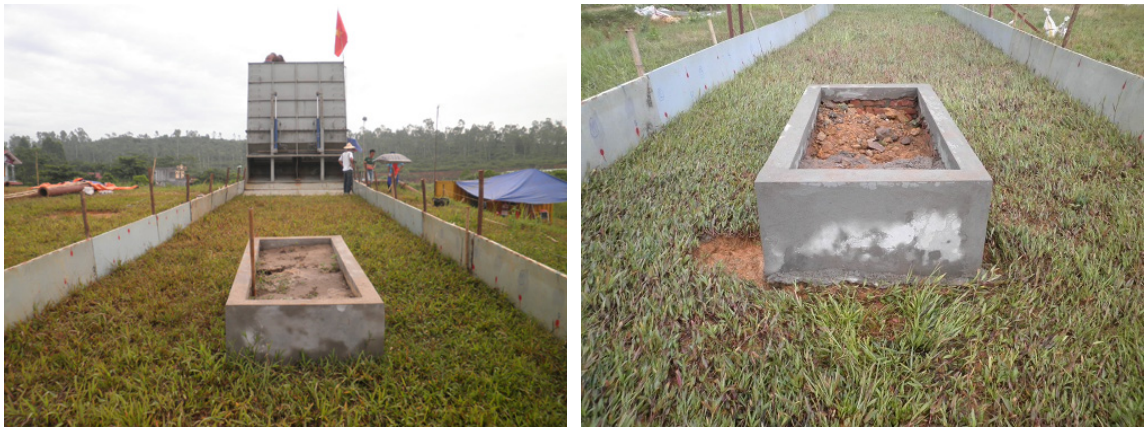

Figure 6.9: Grass mat around the square obstacle at YB4. Left: initial condition. Right: after 40x2 + 60x6.

At YB4, the obstacle was in square shape and about 12 m from the dike crest. The development of the erosion around this obstacle under increasing loads are captured in figures 6.9 and 6.10. After

Figure 6.10: Damage around the square obstacle at YB4. Left: after 0x2 + 60x6 + 80x4. Right: after that 80x2 + 100x4.

more than 10 hours of discharge increasing from 60 to 100 l/s per m, damage on both side of the obstacle extended slowly. These were more considerable than damages around the obstacle at YB1 but insufficient to affect the dike slope function under wave overtopping attack.

6.3 Existing damages

At YB3, after testing 4 hours 60 + 6 hours 80 and 10 hours 100 l/s per m with a significant wave height of 1.5 m, damage was introduced in form of shallow erosion. About 10 cm of the top soil layer where grass roots most distribute were removed at two positions, 5 m from the dike crest on an area of 2 m^2 and 8 m on 1 m^2. Figure 6.11 gives impression of the 2 m^2 grass surface (denoted as 5BC) before being ripped off.

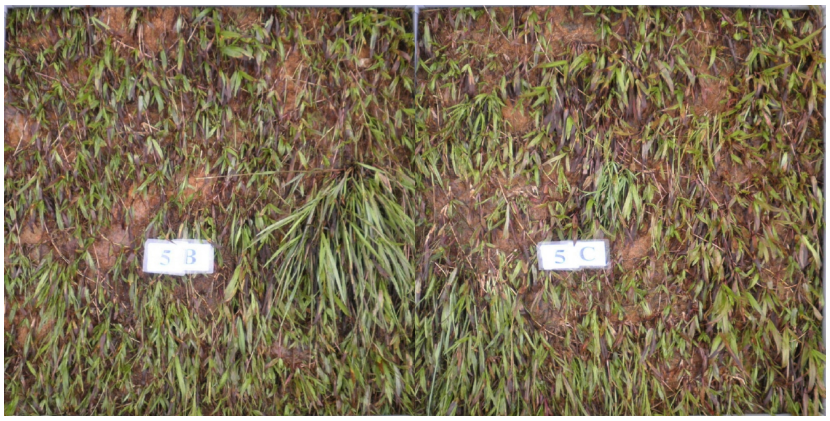

Figure 6.11: The area of 2 m^2 of Mat grass slope before being removed away. Applied discharge 60x4 + 80x6 + 100x10 and wave height of 1.5 m.

The extension of the man-made 5BC damage due to increasing discharges with a wave height of 2.0 m is depicted in Figure 6.12. The erosion area became two time larger in flow direction, from 2 m^2 to about 4 m^2. While its depth and width seemed likely not to change. The damage mechanism is 'roll up' as described in previous sections, flow drag forces at the end of the man-made hole gradually tear and lift up the leading edge of the grass mat to enlarge damage downward.

The mechanism 'roll up' was observed to take place on either Bermuda grass mat or Carpet grass mat as shown in Figure 6.13. Performance can be different depending on the characteristics of these two grass species. Carpet roots distribute more regularly in diameter and density within the first 10 cm under ground surface while Bermuda roots tend to get thiner and fewer [Tuan, 2012]. Bermuda

Figure 6.12: The 5bc damage after 40x1 + 60x2 (left) and after that 60x4 + 80x6 + 100x6 (right), wave height of 2.0 m.

(a) Bermuda grass (b) Carpet grass

Figure 6.13: Mechanism 'roll up' on slopes covered with Bermuda and Carpet grass.

grass creeps on the ground and roots wherever a node reaches the ground, forming a mat of stems and blades. In general, Bermuda grass is eroded by stem by stem or a group of stems close to each others. Due to dense mat of roots, Carpet grass works as a united mat. Due to the high drag forces Carpet grass is lifted and rolled up as shown in Figure 6.13, right panel.

Similarly, two bare spots with areas of 1x1x0.05 m and 0.4x0.4x0.15 m respectively were created on a slope section at Delfzijl, Groningen, the Netherlands [van der Meer et al., 2009]. Gullies developed from these two bare spots and extending to the dike toe under discharge of 50 l/s per m. Damage was observed to have shallow depth when only the grass turf was removed.

6.4 Strength of bare clay

As aforementioned, grass turf (about 10 cm of the top layer) was removed at two positions to expose the underneath soil body. The super dike soil is classified into clay with little erosion resistance according to TAW [1996] as described in chapter 2. The depth of these man-made damage were likely to remain the same under attack of increasing discharges from 40 to 100 l/s per m with significant wave height of 2 m. This means the bare clay body was not eroded. The Dutch erosion-resistance categories in TAW [1996] might need to be adjusted if being applied for the design practice in Viet Nam.

In Delfzijl, Groningen, the Netherlands, the erosion resistance of the bare clay was tested with the simulator (e.g., van der Meer et al. [2009] and Akkerman et al. [2007]). A layer of 0.2 m of the

grass sod was removed on the whole section area, 4 m wide and from crest to toe. The discharge of 1 l/s per m already caused damage to the bare clay slope. In creasing discharge to 5 and then 10 l/s per m lead to a head cut erosion extending towards the dike crest. After 6 hours of 10 l/s per m, the eroded hole reached 1 m deep. The clay was permeable due to a large number of worm holes and small fissures which could encourage the soil structure development. Yen Binh super dike was only one year old after construction, soil structure had not established well. In general, after construction a soil body tends to become more vulnerable when the soil structure develops gradually. On the contrary, the older a grass cover becomes the more resistance erosion it is.

6.5 Loads acting on the super dike slope

In general, loads acting on the super dike slope protected with local grass are in terms of overtopping discharges and applied durations with two significant wave heights, 1.5 m at YB1, YB2 and YB3, and 2.0 m at YB3 and YB4. Values of discharge and corresponding applied duration are plotted together in Figure 6.14. Note that there is no relationship between these two parameters, discharge and duration. The figure graphically illustrates the test conditions and scenarios at each section. During tests, discharge was increased when damage had not been formed or likely to develop further.

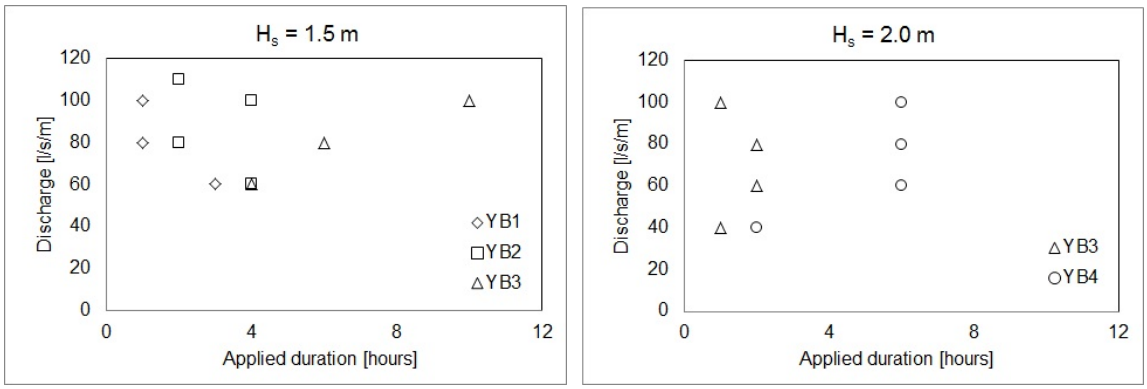

Figure 6.14: Discharges and corresponding durations applied at the four test sections for weight height of 1.5 m (left) and 2.0 m (right).

As aforementioned, the present wave overtopping simulator is capable of generating a maximum discharge of 100 l/s per m and a maximum overtopping volume of 5.5 m^3/m (see more Le et al. [2010] or Le [2011]). On the super dike slope, this discharge could not cause considerable damage to the grass mat. Prolonging duration of 100 l/s per m is a solution to enhance the load impacts because it is impossible to increase the overtopping discharge. The simulator tests on the super dike ended when damages did not reach critical states that might significantly threaten the dike functioning. Accordingly, another device with larger capacity is required to assess the performance of the super dike under extreme weather conditions.

Chapter 7

Main results

Front velocity

The phenomenon of wave overtopping during storms was simulated by the Wave Overtopping Simulator on a 1/15 grass covered slope. The front velocity of overtopping flows were estimated at three positions along the slope using digital camcorders. In general, increasing volume generates higher front velocity and it is likely to become larger downward the slope.

Damage induced by wave overtopping

Under attack of overtopping flows generated by the simulator, the super dike slope covered with Bermuda and Carpet grass was damaged moderately. Damage was in the form of a shallow erosion which took place around the dike crest and toe (geometric transitions). The mechanism is defined as 'roll up' or 'turf set-off', the grass mat of about 5 to 7 cm thick is lifted and rolled up gradually to expose the underneath soil body. Small damaged spots were observed around two obstacles of YB1 and YB4 sections therefore, influence of these objects on slope performance was unclear.

Man-made eroded spots were introduced at two positions on YB3 slope by removing the grass turf which was about 10 cm thick of the top layer including most of roots. Applying discharges of 40, 60, 80 and 100 l/s per m with a wave height of 2.0 m caused a gradual extension of the artificial damage downward while depths and widths remained the same. Apparently, the destructive impact of overtopping flow is most effective in its direction, from crest to toe.

Erosional resistance of the super dike slopes covered with grass

The super dike slope was 1/15 of inclination and protected by two local grass species, Bermuda and Carpet. When being tested, the grass mats were about one year old. The maximum discharge of the simulator 100 l/s per m was applied for 6 to 10 hours, thus resulting in moderate damage to the grass cover. These damaged spots were limited within 7 to 10 cm under the slope surface and insufficiently significant that might threaten the function of the super dike. The simulator was designed to test the normal sea (river) dike slopes with a steepness of 1/3 to 1/6 under a mild wave condition, significant wave heights not above 2.0 m. Therefore, to assess the super dike slope which is unbreachable even in extreme condition, a device with much higher capacity is clearly required.

Bibliography

G.J. Akkerman, P. Bernardini, J.W. van der Meer, H. Verheij, and A. van Hoven. Field tests on sea defences subject to wave overtopping. In *JSCE, Proc. 5th Coastal Structures 2007*, Venice, Italy, 2007.

H. W. M. Hewlett, L. A. Boorman, and M. E. Bramley. *Guide to the design of reinforced grass waterways*. Construction Industry Research and Information Association (CIRIA), London, UK, 1987.

H.T. Le. Destructive tests with the wave overtopping simulator. Comm. on hydraulic and geotechnical eng, 2011-01, Delft University of Technology, Delft, The Netherlands, July 2011.

H.T. Le, J.W. van der Meer, G.J. Schiereck, M.C. Vu, and G. van der Meer. Wave overtopping similator tests in vietnam. In *ASCE, Proc. 32nd ICCE*, Shanghai, China, 2010. Coastal Engineering Research Council. URL `https://journals.tdl.org/ICCE/article/view/1176`.

Voorschrift Toetsen of Veiligheid Primarie Waterkeringen. Ministry of Transport, Public Works and Water Management, 2006.

G. J. Steendam, W. de Vries, J. W. van der Meer, A. van Hoven, G. de Raat, and J. Y. Frissel. Influence of management and maintenance on erosive impact of wave overtopping on grass covered slopes of dikes; tests. In *Proc. FloodRisk*, pages 523–533, Oxford, UK, 2008. ISBN 978-0-415-48507-4.

TAW. Clay for dikes. Technical report, Technical Advisory Committee for Flood Defence in the Netherlands, Delft, The Netherlands, May 1996.

T. Q. Tuan. Characteristics of bermuda grass and carpet grass. Technical report, Water Resources University, Ha Noi, Viet Nam, August 2012.

J.W. van der Meer. Design, construction, calibration and use of the wave overtopping simulator. comcoast, workpackage 3: Development of alternative overtopping-resistant sea defences, phase 3. Final report, Infram and Royal Haskoning, Delft, The Netherlands, 2007.

J.W. van der Meer, W. Snijders, and E. Regeling. The wave overtopping simulator. In *ASCE, Proc. ICCE 2006*, San Diego, US, 2006.

J.W. van der Meer, G.J. Steendam, G. de Raat, and P. Bernardini. Further developments on the wave overtopping simulator. In *ASCE, Proc. ICCE 2008*, Hamburg, Germany, 2008.

J.W. van der Meer, R. Schrijver, B. Hardeman, A. van Hoven, H.J. Verheij, and G.J. Steendam. Guidance on erosion resistance of inner slopes of dikes from 3 years of testing with the wave overtopping simulator. In *ASCE, Proc. ICE 2009*, pages 4654–4666, Endinburgh, UK, 2009.

J.W. van der Meer, B. Hardeman, G.J. Steendam, H. Schüttrumpf, and H.J. Verheij. Flow depths and velocities at crest and inner slope of a dike, in theory and with the wave overtopping simulator. In *ASCE, Proc. 32nd ICCE*, Shanghai, China, 2010.

Soil classification for hydraulic engineering. Viet Nam Ministry of Science and Technology.

Appendix A

Dike slope profiles

A.1 Section YB1, figures

Caption of each table denotes the applied discharges and corresponding durations. For example, a table namely '60x6 + 80x6 + 100x2' means the profile was measured after 6 hours of 60, 6 hours of 80 and 2 hours of 100 l/s per m. The initial situations of the slopes are denoted '0x0'. Coordinate x = 0 at the dike crest and $y = 0$ at the left side wall (eyes to the Simulator).

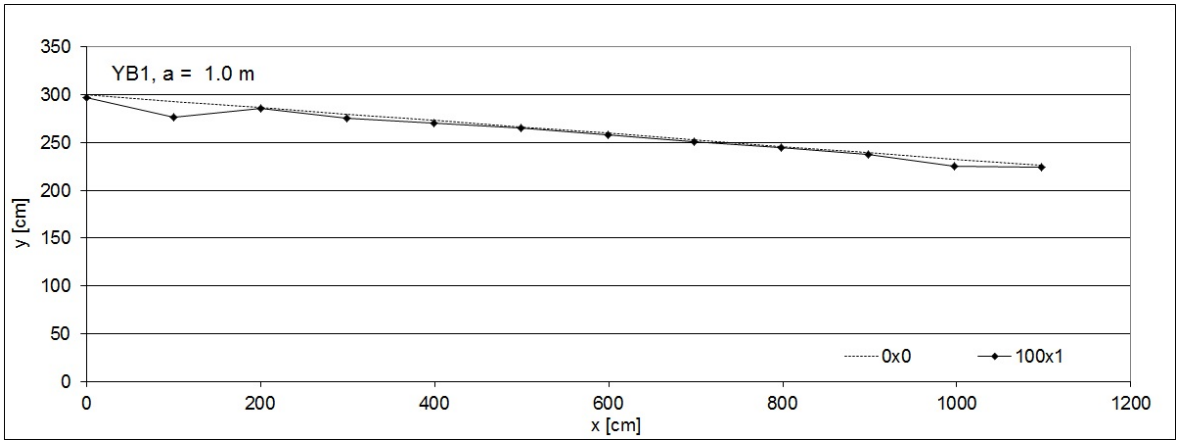

Figure A.1: Changes of slope profile induced by wave overtopping, $a = 1.0$ m, YB1.

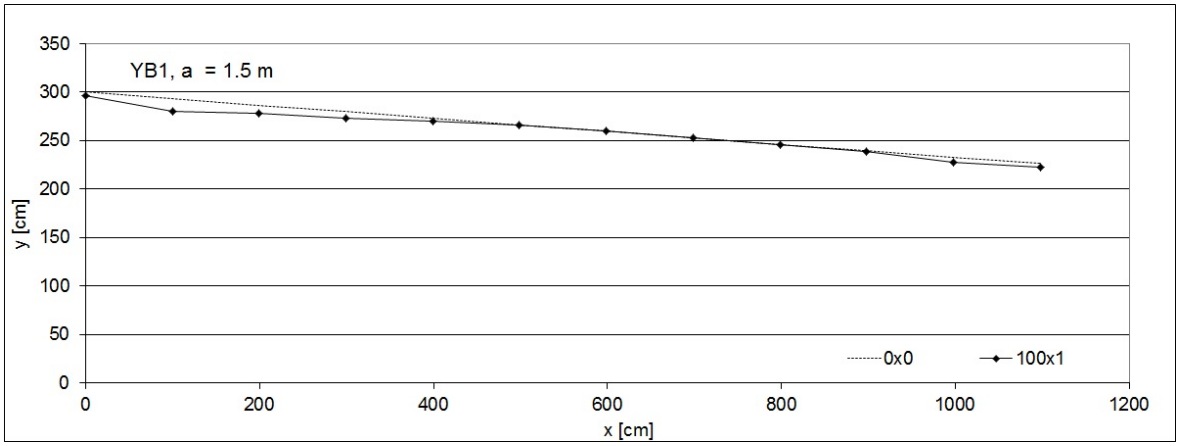

Figure A.2: Changes of slope profile induced by wave overtopping, $a = 1.5$ m, YB1.

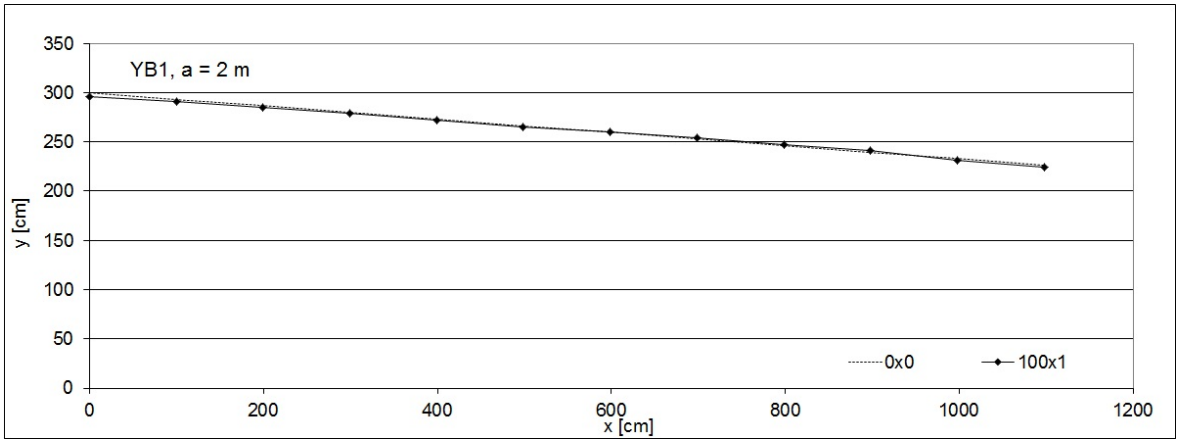

Figure A.3: Changes of slope profile induced by wave overtopping, $a = 2.0$ m, YB1.

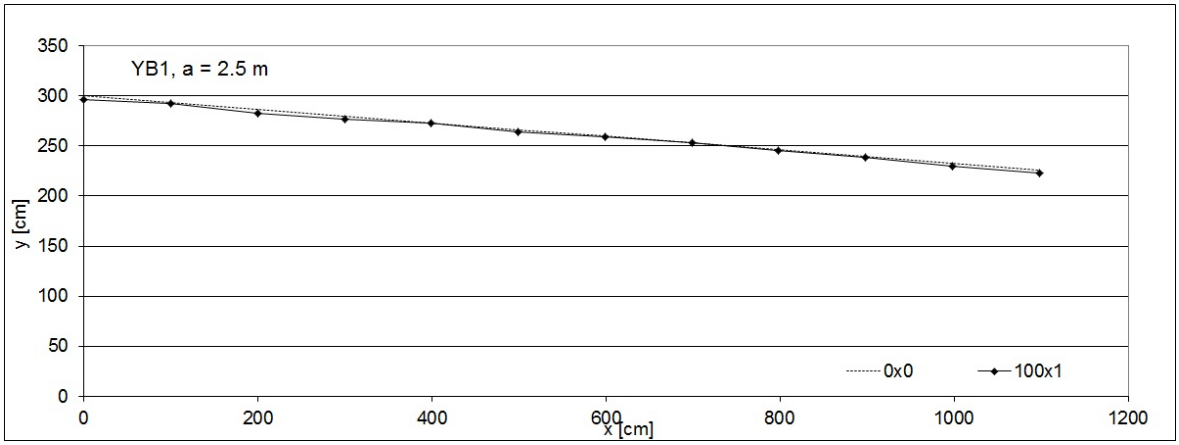

Figure A.4: Changes of slope profile induced by wave overtopping, $a = 2.5$ m, YB1.

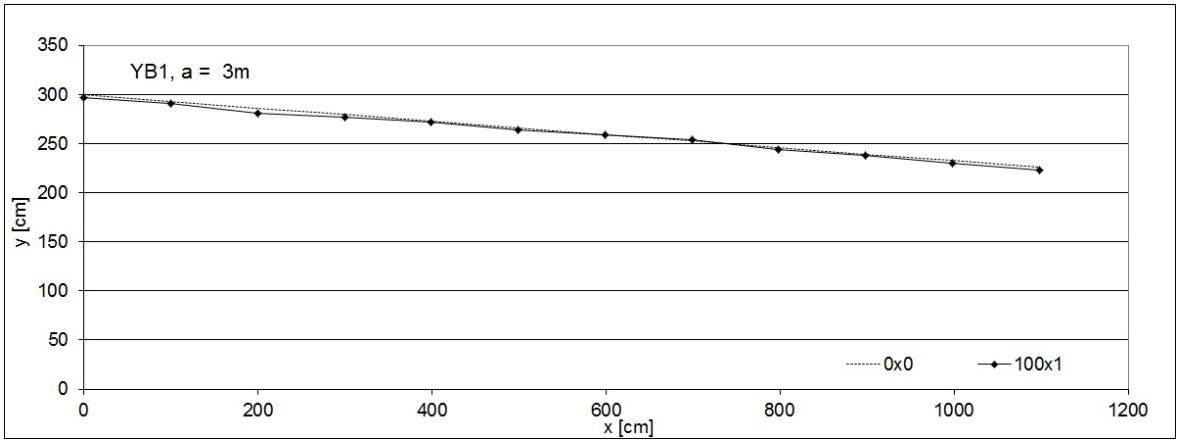

Figure A.5: Changes of slope profile induced by wave overtopping, $a = 3.0$ m, YB1.

A.2 Section YB2, figures

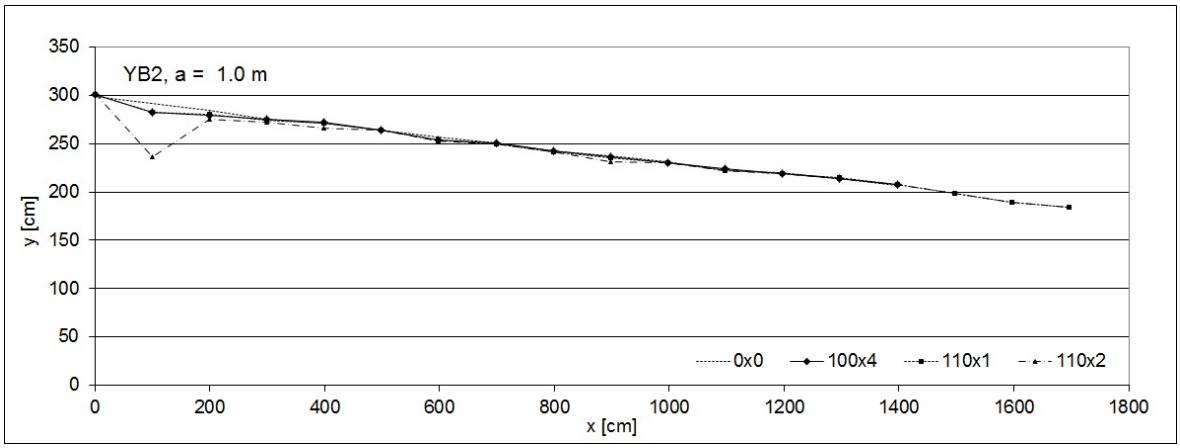

Figure A.6: Changes of slope profile induced by wave overtopping, $a = 1.0$ m, YB2.

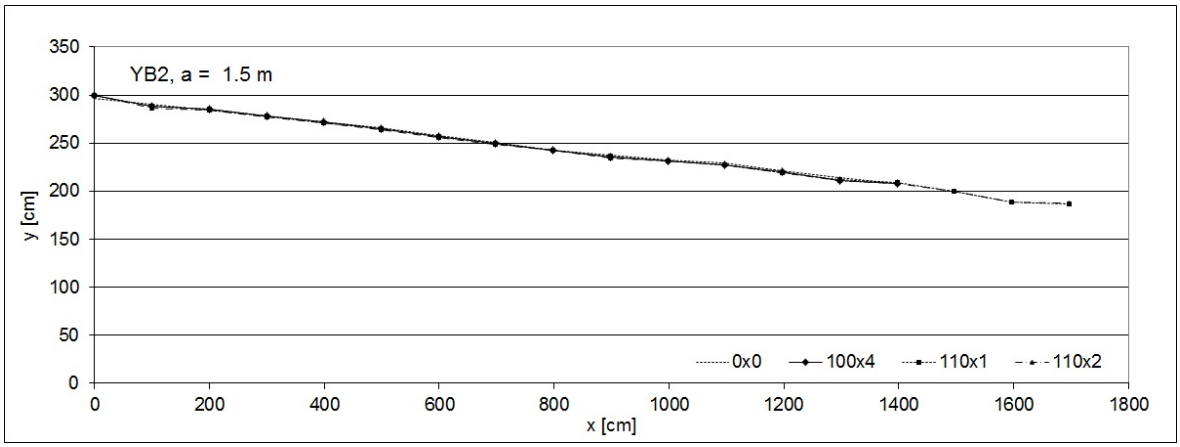

Figure A.7: Changes of slope profile induced by wave overtopping, $a = 1.5$ m, YB2.

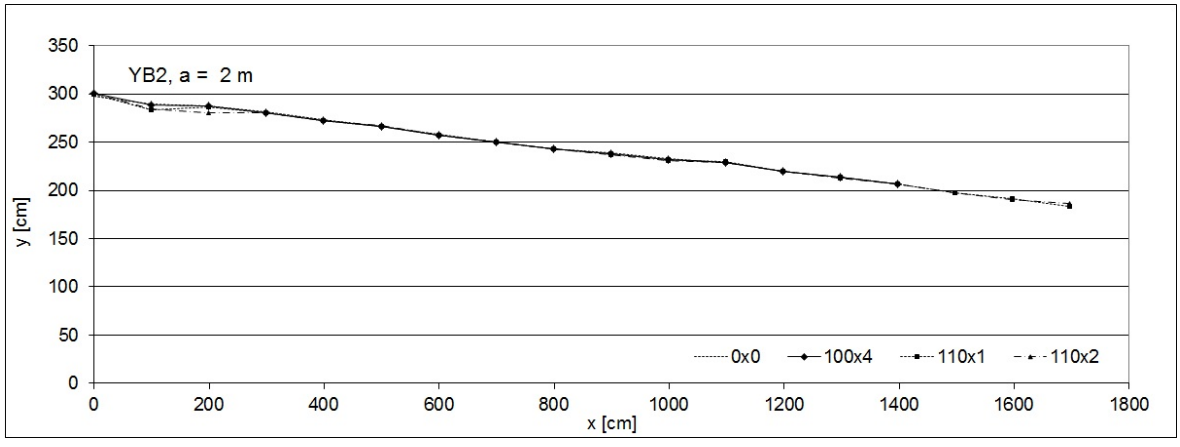

Figure A.8: Changes of slope profile induced by wave overtopping, $a = 2.0$ m, YB2.

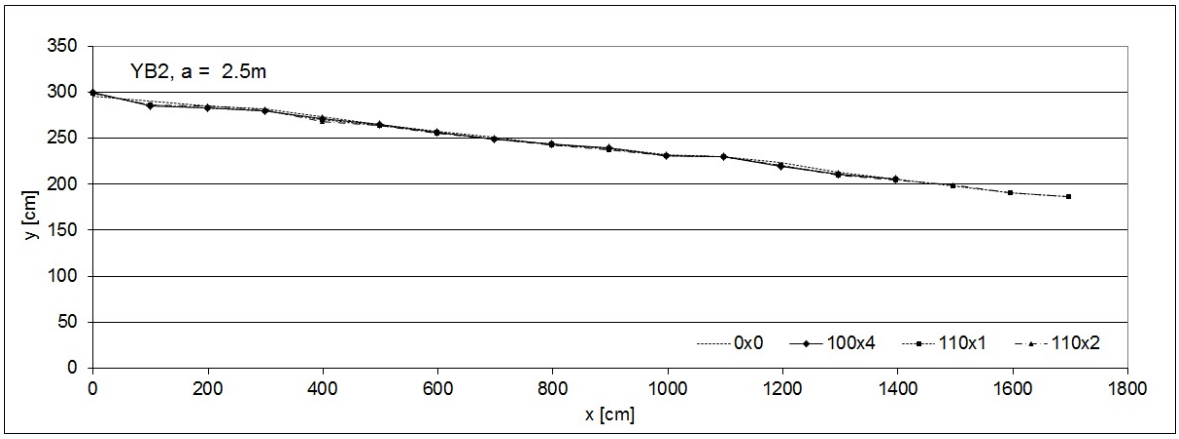

Figure A.9: Changes of slope profile induced by wave overtopping, $a = 2.5$ m, YB2.

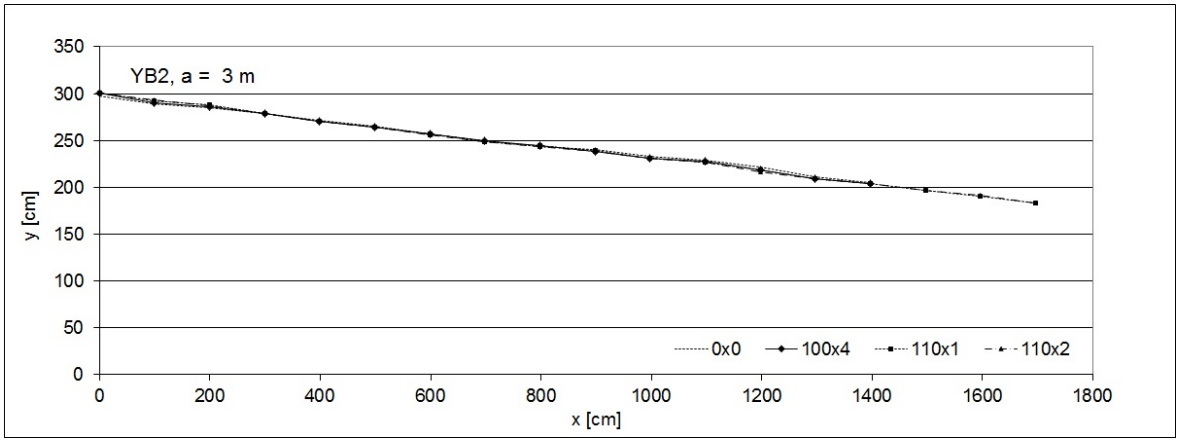

Figure A.10: Changes of slope profile induced by wave overtopping, $a = 3.0$ m, YB2.

A.3 Section YB3, figures

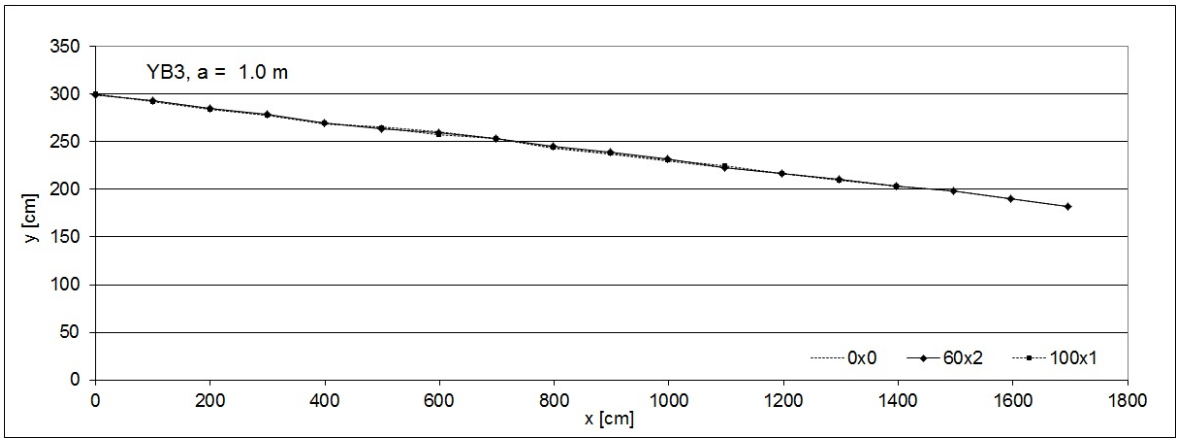

Figure A.11: Changes of slope profile induced by wave overtopping, $a = 1.0$ m, YB3.

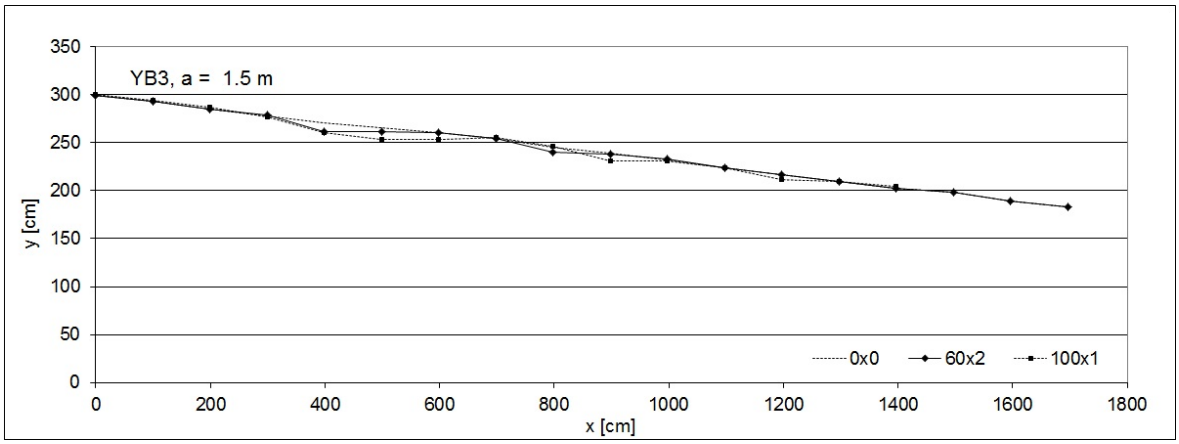

Figure A.12: Changes of slope profile induced by wave overtopping, $a = 1.5$ m, YB3.

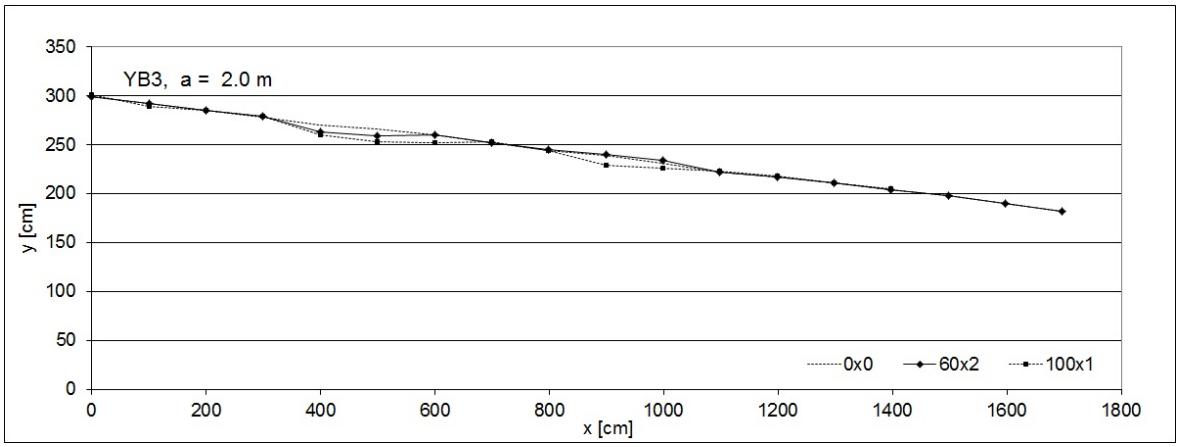

Figure A.13: Changes of slope profile induced by wave overtopping, $a = 2.0$ m, YB3.

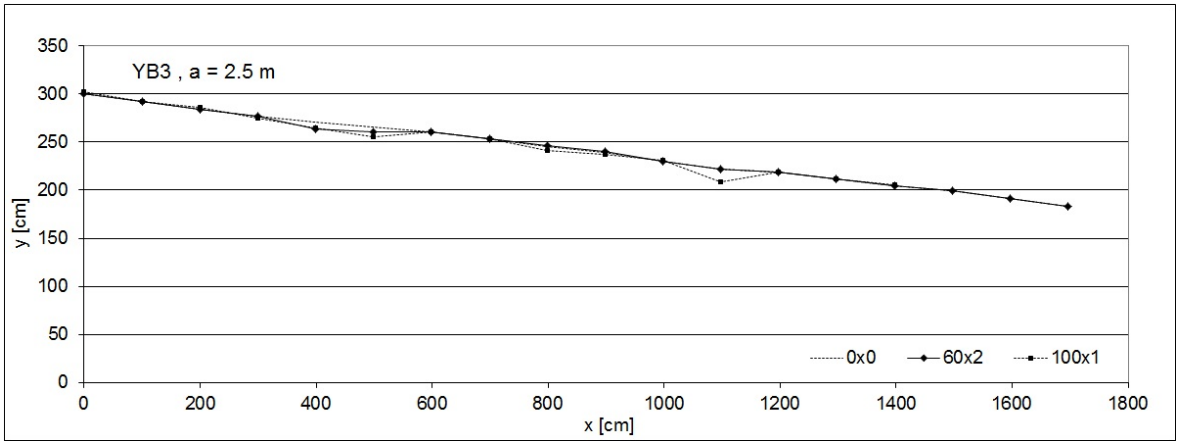

Figure A.14: Changes of slope profile induced by wave overtopping, $a = 2.5$ m, YB3.

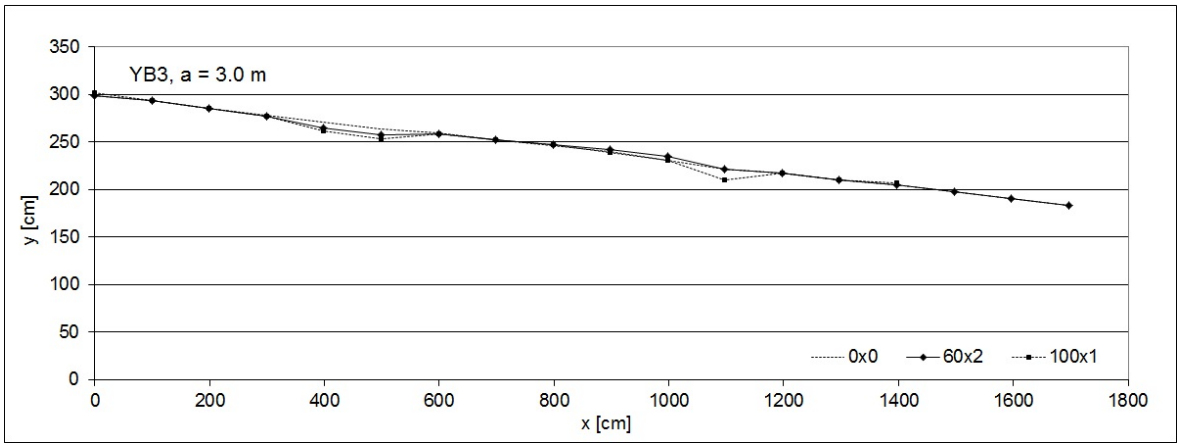

Figure A.15: Changes of slope profile induced by wave overtopping, $a = 3.0$ m, YB3.

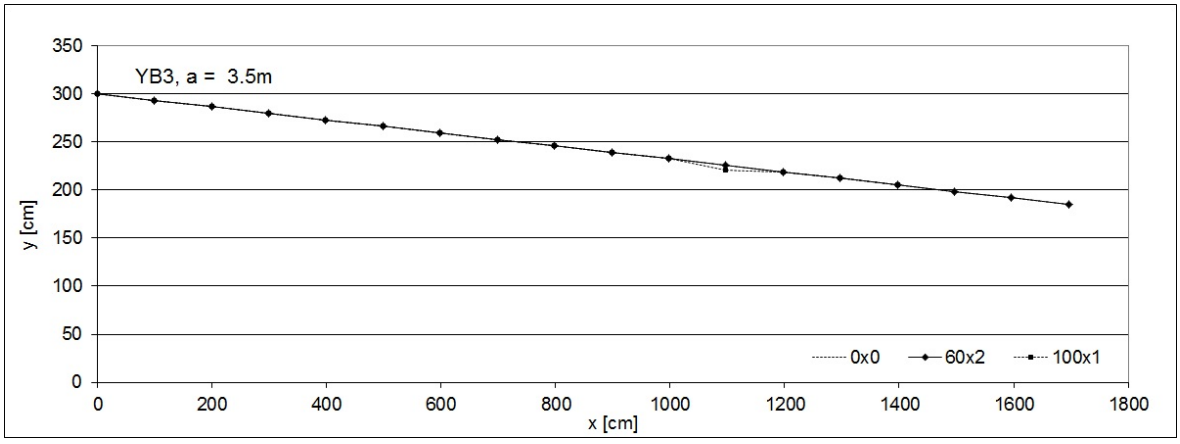

Figure A.16: Changes of slope profile induced by wave overtopping, $a = 3.5$ m, YB3.

A.4 Section YB4, figures

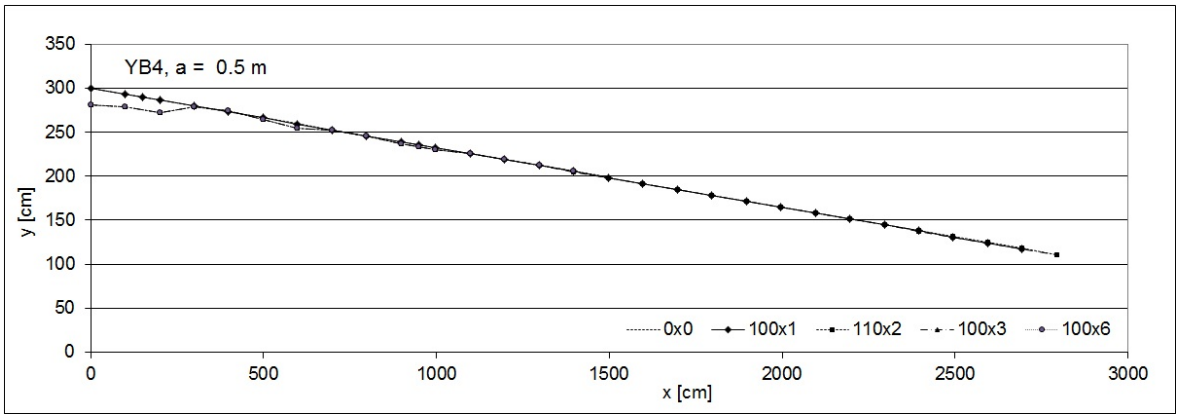

Figure A.17: Changes of slope profile induced by wave overtopping, $a = 0.5$ m, YB4.

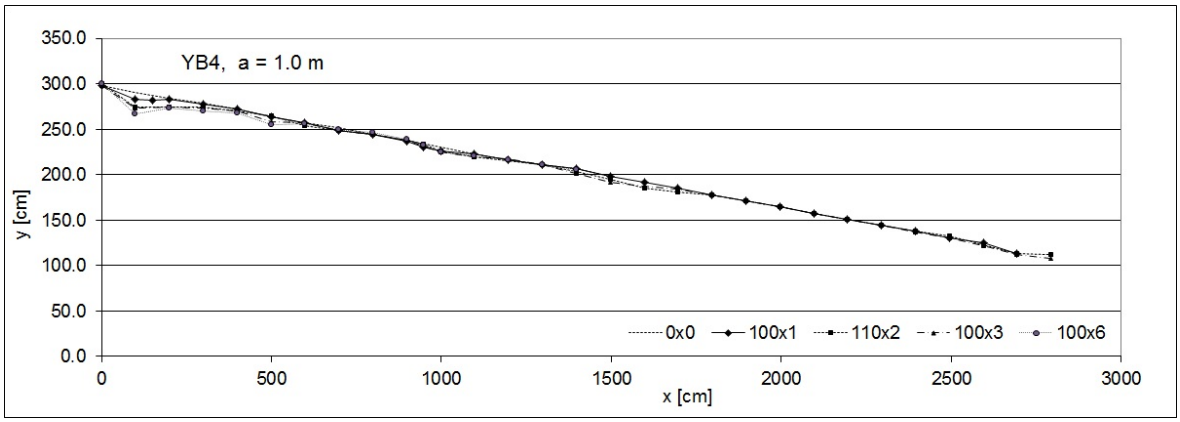

Figure A.18: Changes of slope profile induced by wave overtopping, $a = 1.0$ m, YB4.

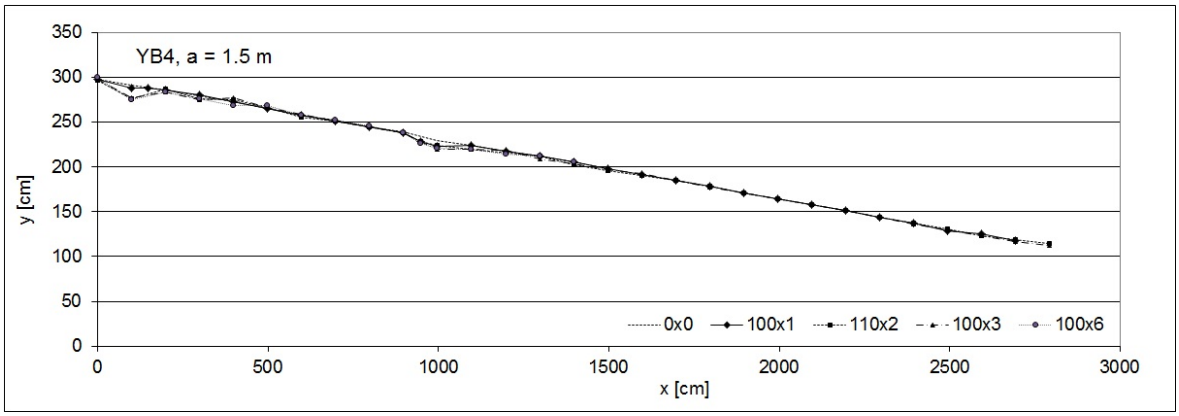

Figure A.19: Changes of slope profile induced by wave overtopping, $a = 1.5$ m, YB4.

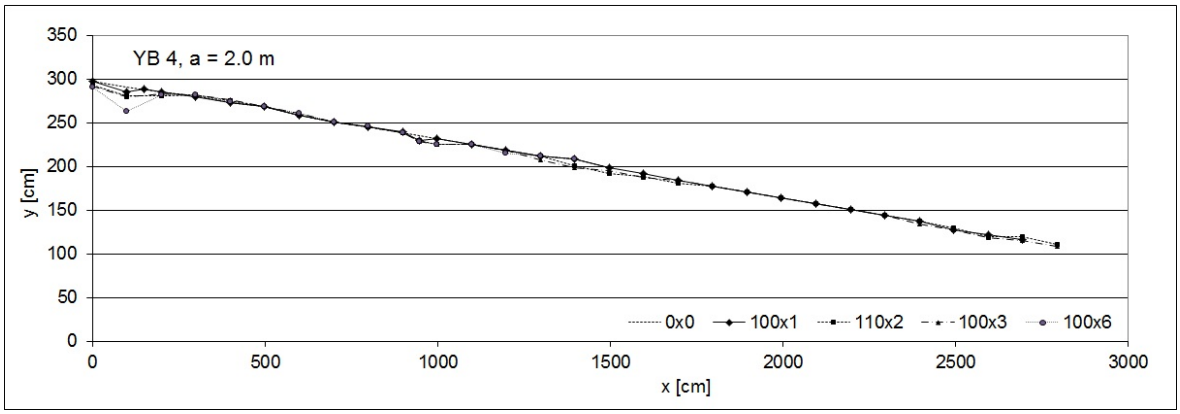

Figure A.20: Changes of slope profile induced by wave overtopping, $a = 2.0$ m, YB4.

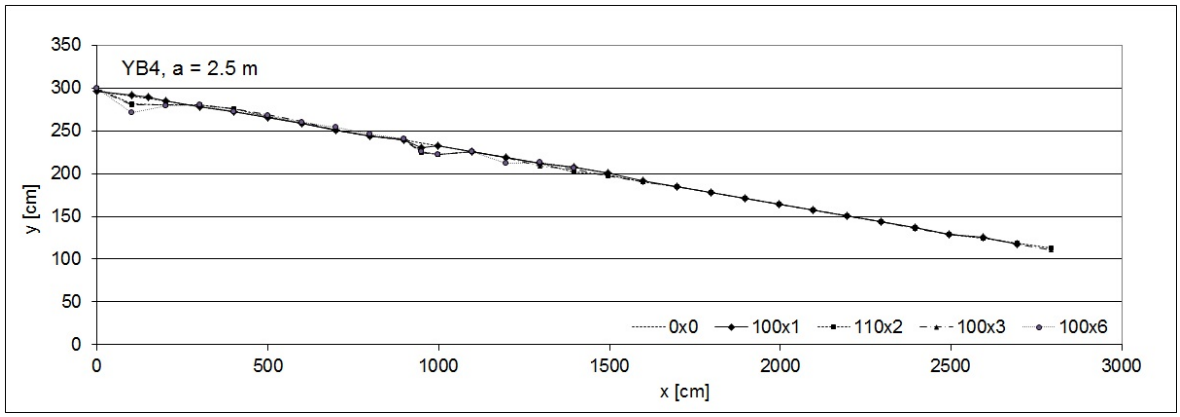

Figure A.21: Changes of slope profile induced by wave overtopping, $a = 2.5$ m, YB4.

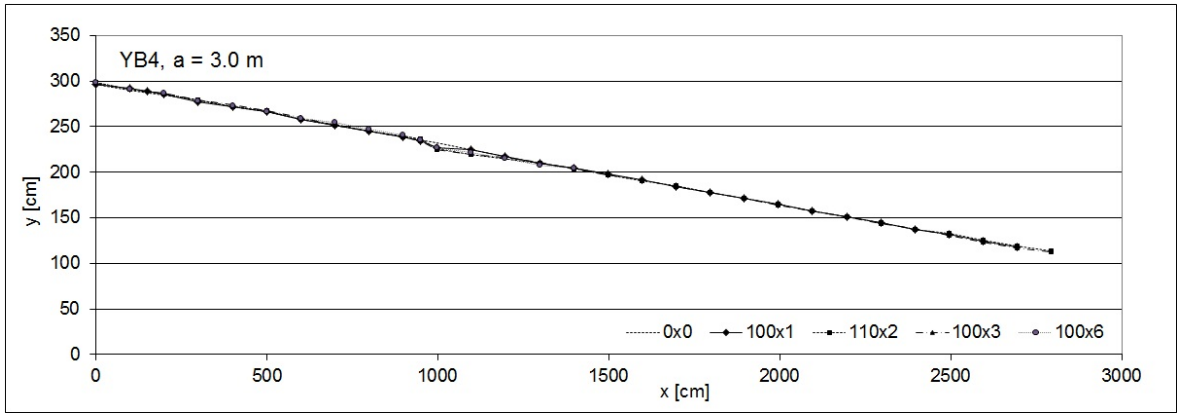

Figure A.22: Changes of slope profile induced by wave overtopping, $a = 3.0$ m, YB4.

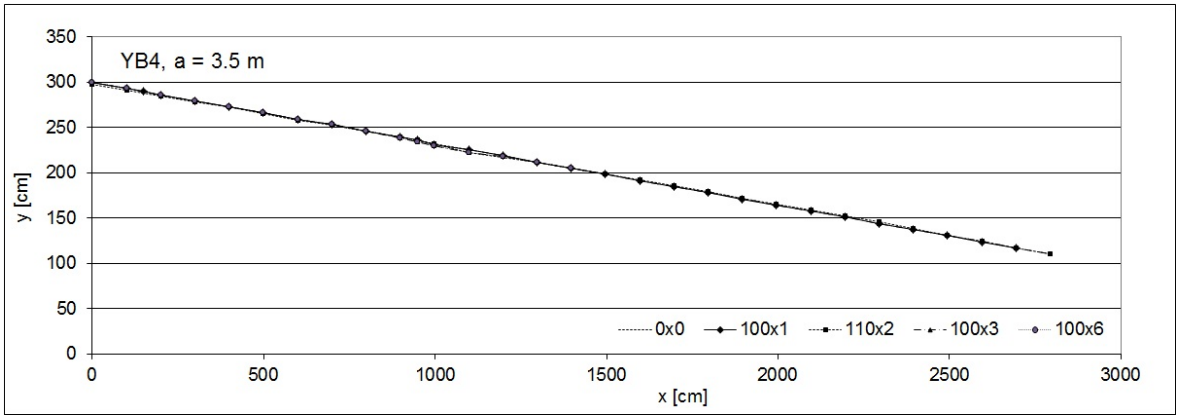

Figure A.23: Changes of slope profile induced by wave overtopping, $a = 3.5$ m, YB4.

A.5 Section YB1, measured data

Table A.1: YB1 slope profiles at 0x0, initial condition.

x [m]	y [m]				
	1.0	1.5	2.0	2.5	3.0
0	70.0	70.0	70.0	70.0	70.0
1	70.1	70.1	70.1	70.1	70.1
2	70.1	70.1	70.1	70.1	70.1
3	70.2	70.2	70.2	70.2	70.2
4	70.3	70.3	70.3	70.3	70.3
5	70.4	70.4	70.4	70.4	70.4
6	70.4	70.4	70.4	70.4	70.4
7	70.5	70.5	70.5	70.5	70.5
8	70.6	70.6	70.6	70.6	70.6
9	70.6	70.6	70.6	70.6	70.6
10	70.7	70.7	70.7	70.7	70.7
11	70.8	70.8	70.8	70.8	70.8

Table A.2: YB1 slope profiles after 60x3 + 80x1 + 100x1.

x [m]	y [m]				
	1.0	1.5	2.0	2.5	3.0
0	73.0	73.5	74.0	73.2	72.5
1	87.0	83.0	72.5	70.5	72.0
2	71.0	79.0	72.0	74.5	75.5
3	74.5	77.5	71.0	73.0	73.0
4	73.5	73.0	71.0	71.0	71.5
5	72.0	71.2	71.5	72.2	72.2
6	72.5	70.2	69.5	70.5	71.0
7	72.2	70.2	69.5	70.0	69.0
8	72.2	71.0	69.5	71.0	73.0
9	73.0	71.5	68.5	71.5	71.5
10	78.0	75.5	72.0	74.0	73.0
11	72.5	74.5	73.0	73.5	73.5

A.6 Section YB2, measured data

Table A.3: YB2 slope profiles at 0x0, initial condition.

x [m]	y [m]				
	1.0	1.5	2.0	2.5	3.0
0	71.5	73.5	72.0	74.5	73.0
1	72.0	72.5	74.0	73.5	73.8
2	72.1	72.0	69.5	71.5	71.5
3	74.5	71.5	69.0	68.5	71.5
4	72.0	71.0	70.0	70.5	71.5
5	72.3	71.0	71.0	72.0	72.0
6	73.5	72.0	71.5	72.5	73.0
7	73.0	73.2	73.5	72.6	74.0
8	74.5	74.0	73.8	74.0	73.0
9	73.0	73.0	71.0	71.0	70.0
10	72.0	71.0	71.0	71.0	70.5
11	74.5	68.0	67.5	66.5	68.5
12	70.0	69.0	70.0	67.0	69.0
13	70.0	70.0	70.0	71.0	72.0
14	70.0	69.0	70.0	71.0	71.5

Table A.4: YB2 slope profiles after 60x4 + 80x2 + 100x4.

x [m]	y [m]				
	1.0	1.5	2.0	2.5	3.0
0	69.0	70.5	69.0	70.5	69.0
1	81.0	74.5	74.5	78.0	73.0
2	77.0	71.5	69.5	73.5	71.0
3	74.5	71.5	70.0	70.0	71.5
4	71.5	71.5	71.0	72.5	72.5
5	72.2	72.0	70.5	72.2	72.2
6	76.0	73.2	72.5	74.0	73.5
7	73.0	73.5	73.5	74.0	74.0
8	74.5	74.0	73.5	73.5	72.5
9	74.0	74.5	72.0	71.0	72.0
10	73.5	72.0	72.0	73.0	72.5
11	73.0	69.5	67.5	67.0	69.5
12	71.0	70.5	70.5	70.5	71.5
13	69.5	73.0	69.5	72.5	74.0
14	69.5	68.5	70.0	71.5	73.5

Table A.5: YB2 slope profiles after 60x4 + 80x2 + 100x4 + 110x1.

x [m]	y [m]				
	1.0	1.5	2.0	2.5	3.0
0	69.0	70.0	70.0	71.0	69.5
1	80.5	74.5	80.0	77.0	71.5
2	76.0	71.0	70.0	73.5	68.5
3	76.0	71.5	69.5	70.5	71.5
4	72.0	72.5	71.5	73.5	72.5
5	72.5	72.0	70.5	72.5	72.5
6	76.0	73.0	72.7	74.2	73.5
7	74.0	74.2	73.5	74.5	75.0
8	75.0	74.0	73.5	73.5	72.5
9	74.5	74.0	72.0	71.5	70.5
10	72.7	72.2	72.0	73.0	72.2
11	73.2	69.5	67.2	66.7	70.5
12	71.0	71.2	70.0	70.0	71.7
13	69.0	72.0	70.0	72.5	74.5
14	69.0	68.0	70.5	71.2	73.5
15	71.5	70.0	73.0	72.0	73.5
16	74.0	74.5	72.5	73.0	73.0
17	72.7	70.0	73.5	71.0	74.0

Table A.6: YB2 slope profiles after 60x4 + 80x2 + 100x4 + 110x2.

x [m]	y [m]				
	1.0	1.5	2.0	2.5	3.0
0	68.5	69.5	69.0	71.0	69.0
1	127.0	77.5	79.0	77.5	70.5
2	81.0	72.2	76.2	72.2	70.0
3	78.0	73.0	69.5	69.0	71.0
4	77.5	72.5	71.2	75.5	72.5
5	73.0	72.5	70.0	72.5	72.5
6	77.0	74.2	73.0	74.5	74.5
7	73.5	74.5	73.5	74.5	74.5
8	75.0	74.0	74.0	74.0	73.0
9	78.5	75.5	73.0	72.5	72.2
10	73.5	72.5	72.5	73.0	73.0
11	75.0	70.0	68.5	67.0	70.0
12	71.5	71.2	70.7	69.5	73.5
13	69.5	72.5	71.0	73.5	74.0
14	69.5	69.0	70.0	72.5	73.5
15	72.0	70.5	73.0	71.0	73.5
16	74.5	75.0	73.0	72.5	72.5
17	72.5	69.5	71.0	71.0	73.5

A.7 Section YB3, measured data

Table A.7: YB3 slope profiles at 0x0, initial condition.

x [m]	y [m]					
	1.0	1.5	2.0	2.5	3.0	3.5
0	71.0	71.0	70.5	70.0	71.5	70.0
1	69.7	70.0	71.5	71.5	69.5	70.1
2	71.5	71.5	72.0	73.0	71.2	70.2
3	72.2	72.0	72.0	73.5	72.0	70.3
4	74.5	73.0	73.5	72.5	72.5	70.4
5	71.5	71.0	71.0	71.0	72.5	70.5
6	70.0	70.0	70.0	70.0	70.5	70.6
7	70.0	69.5	71.5	70.0	70.5	70.7
8	73.5	72.0	72.5	72.0	71.0	70.8
9	73.0	71.5	71.5	71.0	70.0	70.9
10	73.5	72.0	72.0	73.0	73.0	71.0
11	73.5	73.5	74.5	75.0	75.5	71.1
12	73.5	74.0	73.0	71.0	73.0	71.2
13	73.0	73.5	73.0	72.0	73.5	71.3
14	73.0	74.0	72.5	72.0	72.0	71.4
15	72.0	72.0	72.5	71.0	72.0	71.5
16	73.0	74.0	74.0	72.5	73.0	71.6
17	74.5	74.0	75.0	74.0	74.0	71.7

A.8 Section YB4, measured data

Table A.8: YB3 slope profiles after (60x4 + 80x6 + 100x10) with H_s 1.5 m + (40x1 + 60x2) with H_s 2.0 m.

x [m]	y [m]					
	1.0	1.5	2.0	2.5	3.0	3.5
0	71.0	71.0	70.5	70.0	71.5	70.0
1	69.7	70.0	71.5	71.5	69.5	70.1
2	71.5	71.5	72.0	73.0	71.2	70.2
3	71.5	71.0	70.5	73.0	72.5	70.3
4	74.0	82.0	80.7	80.0	79.0	70.4
5	73.5	75.5	77.5	76.5	79.0	70.5
6	71.0	70.0	70.0	70.0	71.0	70.6
7	70.0	69.5	71.5	70.0	70.5	70.7
8	71.5	76.5	71.5	70.5	69.0	70.8
9	71.5	72.5	70.0	69.5	68.5	70.9
10	71.5	70.5	69.5	73.0	68.2	71.0
11	73.5	73.5	74.5	75.0	75.5	71.1
12	73.5	74.0	73.0	71.0	73.0	71.2
13	73.0	73.5	73.0	72.0	73.5	71.3
14	73.0	74.0	72.5	72.0	72.0	71.4
15	72.0	72.0	72.5	71.0	72.0	71.5
16	73.0	74.0	74.0	72.5	73.0	71.6
17	74.5	74.0	75.0	74.0	74.0	71.7

Table A.9: YB3 slope profiles after (60x4 + 80x6 + 100x10) with H_s 1.5 m + (40x1 + 60x2 + 80x2 + 100x1) with H_s 2.0 m.

x [m]	y [m]					
	1.0	1.5	2.0	2.5	3.0	3.5
0	70.0	69.5	68.5	68.0	68.5	70.0
1	71.0	69.5	74.5	71.0	70.0	70.1
2	73.2	70.0	71.5	71.0	71.0	70.2
3	72.0	73.0	71.2	75.0	73.0	70.3
4	74.0	83.0	83.0	79.0	81.5	70.4
5	72.0	83.5	83.5	81.0	83.0	70.5
6	72.5	77.0	77.5	70.0	71.5	70.6
7	70.0	68.5	70.0	70.0	71.0	70.7
8	73.0	71.0	72.5	76.0	70.0	70.8
9	72.5	79.0	81.5	73.0	71.0	70.9
10	73.0	72.5	77.0	72.0	73.0	71.0
11	71.5	73.5	74.0	88.0	87.0	76.5
12	73.5	79.0	72.5	71.0	72.5	71.3
13	73.5	74.0	72.5	72.0	73.0	71.4
14	73.5	72.0	71.5	71.0	70.0	71.5

Table A.10: YB4 slope profiles at 0x0, initial condition.

x [m]	y [m]						
	0.5	1.0	1.5	2.0	2.5	3.0	3.5
0.0	70.0	72.0	72.0	72.0	73.0	74.0	70.0
1.0	70.1	73.0	72.5	72.0	73.0	73.5	70.1
2.0	70.2	73.0	71.0	71.5	72.0	72.0	70.2
3.0	70.3	71.0	71.0	69.0	71.5	71.0	70.3
4.0	70.4	71.0	71.0	70.0	71.0	72.0	70.4
5.0	70.5	73.0	71.5	68.5	70.5	70.5	70.5
6.0	70.6	73.2	73.0	71.0	71.5	72.5	70.6
7.0	70.7	72.0	71.0	72.0	72.0	70.5	70.7
8.0	70.8	73.0	72.5	71.5	72.5	72.0	70.8
9.0	70.9	72.2	71.5	71.5	70.5	71.0	70.9
10.0	71.0	73.5	74.0	71.5	70.5	71.0	71.0
11.0	71.1	73.5	72.5	71.5	70.5	72.0	71.1
12.0	71.2	74.0	73.0	71.0	71.5	73.0	71.2
13.0	71.3	73.0	72.0	72.0	71.5	74.0	71.3
14.0	71.4	70.5	71.0	68.5	69.0	72.0	71.4
15.0	71.5	72.0	72.5	72.0	70.0	72.0	71.5

Table A.11: YB4 slope profiles after 40x2 + 60x6 + 80x6 + 100x1.

x [m]	y [m]						
	0.5	1.0	1.5	2.0	2.5	3.0	3.5
0.0	70.0	72.0	72.0	72.0	73.0	74.0	70.0
1.0	70.1	80.0	75.0	78.0	71.0	71.5	70.1
1.5	70.2	78.5	72.0	71.5	70.5	71.0	70.2
2.0	70.3	74.0	70.5	71.5	71.5	71.5	70.3
3.0	70.4	72.5	70.0	70.0	71.5	73.0	70.4
4.0	70.5	71.0	71.0	70.0	71.0	72.0	70.4
5.0	70.6	73.0	71.5	68.5	70.5	70.5	70.5
6.0	70.7	73.2	73.0	71.0	71.5	72.5	70.6
7.0	70.8	74.5	72.5	72.5	72.5	71.5	70.0
8.0	70.9	73.0	72.5	71.5	72.5	72.0	70.8
9.0	71.0	73.0	72.0	70.5	70.5	71.0	70.8
9.5	71.1	76.5	79.0	77.5	76.0	72.0	70.8
10.0	71.2	77.5	81.0	71.5	70.5	77.0	72.5
11.0	71.3	73.5	72.5	71.5	70.5	72.0	71.1
12.0	71.4	74.0	73.0	71.0	71.5	73.0	71.2
13.0	71.5	73.0	72.0	72.0	71.5	74.0	71.3
14.0	71.6	70.5	71.0	68.5	69.0	72.0	71.4
15.0	71.7	72.0	72.5	72.0	70.0	72.0	71.5
16.0	71.8	72.1	72.1	72.1	72.1	72.1	72.1
17.0	71.9	72.2	72.2	72.2	72.2	72.2	72.2
18.0	72.0	72.3	72.3	72.3	72.3	72.3	72.3
19.0	72.1	72.4	72.4	72.4	72.4	72.4	72.4
20.0	72.2	72.5	72.5	72.5	72.5	72.5	72.5
21.0	72.3	72.6	72.6	72.6	72.6	72.6	72.6
22.0	72.4	72.7	72.7	72.7	72.7	72.7	72.7
23.0	72.5	72.8	72.8	72.8	72.8	72.8	72.8
24.0	72.6	72.9	72.9	72.9	72.9	72.9	72.9
25.0	72.7	73.0	75.0	76.0	75.0	71.5	73.0
26.0	72.8	72.0	71.5	75.5	71.0	72.5	73.1
27.0	72.9	77.0	73.0	74.0	72.5	72.5	73.2

Table A.12: YB4 slope profiles at 40x2 + 60x6 + 80x6 + 100x2.

x [m]	y [m]						
	0.5	1.0	1.5	2.0	2.5	3.0	3.5
0.0	88.5	70.0	73.0	76.5	70.0	72.0	72.5
1.0	84.5	89.5	87.0	82.0	81.5	72.0	72.0
2.0	84.5	82.5	70.0	76.0	76.0	71.0	72.0
3.0	71.5	76.0	74.5	68.0	69.5	70.5	71.5
4.0	69.0	73.5	69.0	68.5	68.0	71.5	70.5
5.0	72.5	72.0	71.0	68.5	70.0	69.5	71.0
6.0	76.0	76.5	75.0	71.0	71.5	72.0	72.5
7.0	70.7	74.5	72.5	72.5	72.5	71.5	70.0
8.0	70.9	73.0	72.5	71.5	72.5	72.0	70.8
9.0	73.5	72.0	72.0	71.0	70.0	70.0	70.0
9.5	73.5	73.5	79.0	77.5	81.0	70.0	70.5
10.0	73.5	77.0	80.0	77.6	81.0	77.5	71.5
11.0	71.3	77.0	77.5	71.5	70.5	77.5	74.0
13.0	71.5	73.0	72.0	72.0	71.5	74.0	71.3
14.0	71.6	73.0	74.5	76.5	75.0	72.5	71.3
15.0	71.7	75.5	74.0	78.5	72.0	73.5	71.3
16.0	71.8	78.5	73.5	75.0	72.5	73.0	71.3
17.0	71.9	76.0	71.5	75.5	72.5	71.5	71.3
18.0	72.0	72.3	72.3	72.3	72.3	72.3	71.3
19.0	72.1	72.4	72.4	72.4	72.4	72.4	71.3
20.0	72.2	72.5	72.5	72.5	72.5	72.5	71.3
21.0	72.3	72.6	72.6	72.6	72.6	72.6	71.3
22.0	72.4	72.7	72.7	72.7	72.7	72.7	71.3
23.0	72.5	72.8	72.8	72.8	72.8	72.8	71.3
24.0	72.6	72.9	72.9	72.9	72.9	72.9	71.3
25.0	72.0	71.5	72.5	73.5	74.5	71.0	73.0
26.0	72.0	74.0	73.5	77.0	72.5	71.5	73.0
27.0	72.0	77.0	72.0	71.0	72.0	71.0	73.0
28.0	73.0	72.0	69.0	73.0	71.0	70.5	73.0

Table A.13: YB4 slope profiles at 40x2 + 60x6 + 80x6 + 100x3.

x [m]	y [m]						
	0.5	1.0	1.5	2.0	2.5	3.0	3.5
0.0	88.5	72.0	72.0	78.0	71.5	72.5	70.0
1.0	84.5	90.5	86.5	84.0	82.5	72.0	70.1
2.0	84.5	82.5	73.0	73.2	76.0	70.0	70.2
3.0	71.5	77.0	75.0	68.0	70.0	71.0	70.3
4.0	69.0	73.5	66.5	66.5	67.5	69.0	70.4
5.0	72.5	79.0	70.5	68.0	68.0	69.5	70.5
6.0	76.0	73.0	71.5	69.0	69.5	70.0	70.6
7.0	70.7	74.5	72.5	72.5	72.5	71.5	70.0
8.0	70.9	73.0	72.5	71.5	72.5	72.0	70.8
9.0	73.5	72.5	72.5	71.5	70.5	71.0	72.0
9.5	73.5	75.5	79.0	78.5	82.0	72.0	72.5
10.0	73.5	79.0	83.5	77.6	81.0	79.0	73.0
11.0	71.3	77.0	77.5	71.5	70.5	77.5	74.0
12.0	71.5	73.0	72.0	72.0	71.5	74.0	71.5
13.0	71.6	73.0	74.5	76.5	75.0	72.5	71.6
14.0	71.7	75.5	74.0	78.5	72.0	73.5	71.7
15.0	71.8	78.5	73.5	75.0	72.5	73.0	71.8
16.0	71.9	76.0	71.5	75.5	72.5	71.5	71.9
17.0	72.0	72.3	72.3	72.3	72.3	72.3	72.0
18.0	72.1	72.4	72.4	72.4	72.4	72.4	72.1
19.0	72.2	72.5	72.5	72.5	72.5	72.5	72.2
20.0	72.3	72.6	72.6	72.6	72.6	72.6	72.3
21.0	72.4	72.7	72.7	72.7	72.7	72.7	72.4
22.0	72.5	72.8	72.8	72.8	72.8	72.8	72.5
23.0	72.6	72.9	72.9	72.9	72.9	72.9	72.6
24.0	72.7	73.0	74.5	76.5	75.0	72.5	72.7
25.0	72.8	73.0	74.5	76.5	75.0	72.5	72.8
26.0	72.9	75.5	74.0	78.5	72.0	73.5	72.9
27.0	73.0	78.5	73.5	75.0	72.5	73.0	73.0
28.0	73.0	76.0	71.5	75.5	72.5	71.5	73.0

Table A.14: YB4 slope profiles at 40x2 + 60x6 + 80x6 + 100x6.

x [m]	y [m]						
	0.5	1.0	1.5	2.0	2.5	3.0	3.5
0.0	88.5	70.0	70.0	79.5	70.0	71.2	70.0
1.0	84.5	96.5	88.0	100.0	92.0	72.5	70.1
2.0	84.5	83.5	73.0	74.5	77.5	70.0	70.2
3.0	71.5	80.5	74.5	68.0	70.0	71.5	70.3
4.0	69.0	75.5	75.5	69.0	71.0	71.0	70.4
5.0	72.5	82.0	68.5	68.0	68.5	70.5	70.5
6.0	76.0	74.0	72.0	69.0	70.0	71.0	70.6
7.0	70.7	73.5	71.0	72.0	69.0	68.5	70.0
.0	70.9	70.0	71.0	70.0	70.0	69.5	70.8
9.0	73.5	71.5	72.0	71.0	69.5	69.5	71.0
9.5	73.5	74.0	81.0	78.5	80.5	71.5	72.5
10.0	73.5	78.5	82.5	77.6	81.0	76.5	73.0
11.0	71.3	76.0	77.0	71.5	70.5	75.0	74.0
12.0	71.5	74.0	75.5	74.5	78.0	74.5	71.5
13.0	71.6	72.5	71.5	71.0	70.5	76.0	71.6
14.0	71.6	71.0	71.5	68.0	70.5	72.0	71.7

Appendix B

Photographs of the 1/15 grass covered slopes

The appendix B contents of all photographs of the four slope sections at different moments during the tests illustrating the erosion development due to wave overtopping. Caption of each figure denotes the applied discharges and corresponding durations. For example, a figure namely '60x6 + 80x6 + 100x2' means the photograph was taken after 6 hours of 60, 6 hours of 80 and 2 hours of 100 l/s per m. The initial situations of the slopes are denoted '0x0'. The whole slope sections can be split into two or three consecutive parts as the photographs' lengths exceed the paper size.

B.1 Section YB1

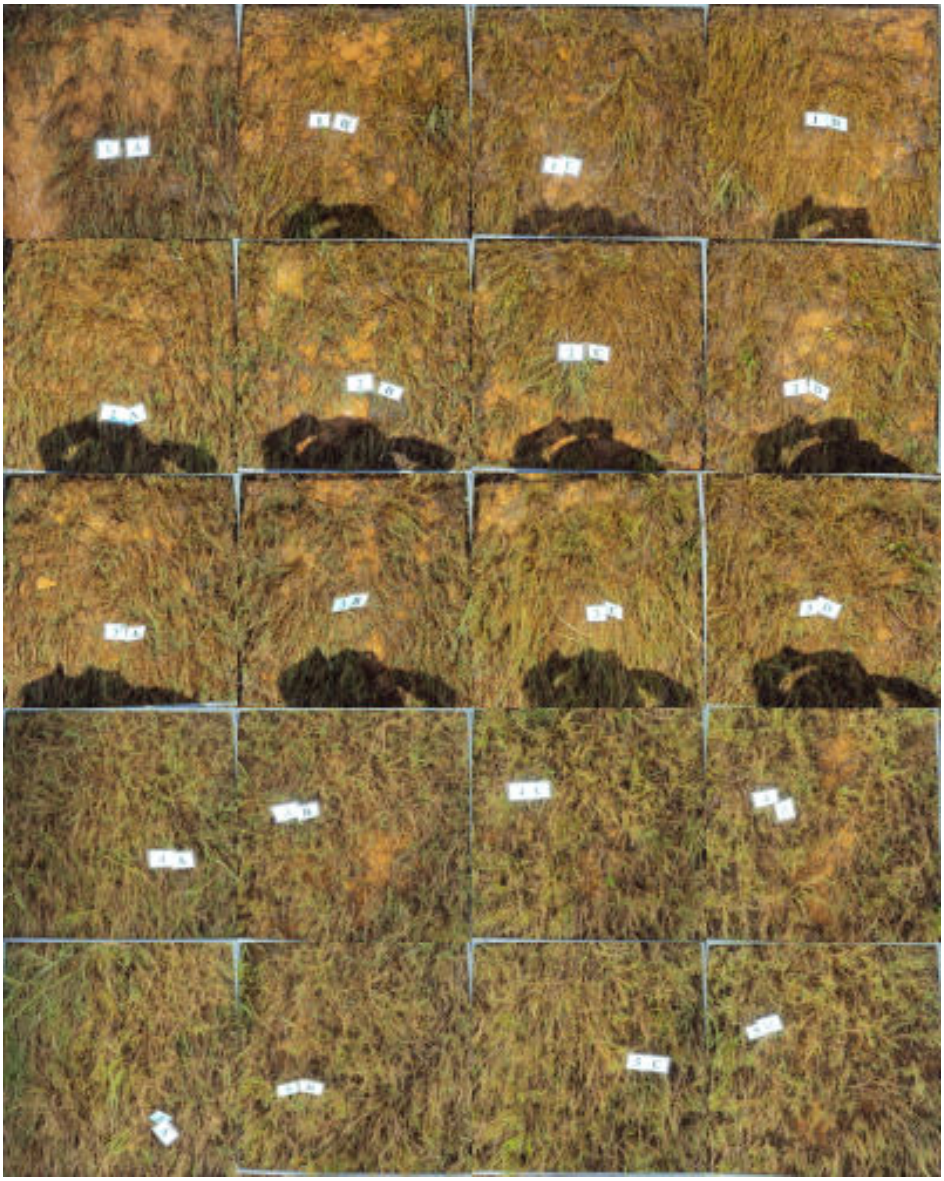

Figure B.1: 60x1, 1 to 5 m from the dike crest, section YB1.

Figure B.2: 60x1, 6 to 11 m from the dike crest, section YB1.

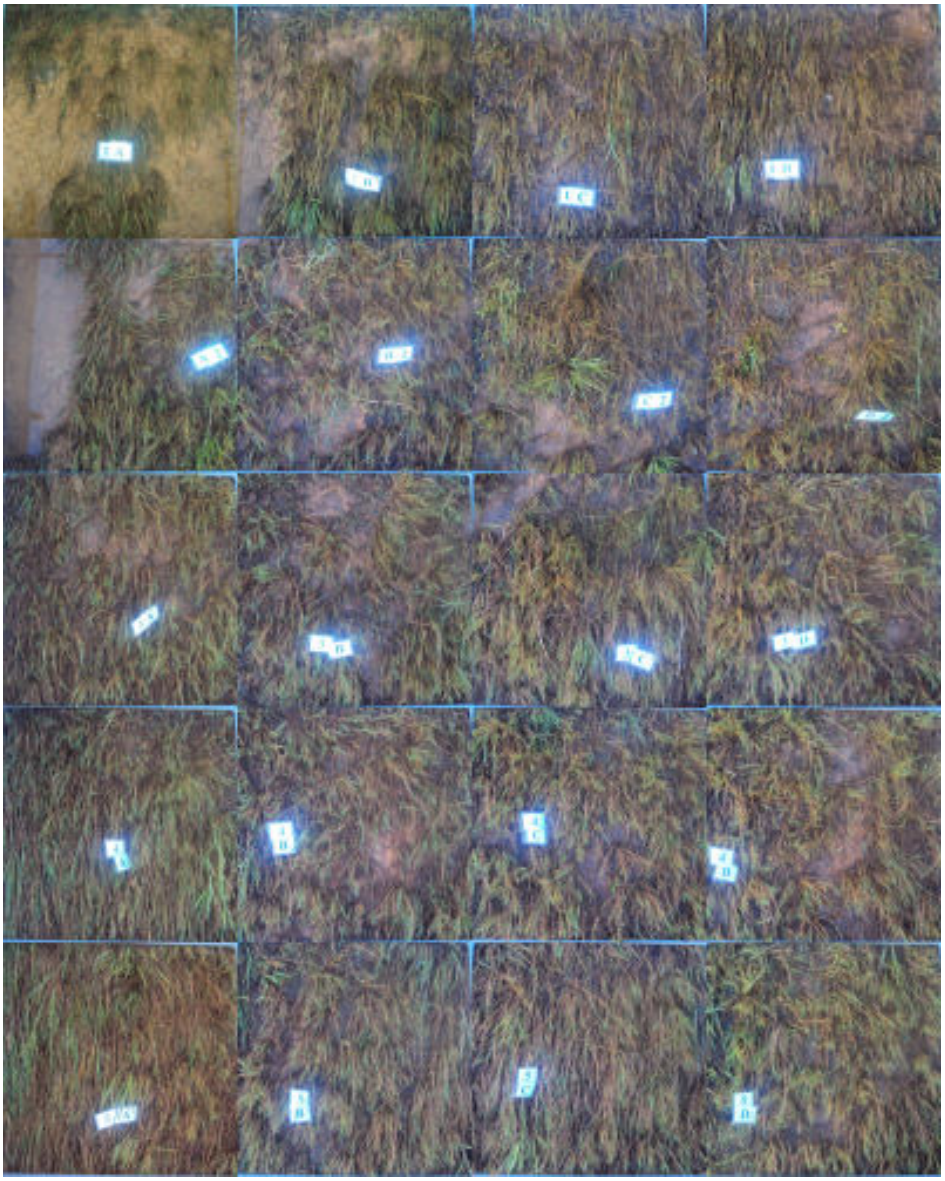

Figure B.3: 60x2, 1 to 5 m from the dike crest, section YB1.

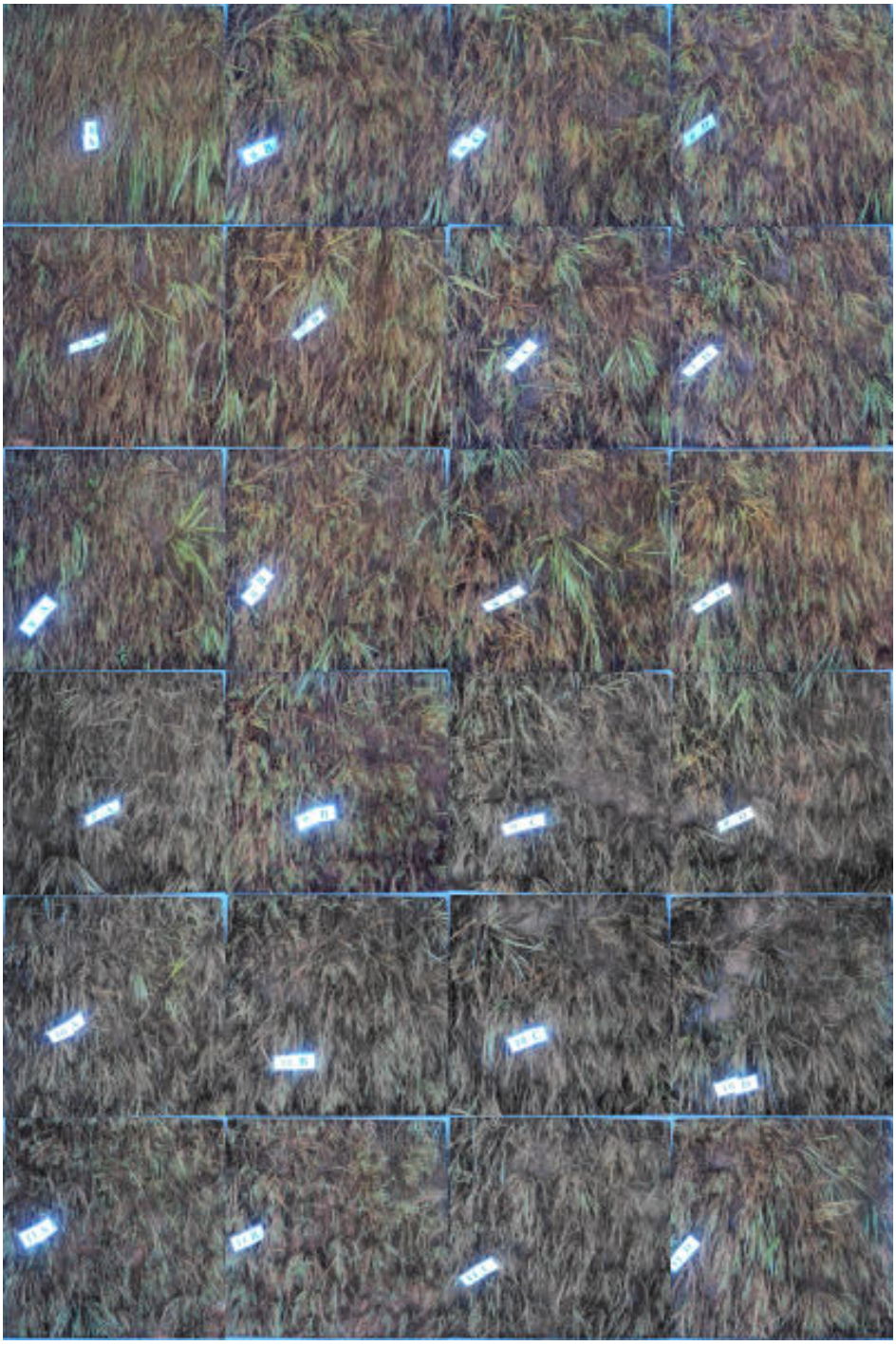

Figure B.4: 60x2, 6 to 11 m from the dike crest, section YB1.

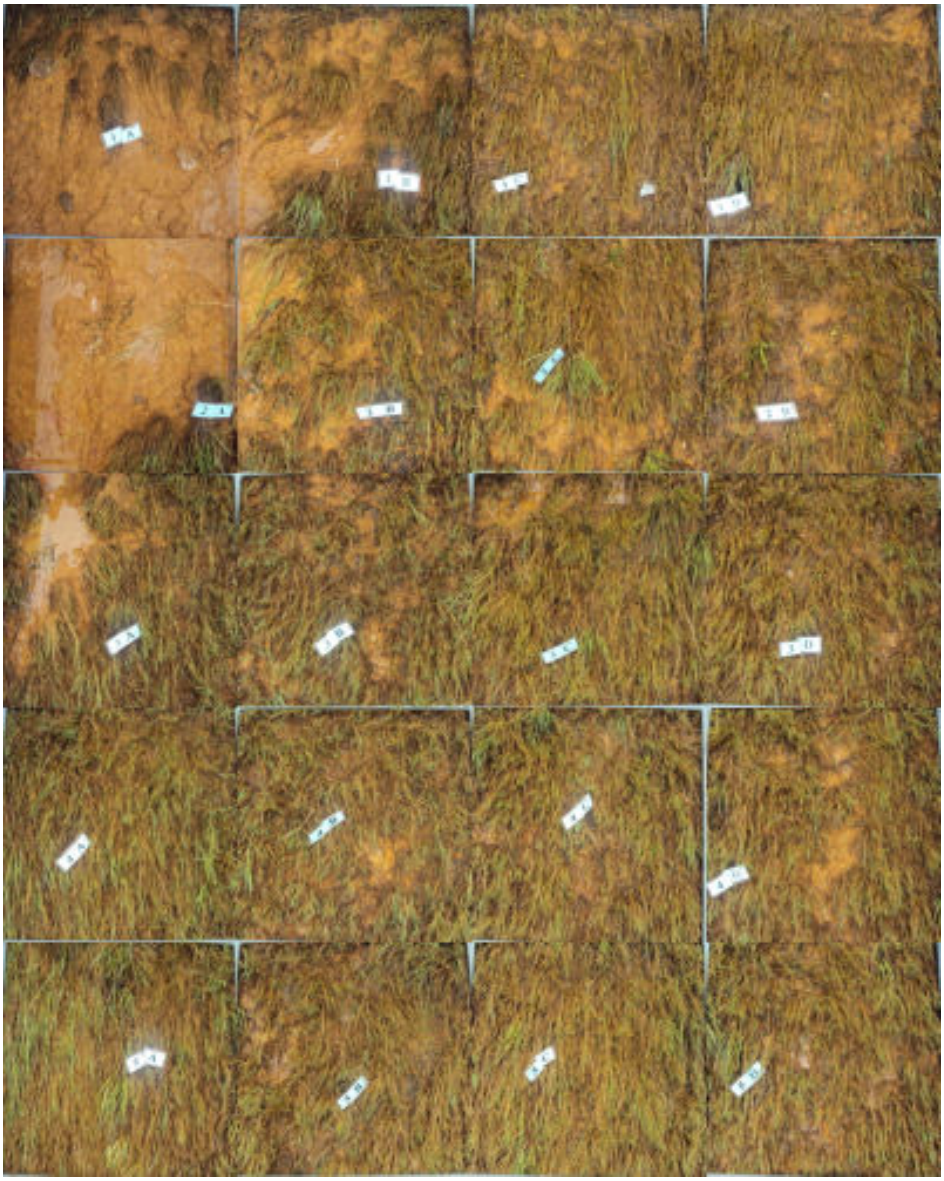

Figure B.5: 60x3, 1 to 5 m from the dike crest, section YB1.

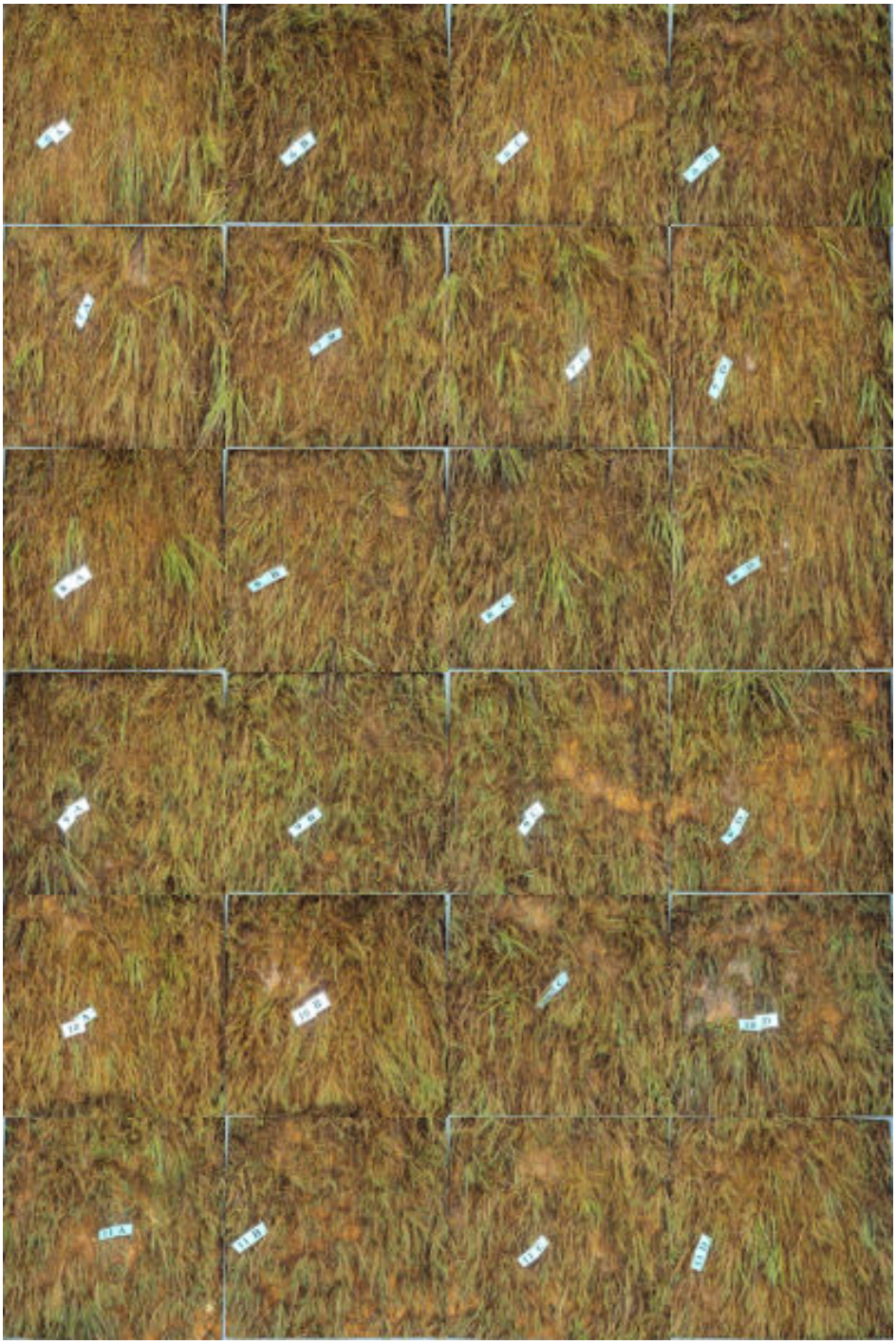

Figure B.6: 60x3, 6 to 11 m from the dike crest, section YB1.

Figure B.7: 60x3 + 100x1, 1 to 5 m from the dike crest, section YB1.

Figure B.8: 100x1, 6 to 11 m from the dike crest, section YB1.

B.2 Section YB2

Figure B.9: 0x0, 1 to 7 m from the dike crest, section YB2.

Figure B.10: 0x0, 8 to 14 m from the dike crest, section YB2.

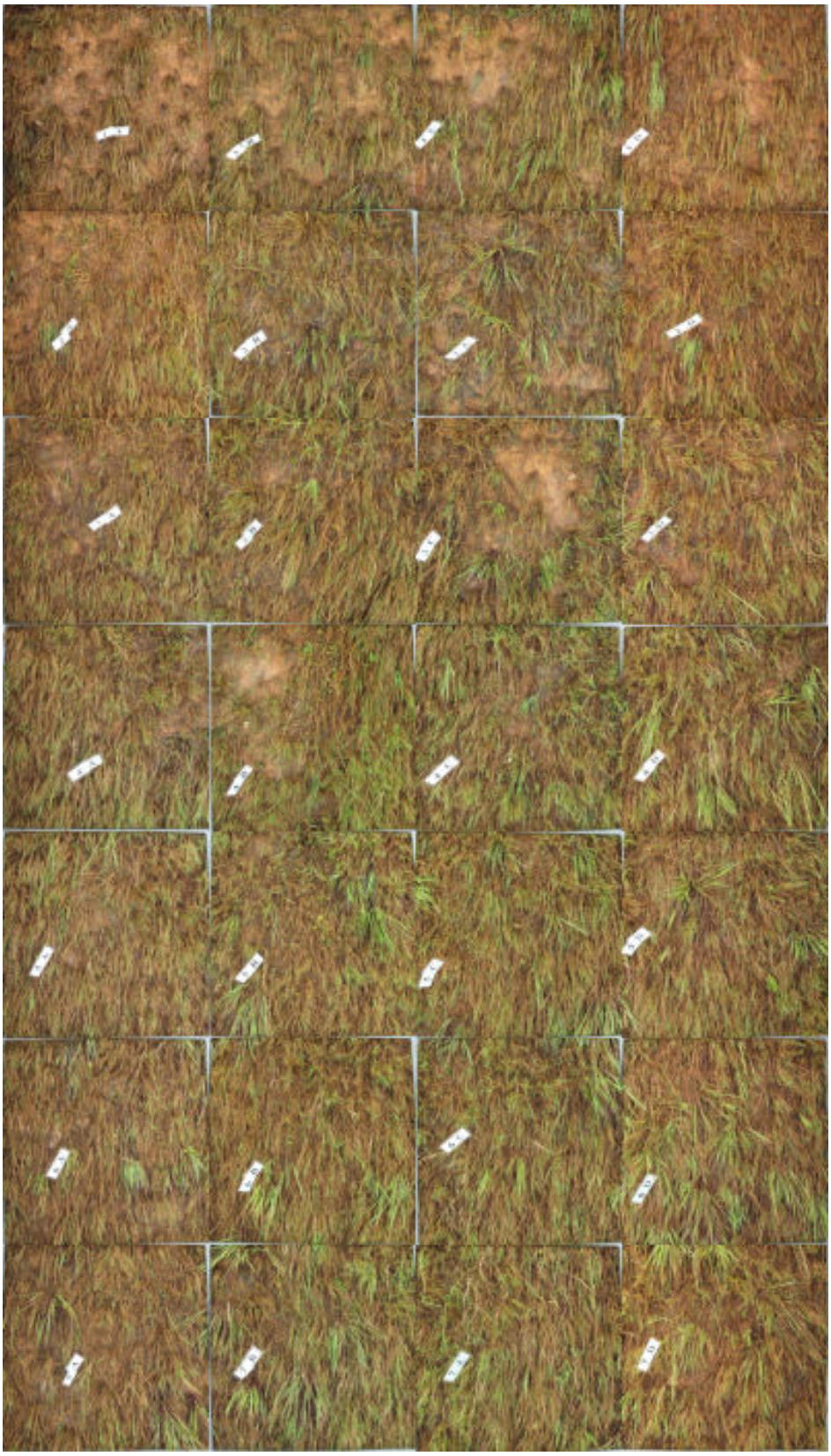

Figure B.11: 60x1, 1 to 7 m from the dike crest, section YB2.

Figure B.12: 60x1, 8 to 14 m from the dike crest, section YB2.

Figure B.13: 60x2, 1 to 7 m from the dike crest, section YB2.

Figure B.14: 60x2, 8 to 14 m from the dike crest, section YB2.

Figure B.15: 60x2 + 80x1, 1 to 7 m from the dike crest, section YB2.

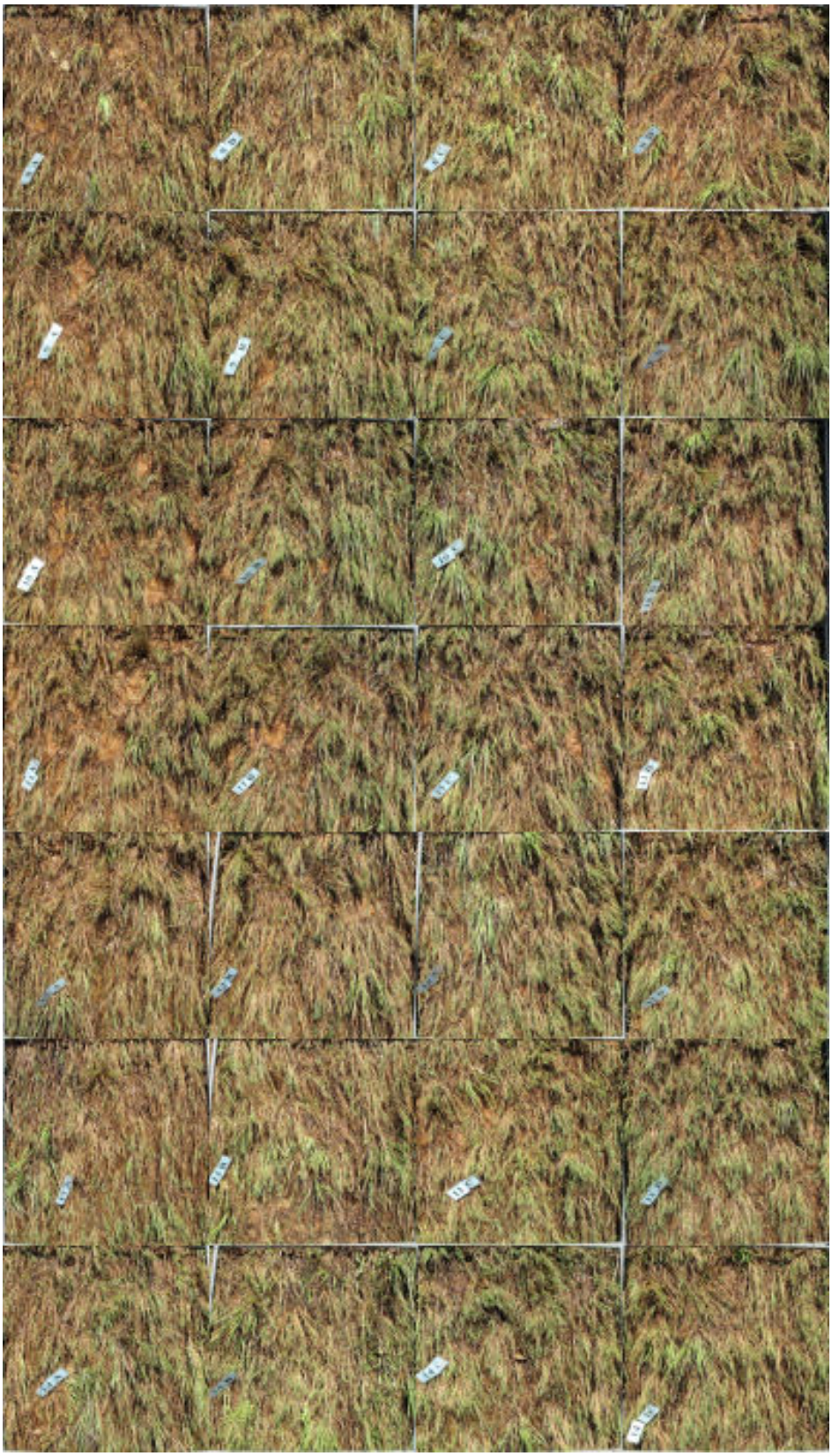

Figure B.16: 60x2 + 80x1, 8 to 14 m from the dike crest, section YB2.

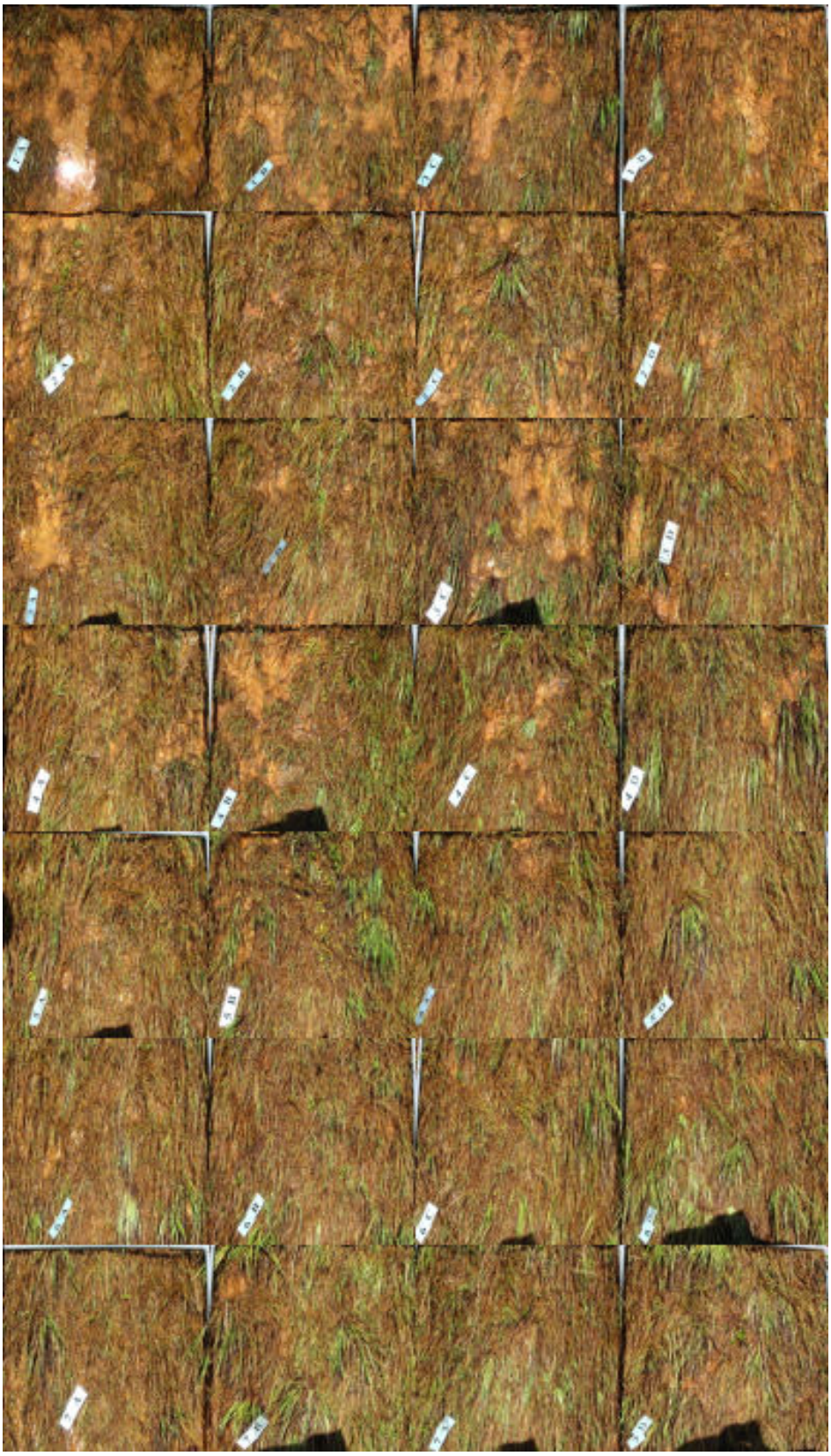

Figure B.17: 60x2 + 80x2, 1 to 7 m from the dike crest, section YB2.

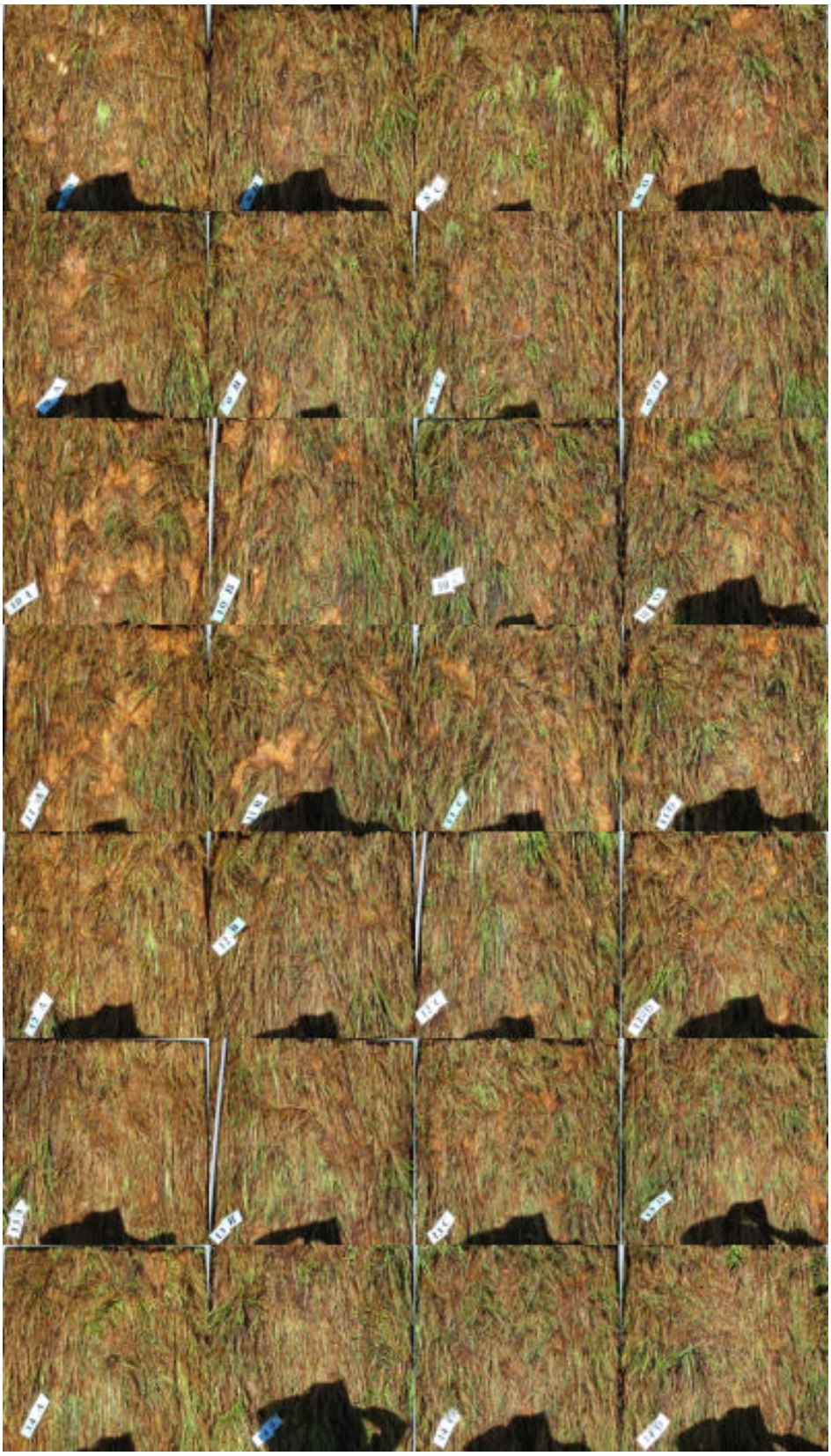

Figure B.18: 60x2 + 80x2, 8 to 14 m from the dike crest, section YB2.

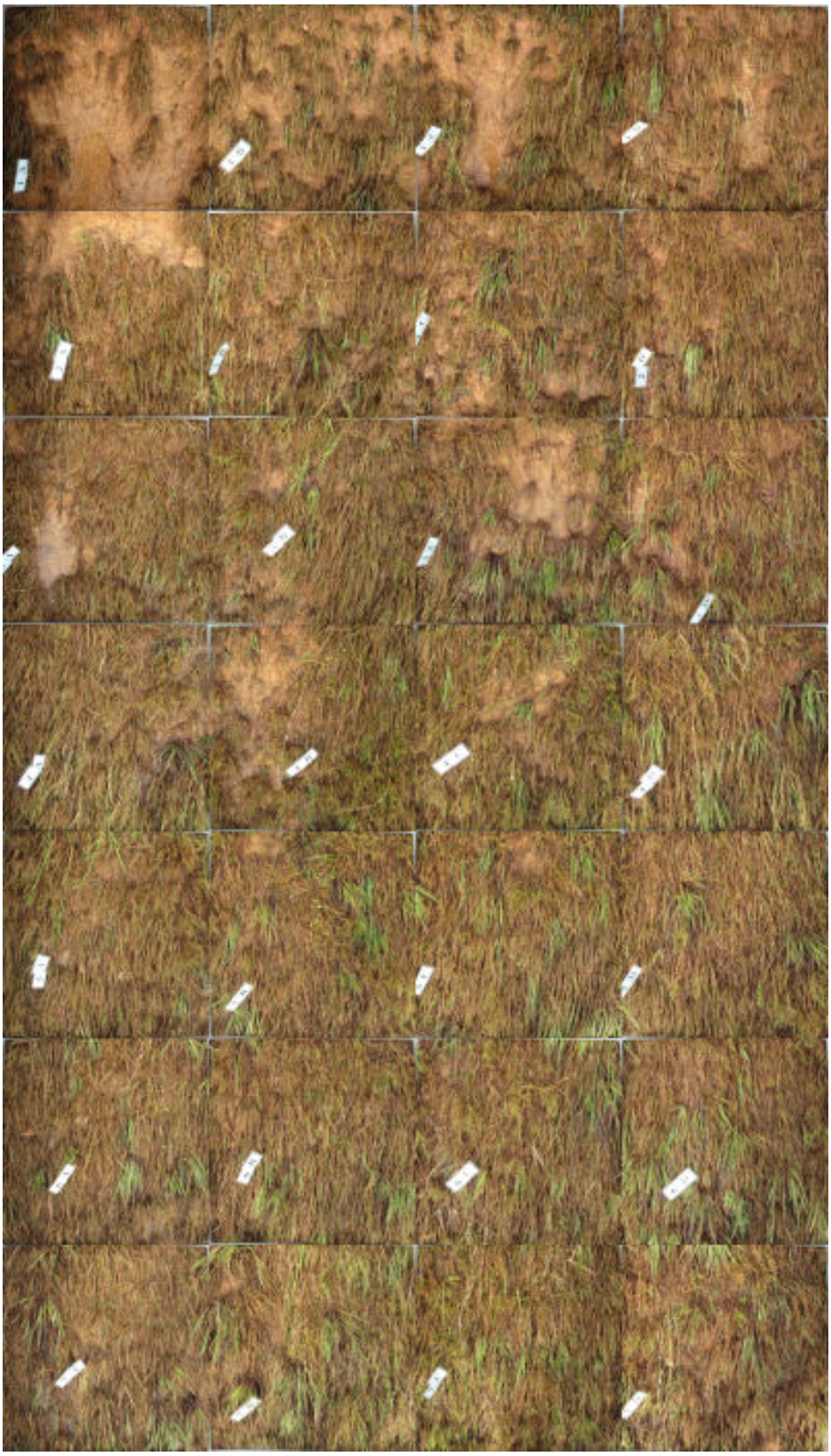

Figure B.19: 60x2 + 80x2 + 100x1, 1 to 7 m from the dike crest, section YB2.

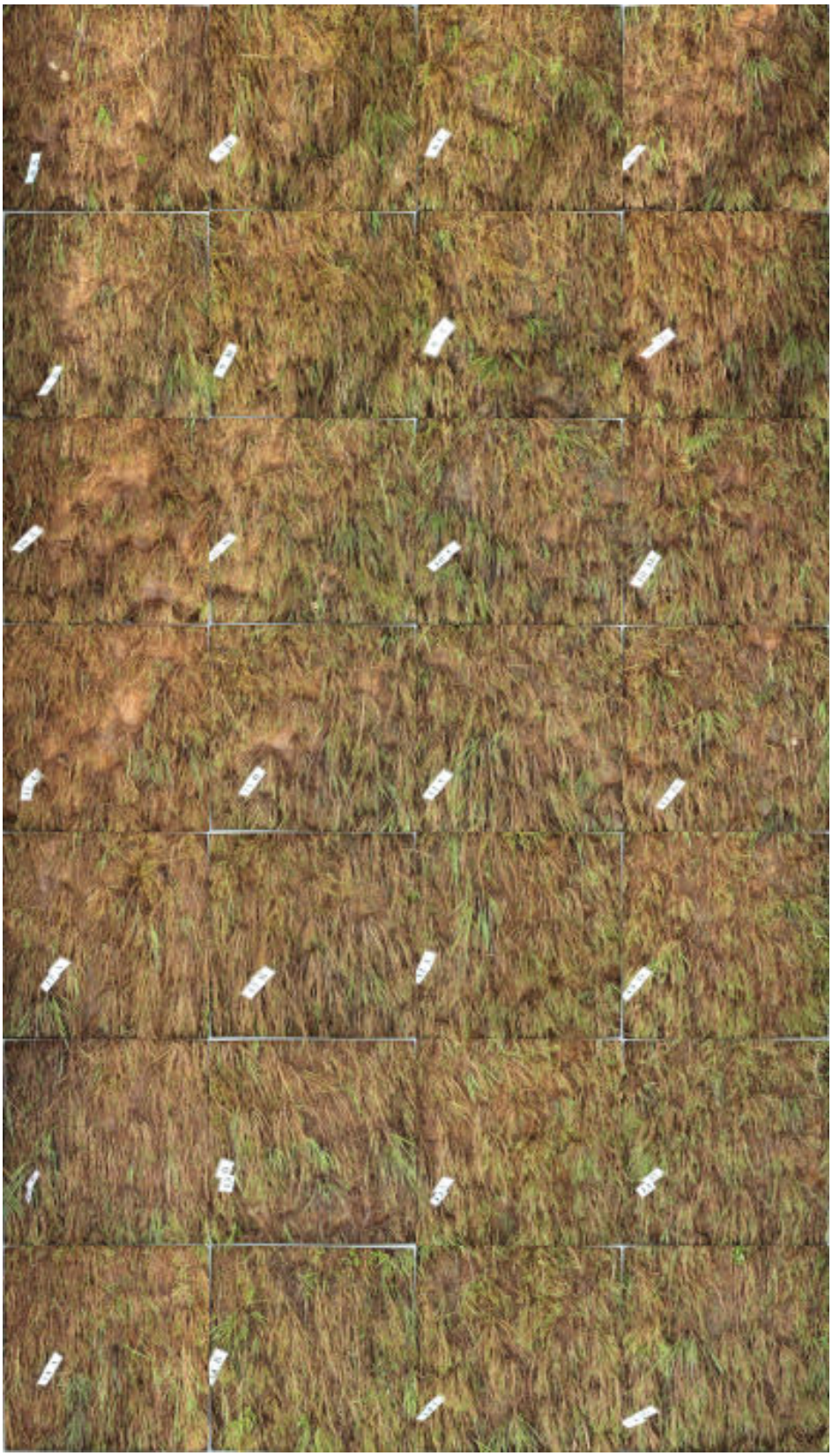

Figure B.20: 60x2 + 80x2 + 100x1, 8 to 14 m from the dike crest, section YB2.

Figure B.21: 60x2 + 80x2 + 100x2, 1 to 7 m from the dike crest, section YB2.

Figure B.22: 60x2 + 80x2 + 100x2, 8 to 14 m from the dike crest, section YB2.

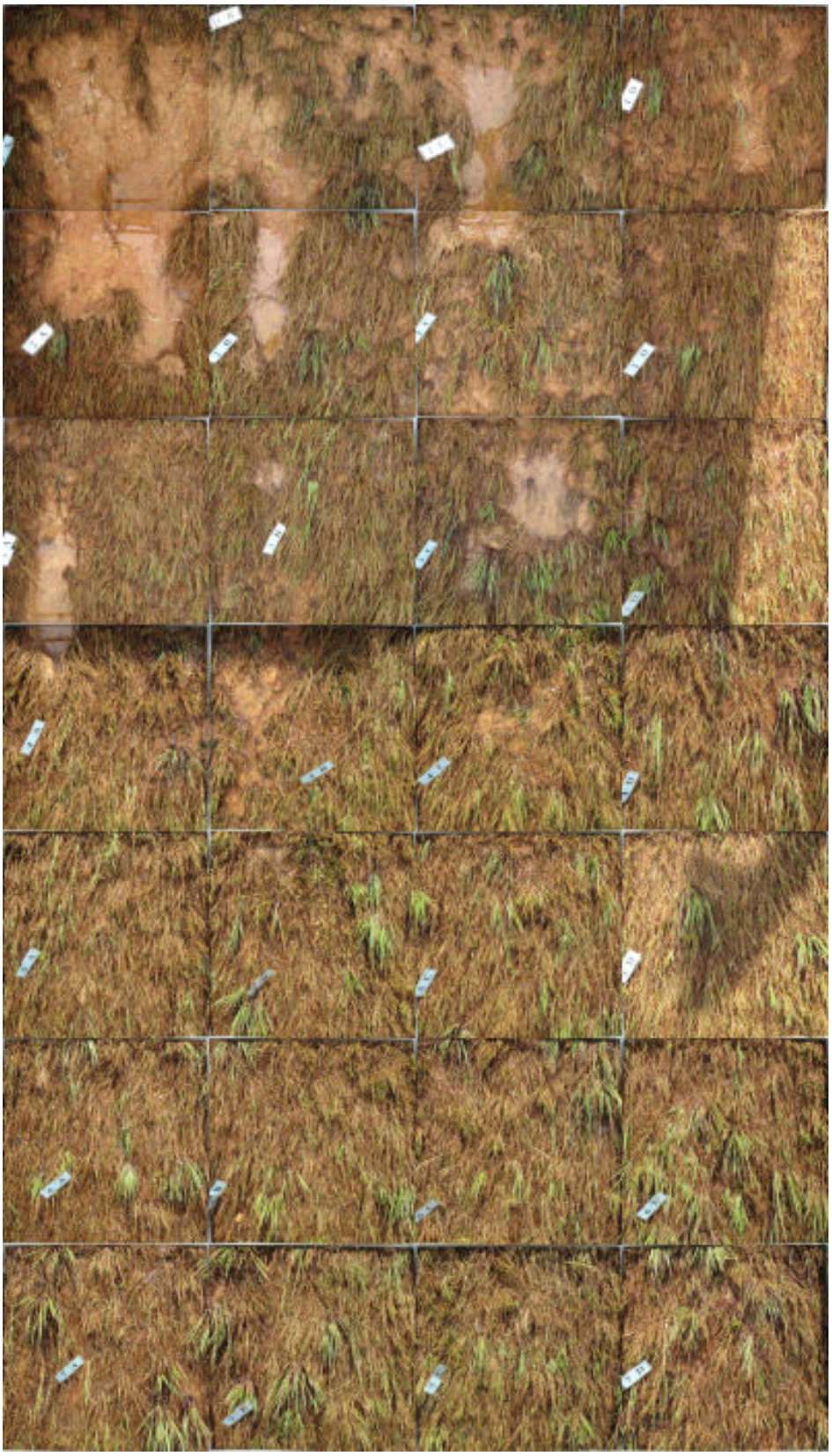

Figure B.23: 60x2 + 80x2 + 100x3, 1 to 7 m from the dike crest, section YB2.

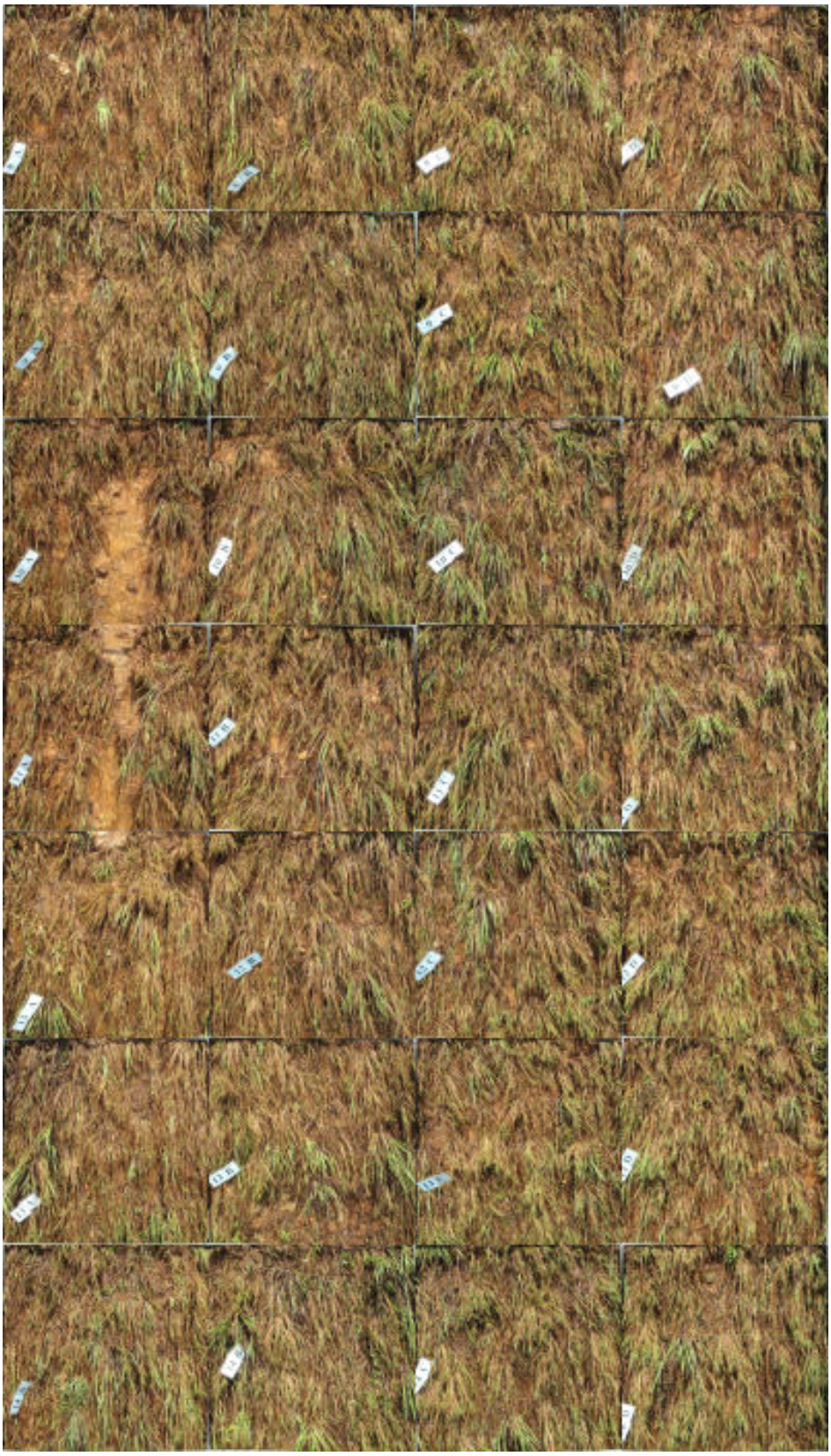

Figure B.24: 60x2 + 80x2 + 100x3, 8 to 14 m from the dike crest, section YB2.

Figure B.25: 60x2 + 80x2 + 100x4, 1 to 7 m from the dike crest, section YB2.

Figure B.26: 60x2 + 80x2 + 100x4, 8 to 14 m from the dike crest, section YB2.

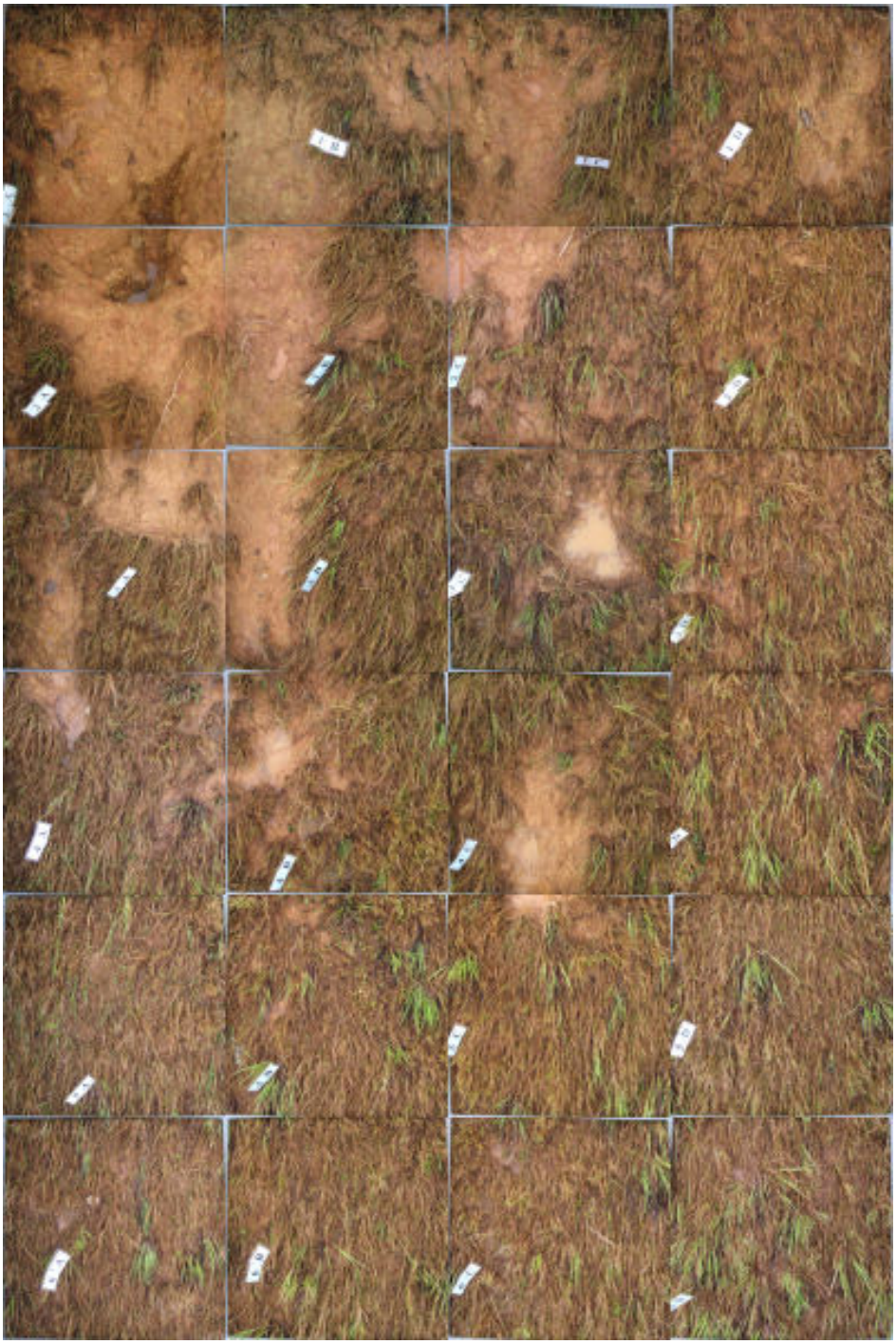

Figure B.27: 60x2 + 80x2 + 100x4 + 110x1, 1 to 6 m from the dike crest, section YB2.

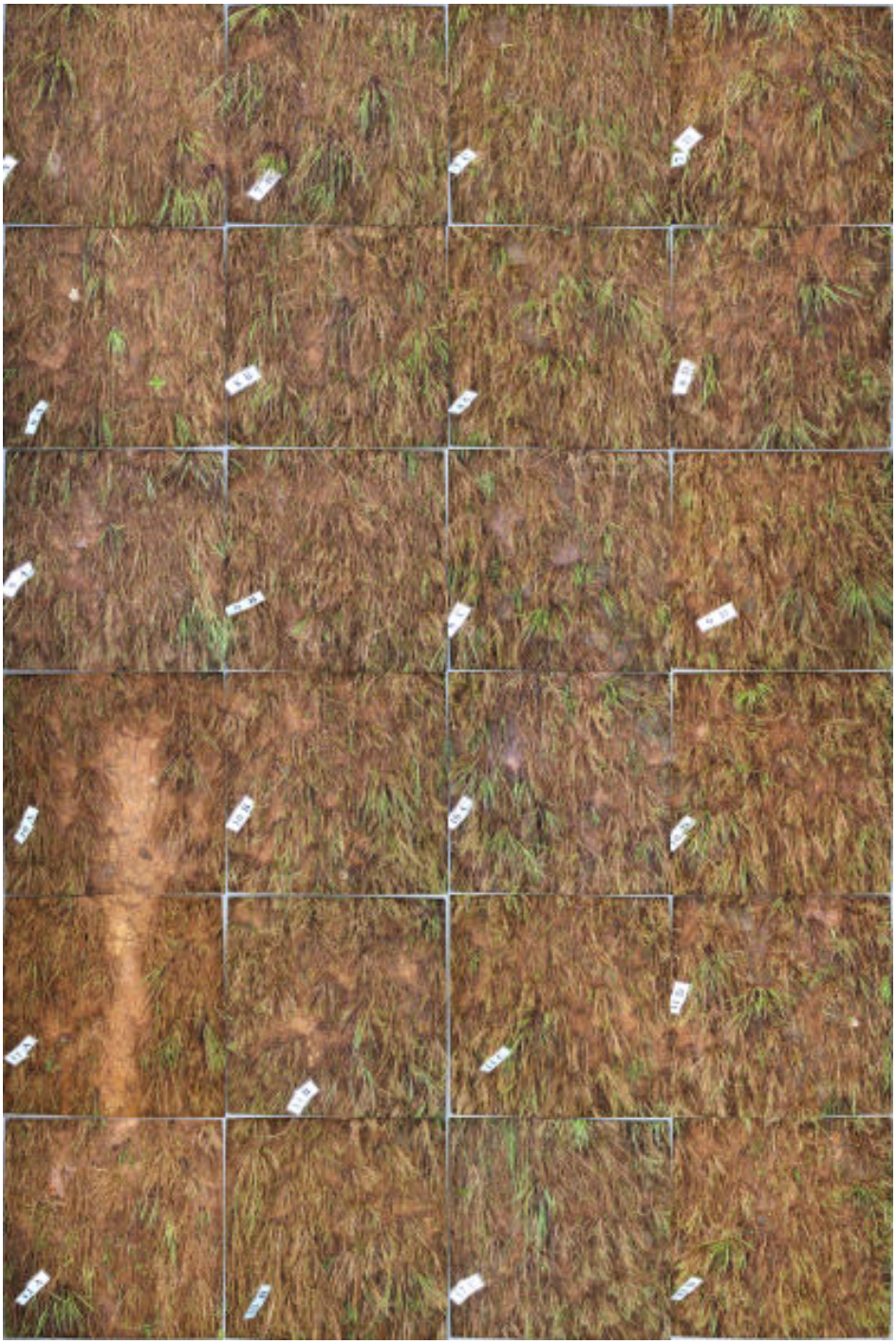

Figure B.28: 60x2 + 80x2 + 100x4 + 110x1, 7 to 12 m from the dike crest, section YB2.

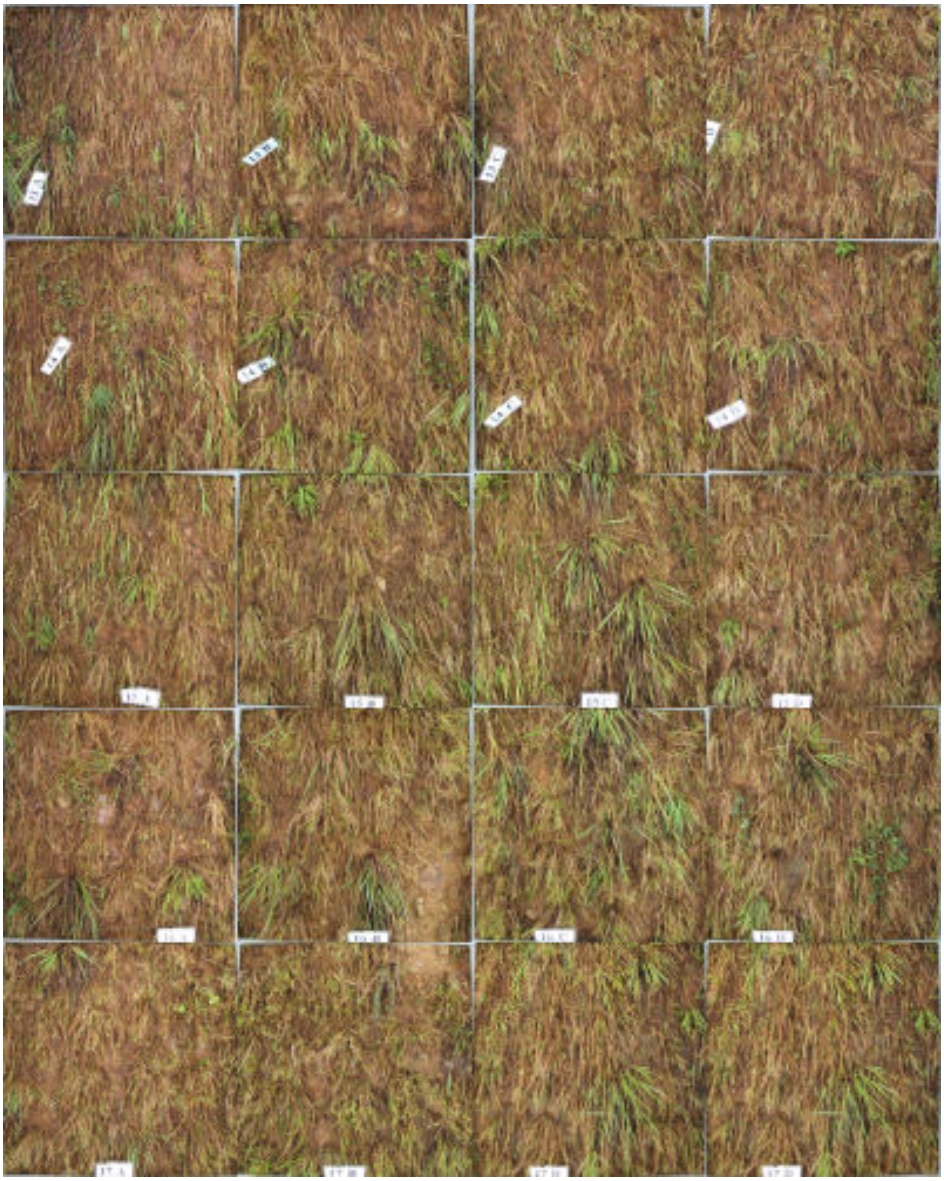

Figure B.29: 60x2 + 80x2 + 100x4 + 110x1, 13 to 17 m from the dike crest, section YB2.

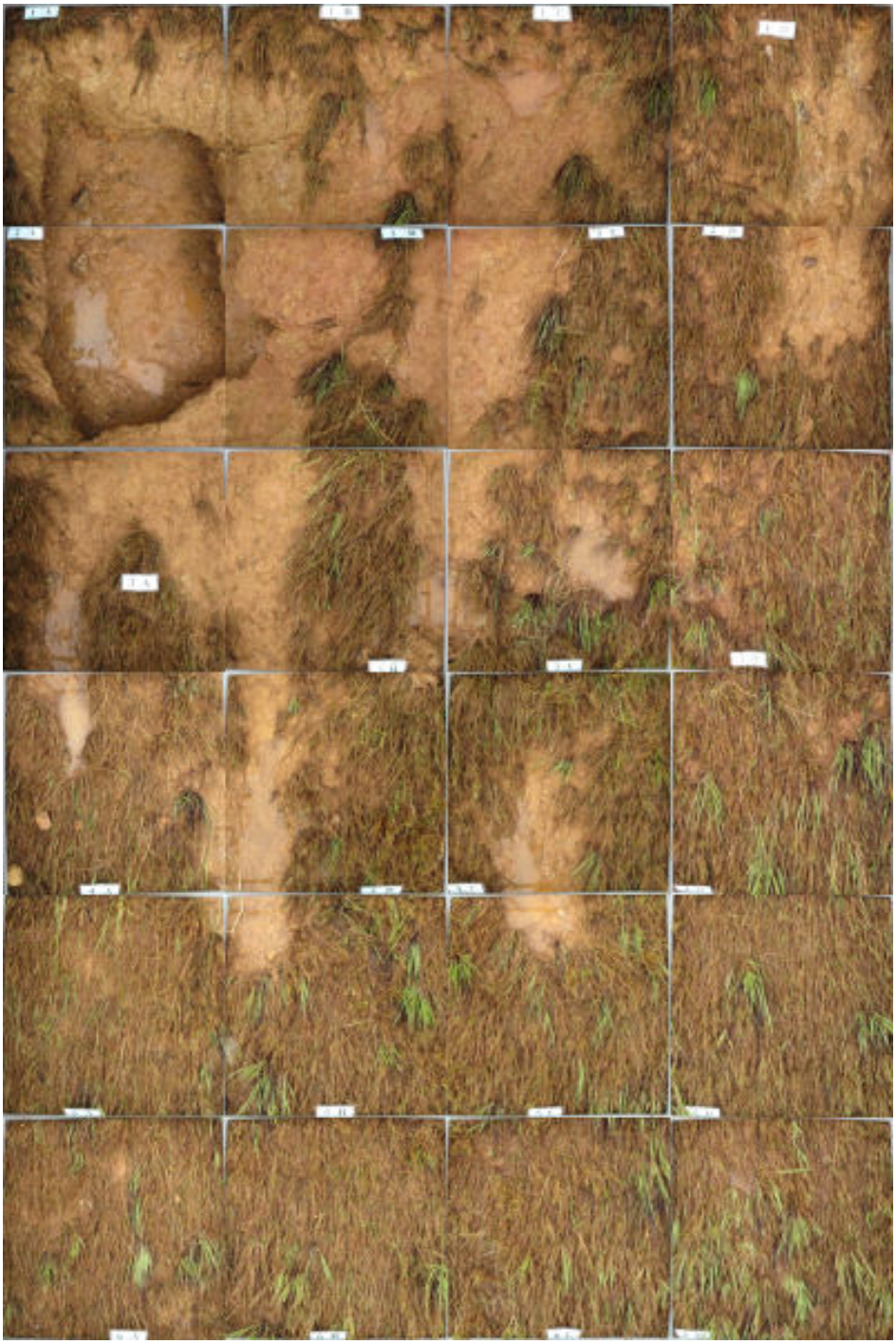

Figure B.30: 60x2 + 80x2 + 100x4 + 110x2, 1 to 6 m from the dike crest, section YB2.

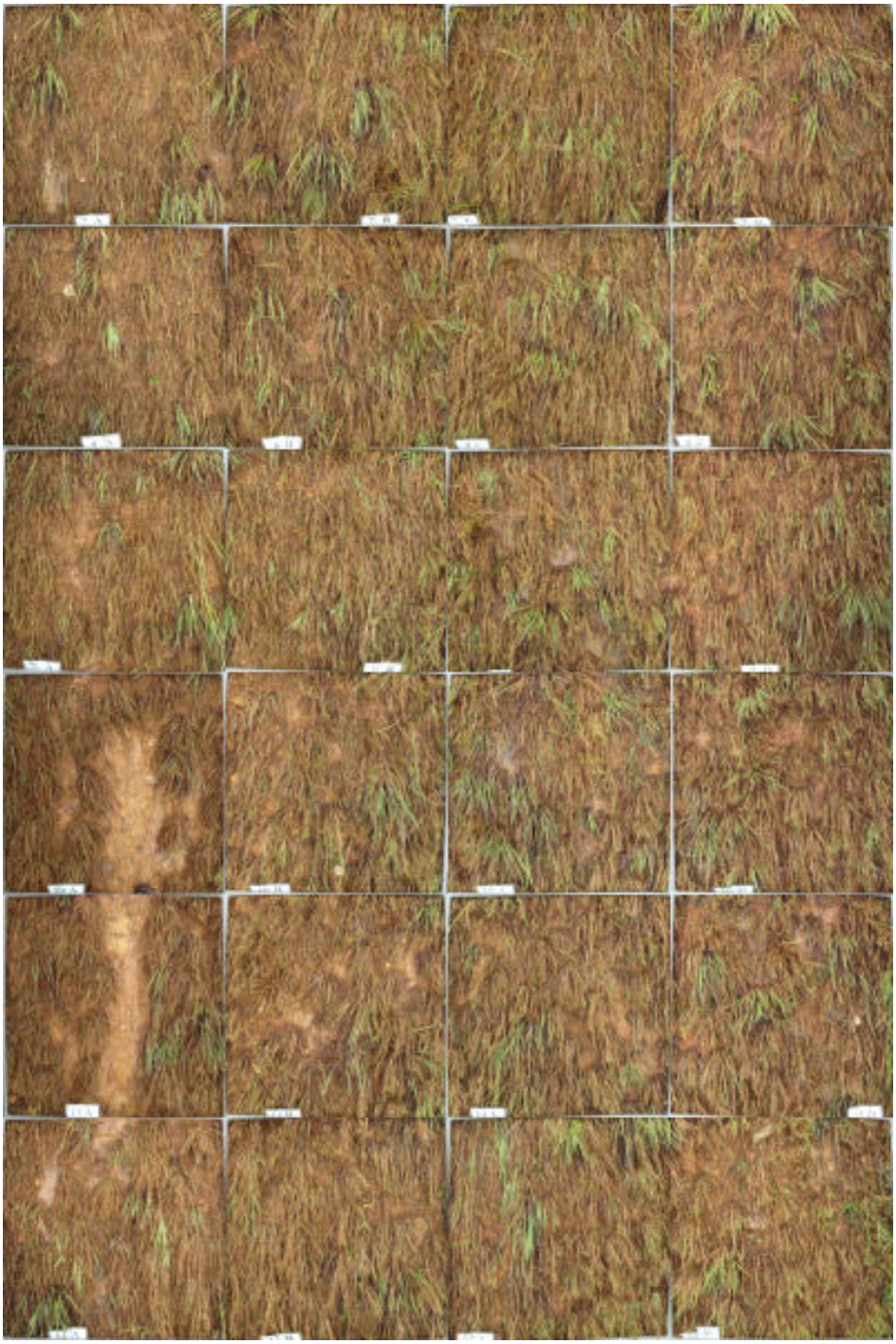

Figure B.31: 60x2 + 80x2 + 100x4 + 110x2, 7 to 12 m from the dike crest, section YB2.

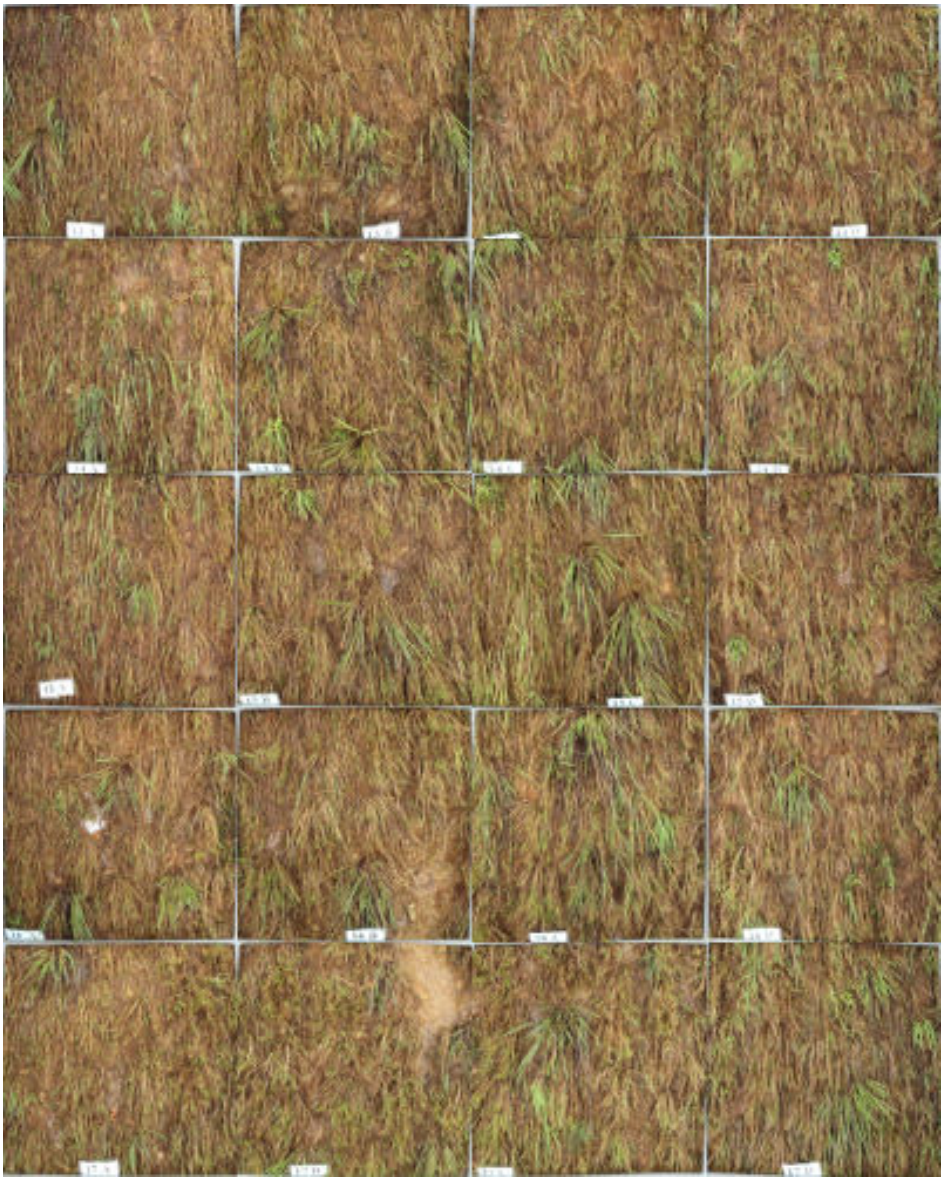

Figure B.32: 60x2 + 80x2 + 100x4 + 110x2, 13 to 17 m from the dike crest, section YB2.

B.3 Section YB3

At the section YB3, two different wave conditions were deployed. A wave height of 1.5 m was used till '60x4 + 80x6 + 100x10' l/s per m. After that, a wave height of 2.0 m was applied for '40x1 + 60x2 + 80x2 + 100x1' l/s per m.

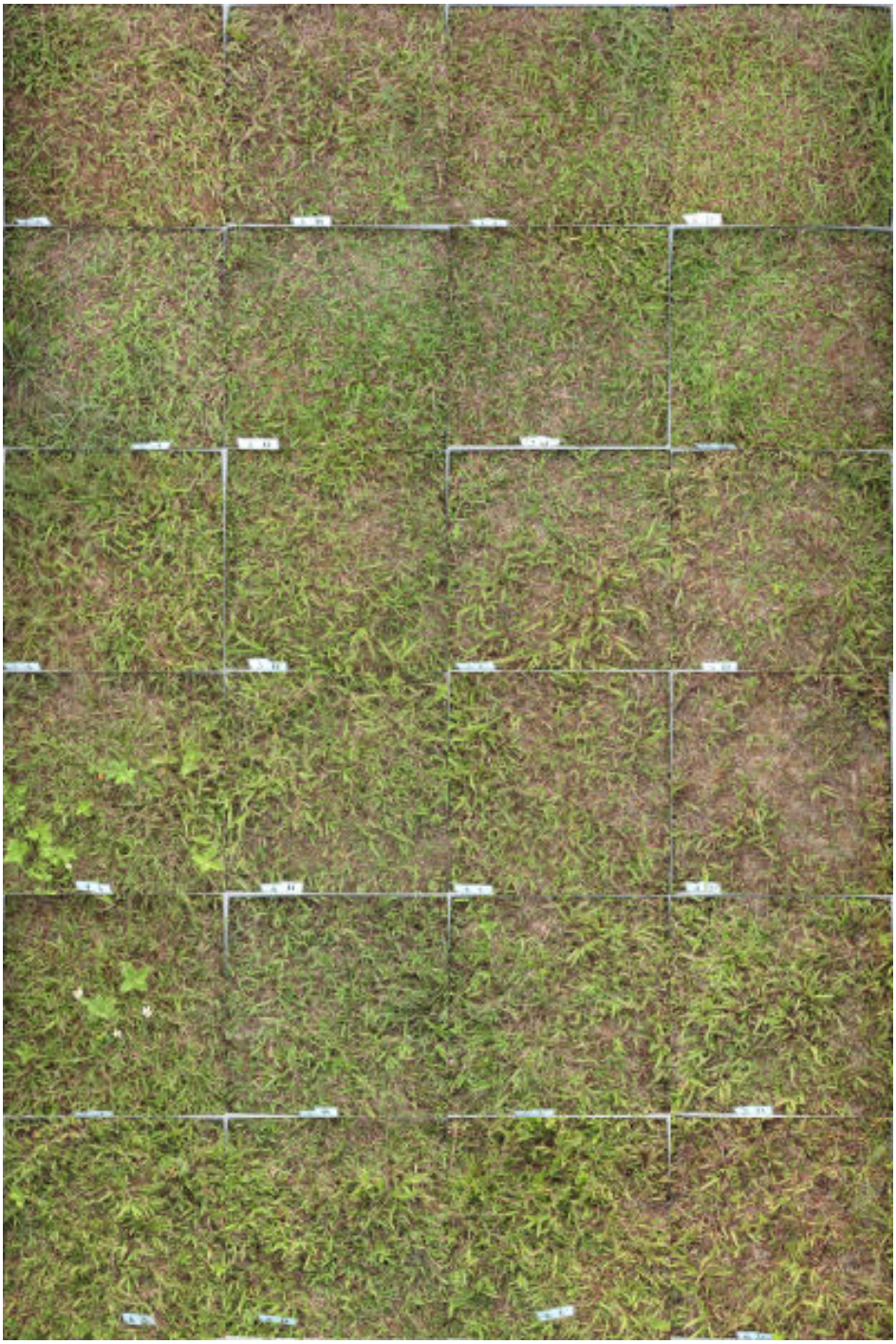

Figure B.33: 0x0, 1 to 6 m from the dike crest, section YB3.

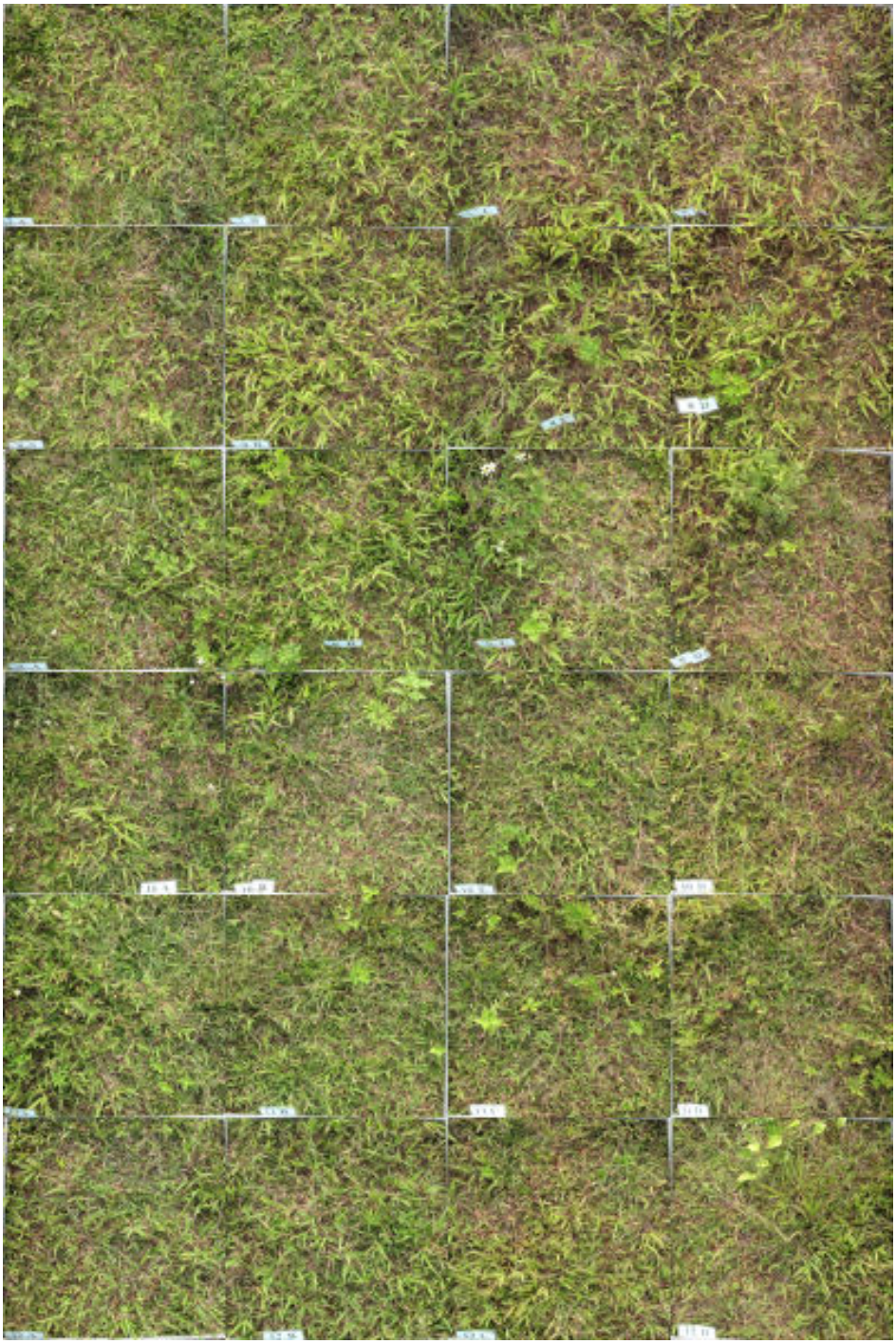

Figure B.34: 0x0, 7 to 12 m from the dike crest, section YB3.

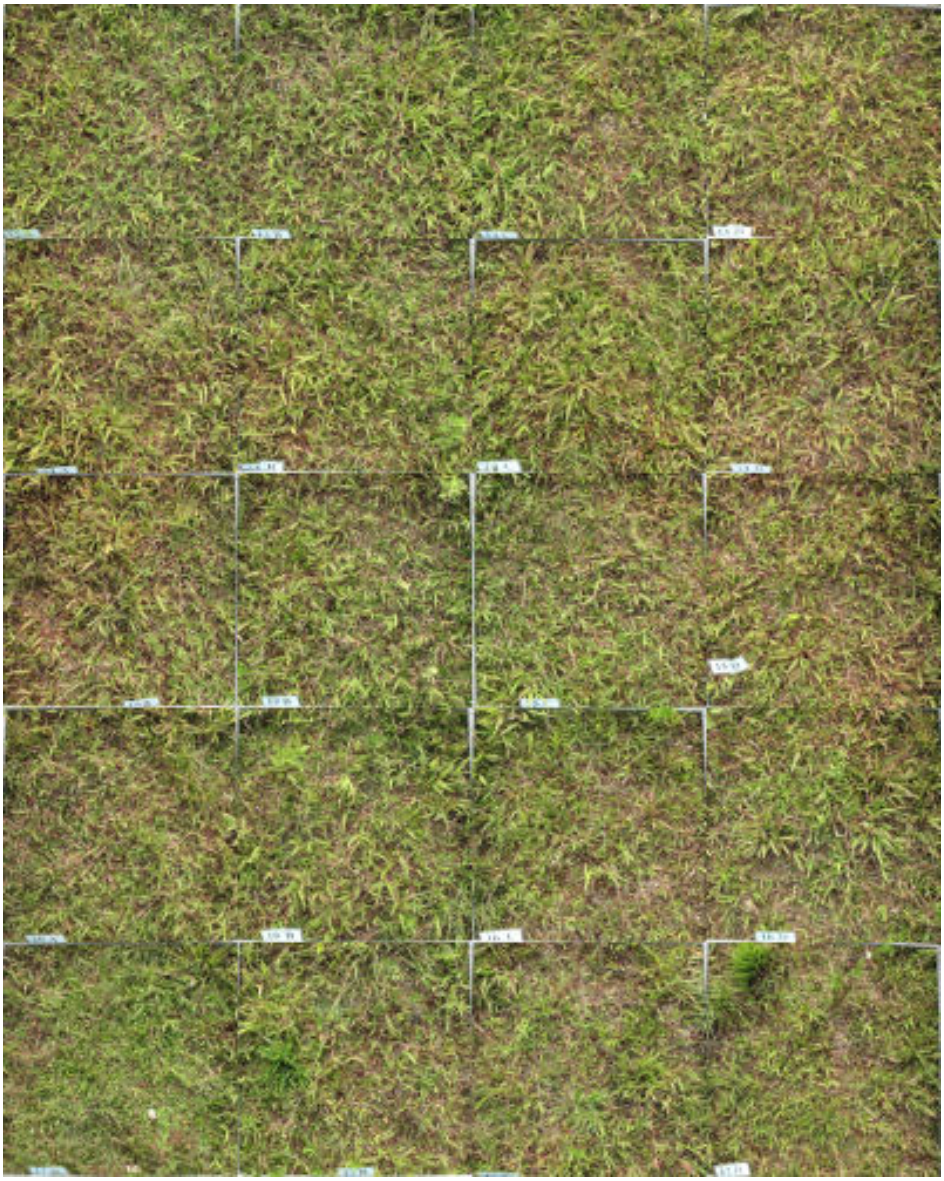

Figure B.35: 0x0, 13 to 17 m from the dike crest, section YB3.

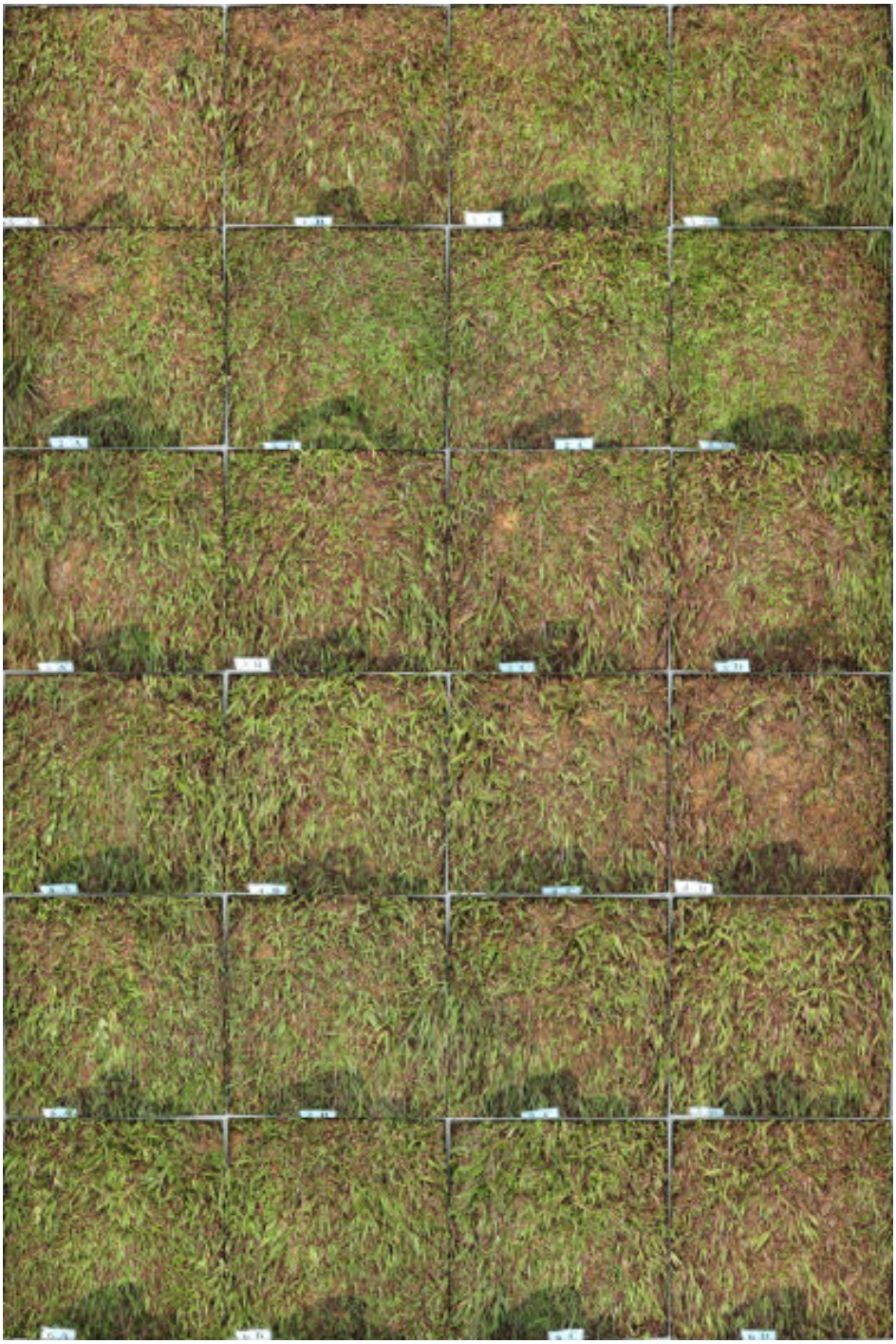

Figure B.36: 60x1, 1 to 6 m from the dike crest, section YB3.

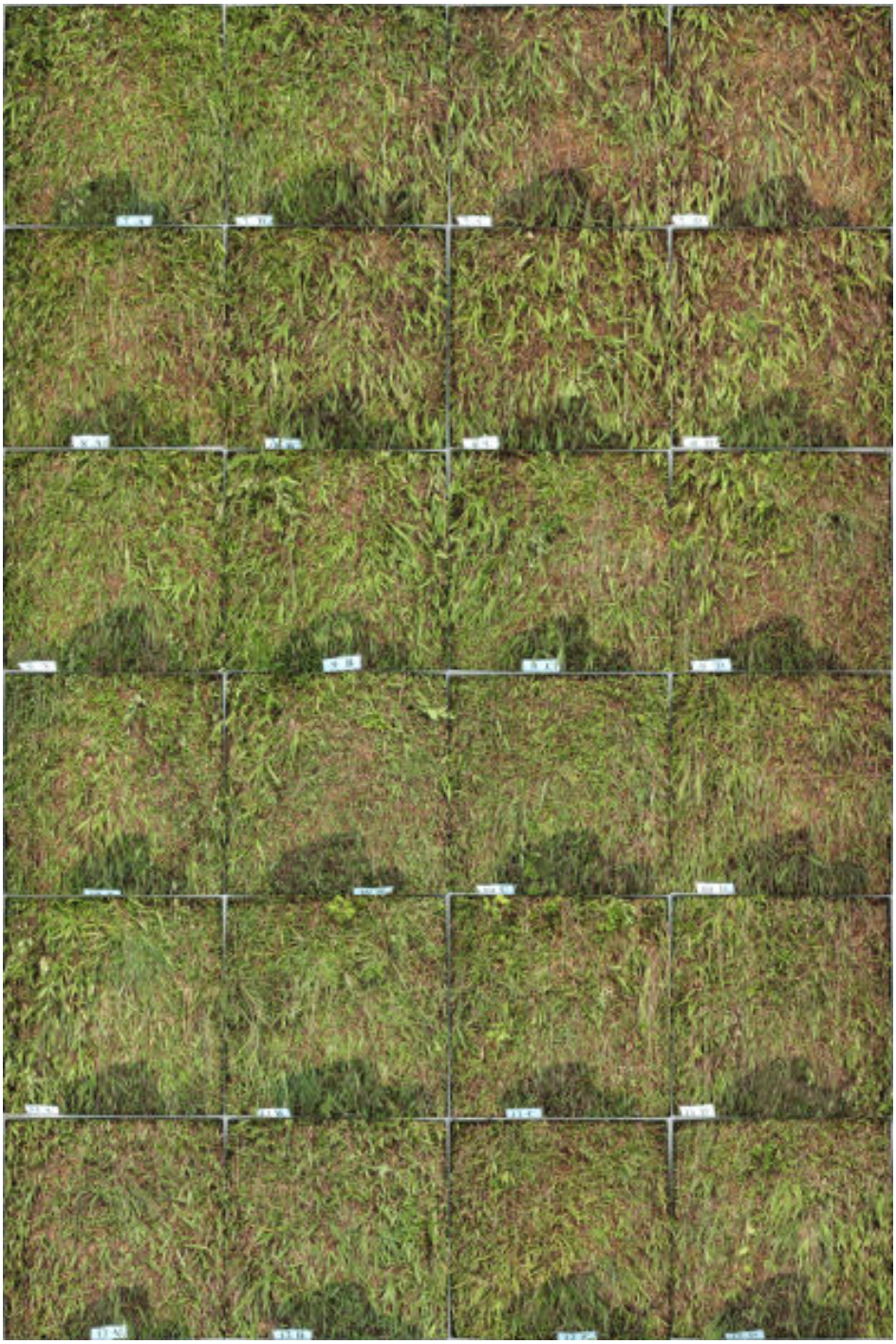

Figure B.37: 60x1, 7 to 12 m from the dike crest, section YB3.

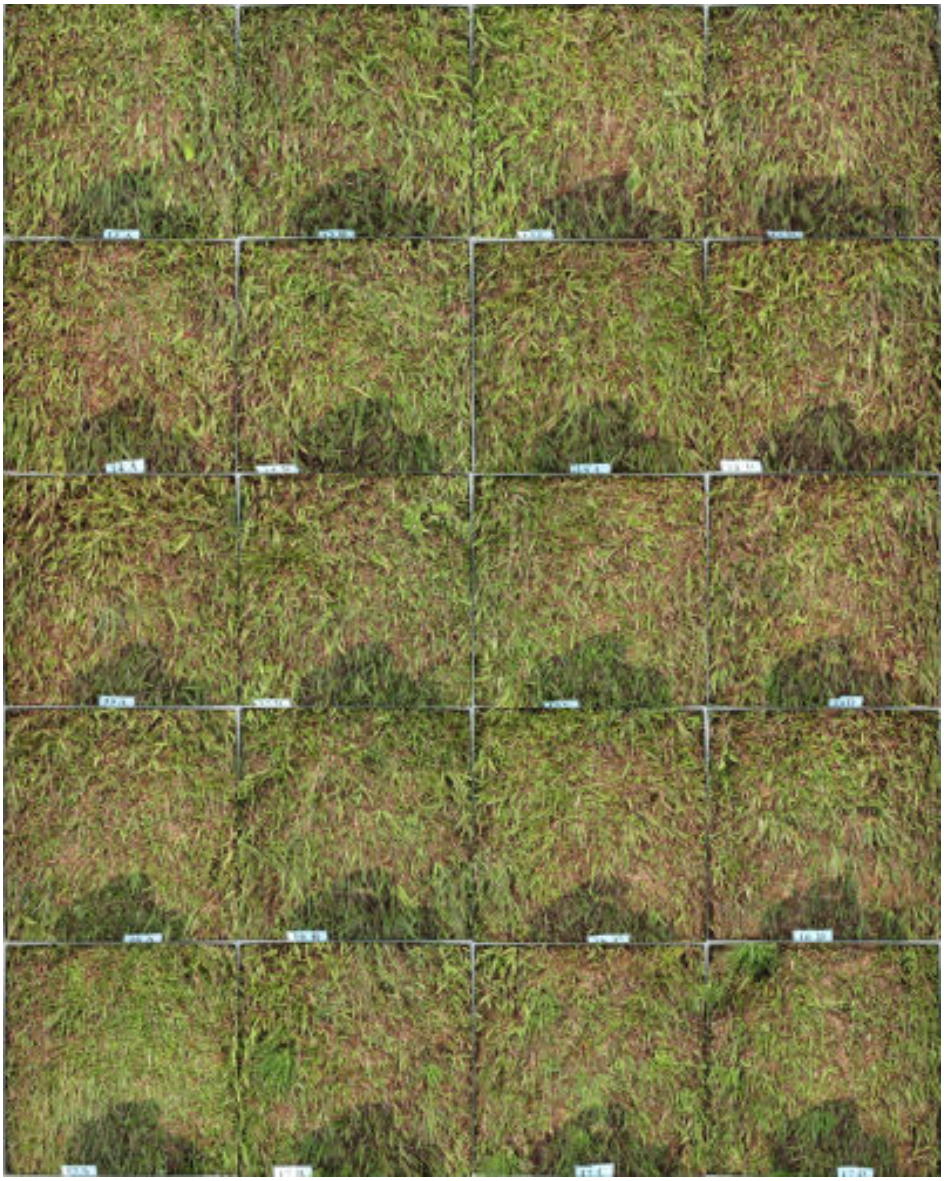

Figure B.38: 60x1, 13 to 17 m from the dike crest, section YB3.

Figure B.39: 60x4 + 80x6 + 100x10, 30 to 34 m from the dike crest, section YB3.

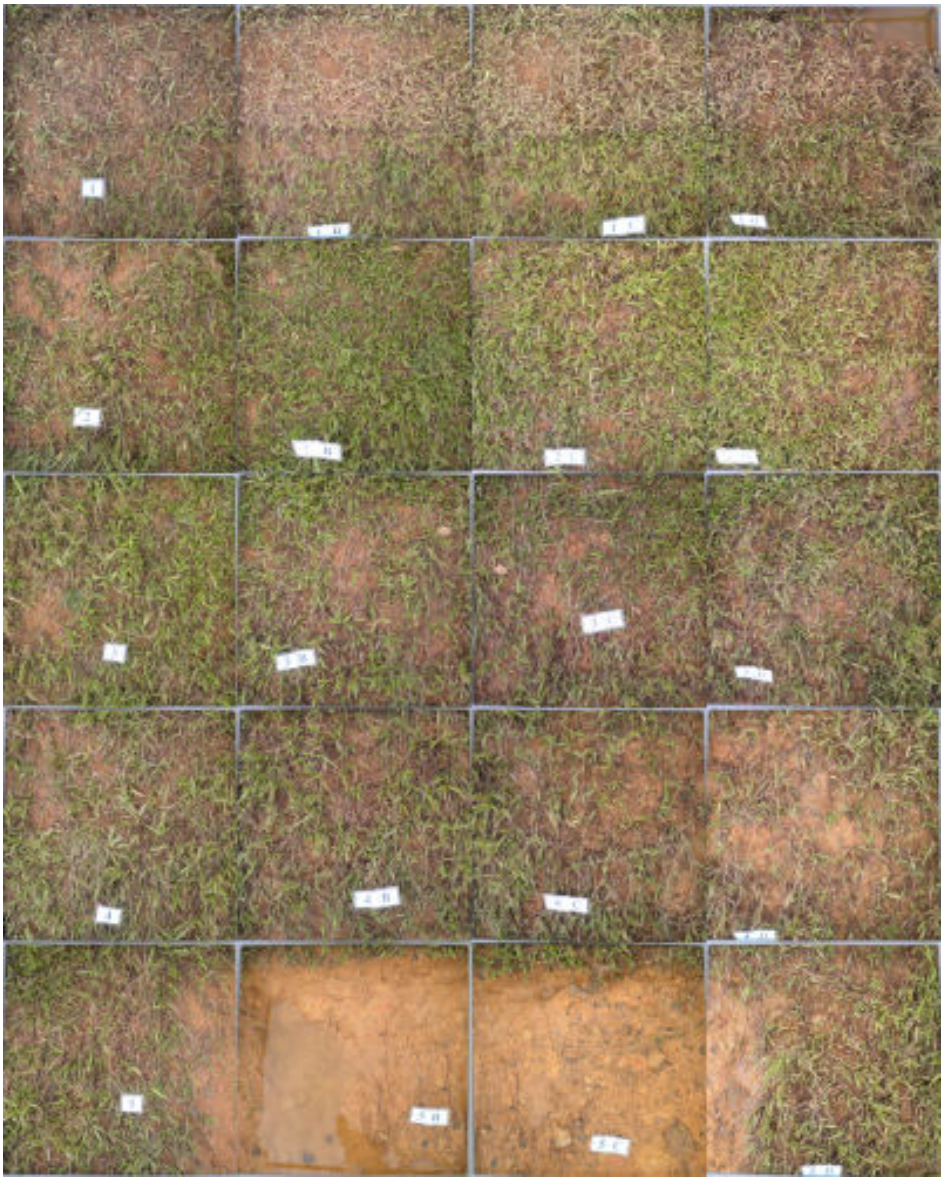

Figure B.40: (60x4 + 80x6 + 100x10) with H_s = 1.5 m and (40x1 + 60x2 + 80x2 + 100x1) with H_s = 2.0 m, 1 to 5 m from the dike crest, section YB3.

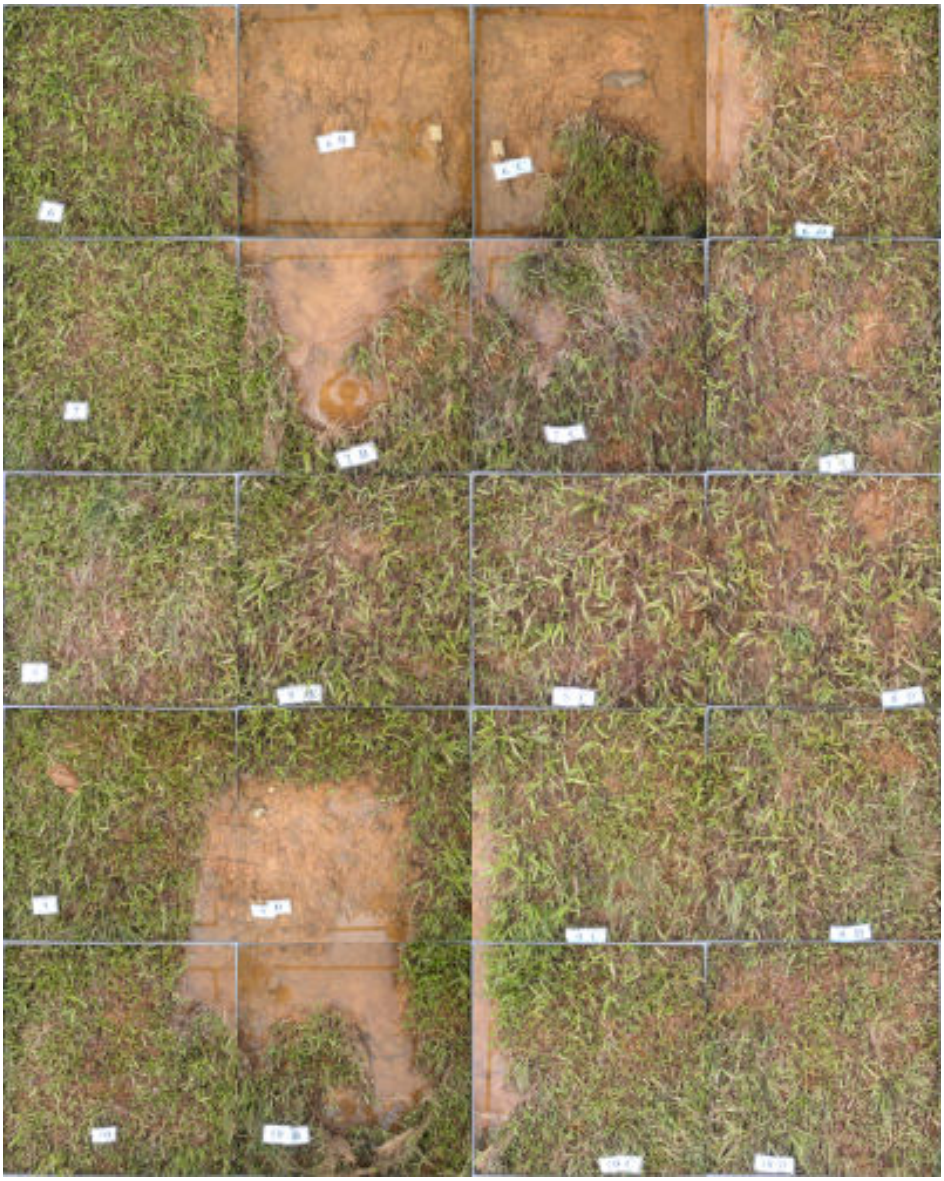

Figure B.41: (60x4 + 80x6 + 100x10) with H_s = 1.5 m and (40x1 + 60x2 + 80x2 + 100x1) with H_s = 2.0 m, 6 to 10 m from the dike crest, section YB3.

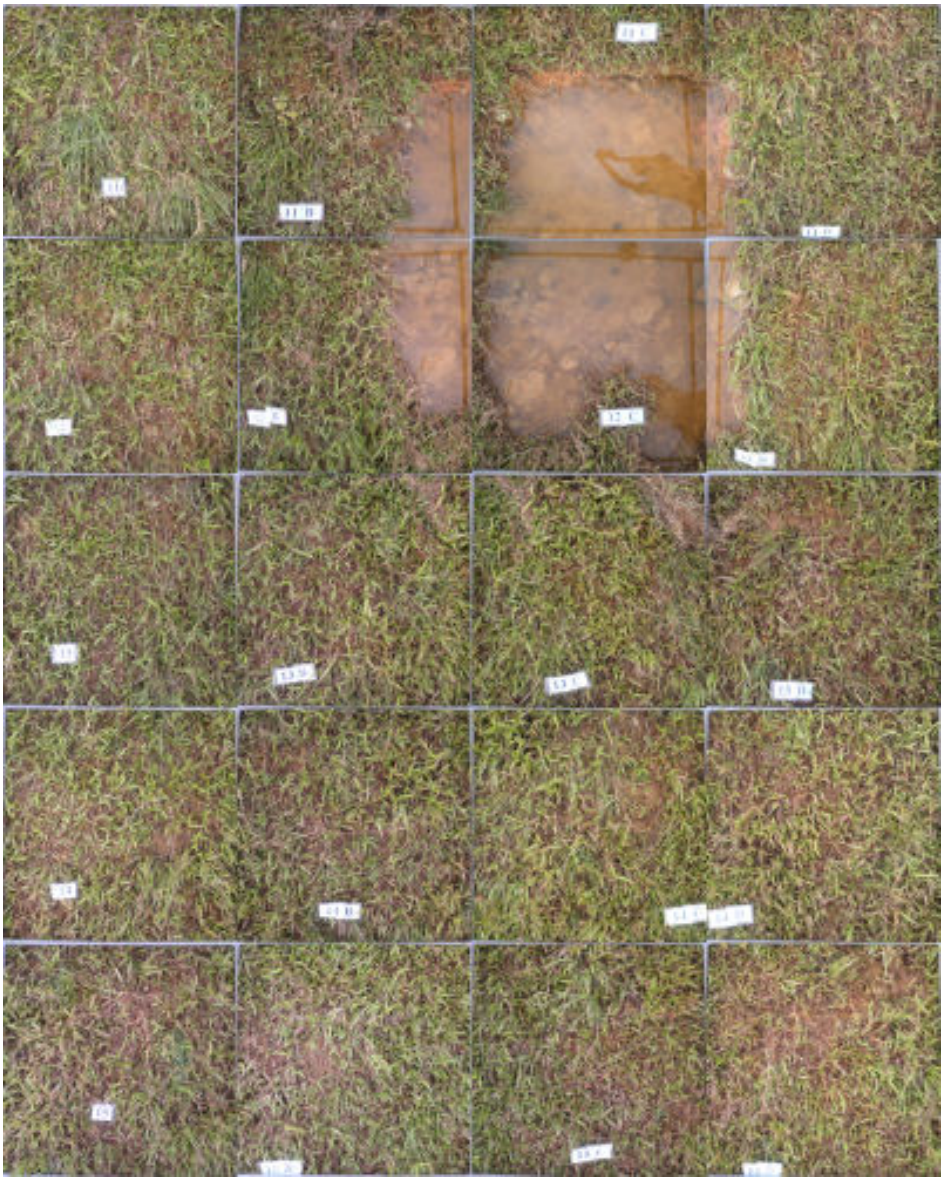

Figure B.42: (60x4 + 80x6 + 100x10) with H_s = 1.5 m and (40x1 + 60x2 + 80x2 + 100x1) with H_s = 2.0 m, 11 to 15 m from the dike crest, section YB3.

Figure B.43: (60x4 + 80x6 + 100x10) with H_s = 1.5 m and (40x1 + 60x2 + 80x2 + 100x1) with H_s = 2.0 m, 30 to 34 m from the dike crest, section YB3.

B.4 Section YB4

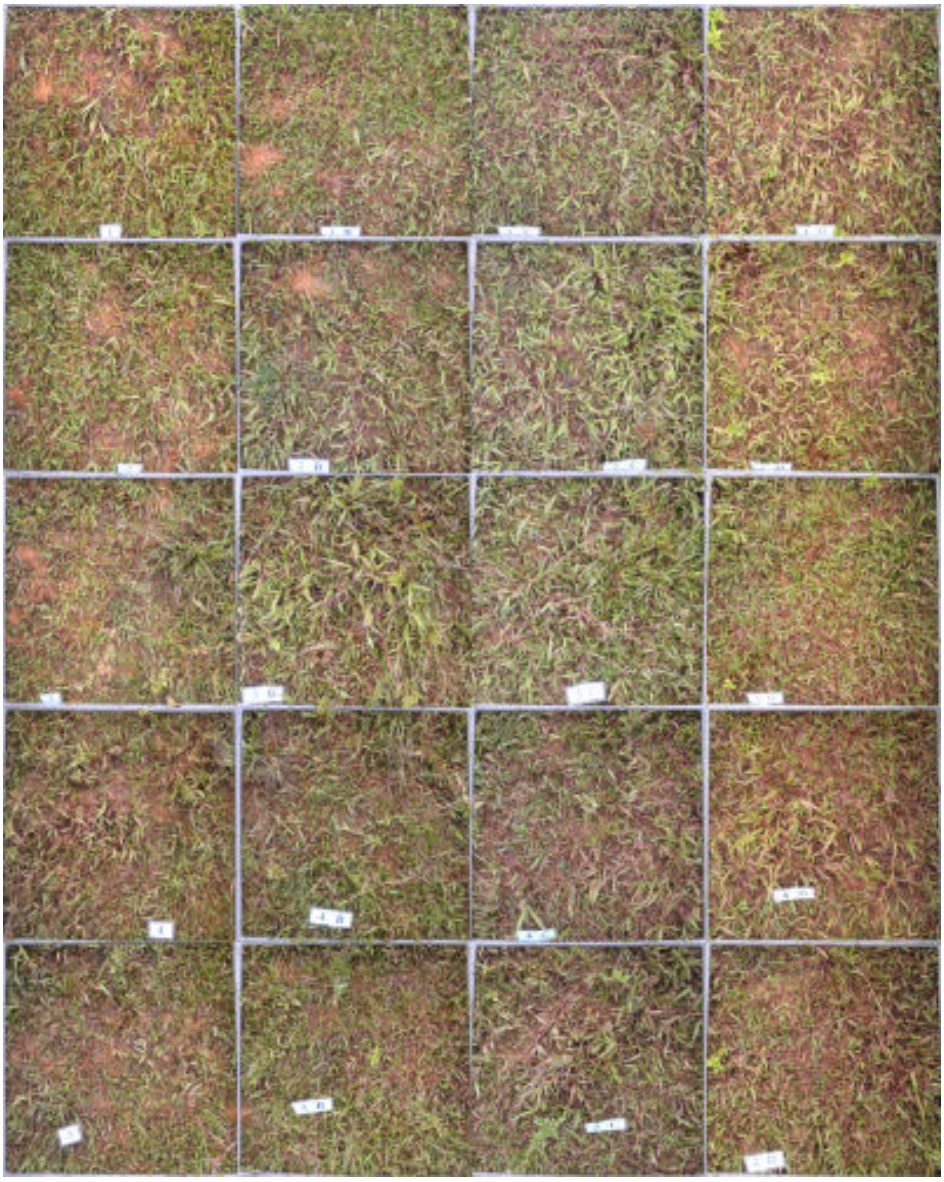

Figure B.44: 0x0, 1 to 5 m from the dike crest, section YB4.

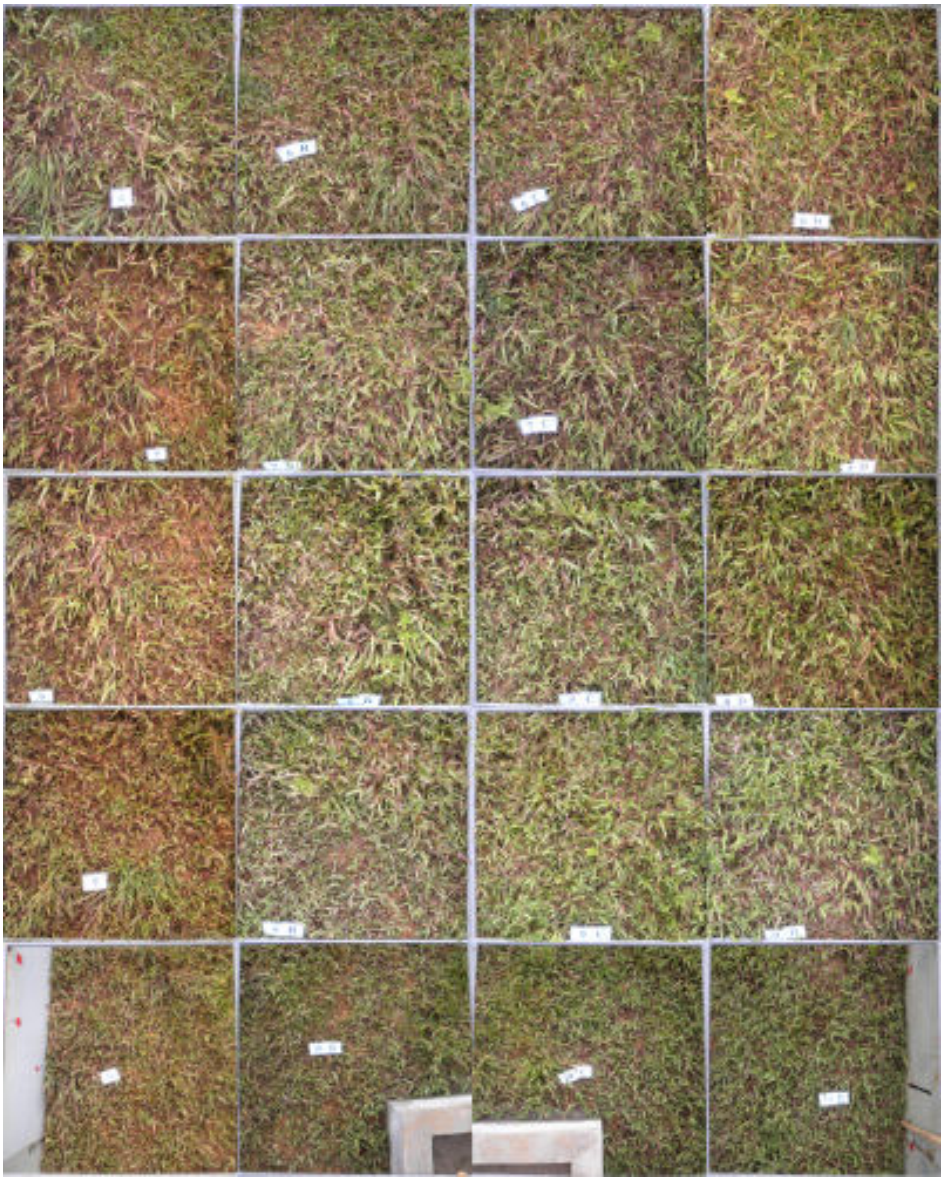

Figure B.45: 0x0, 6 to 10 m from the dike crest, section YB4.

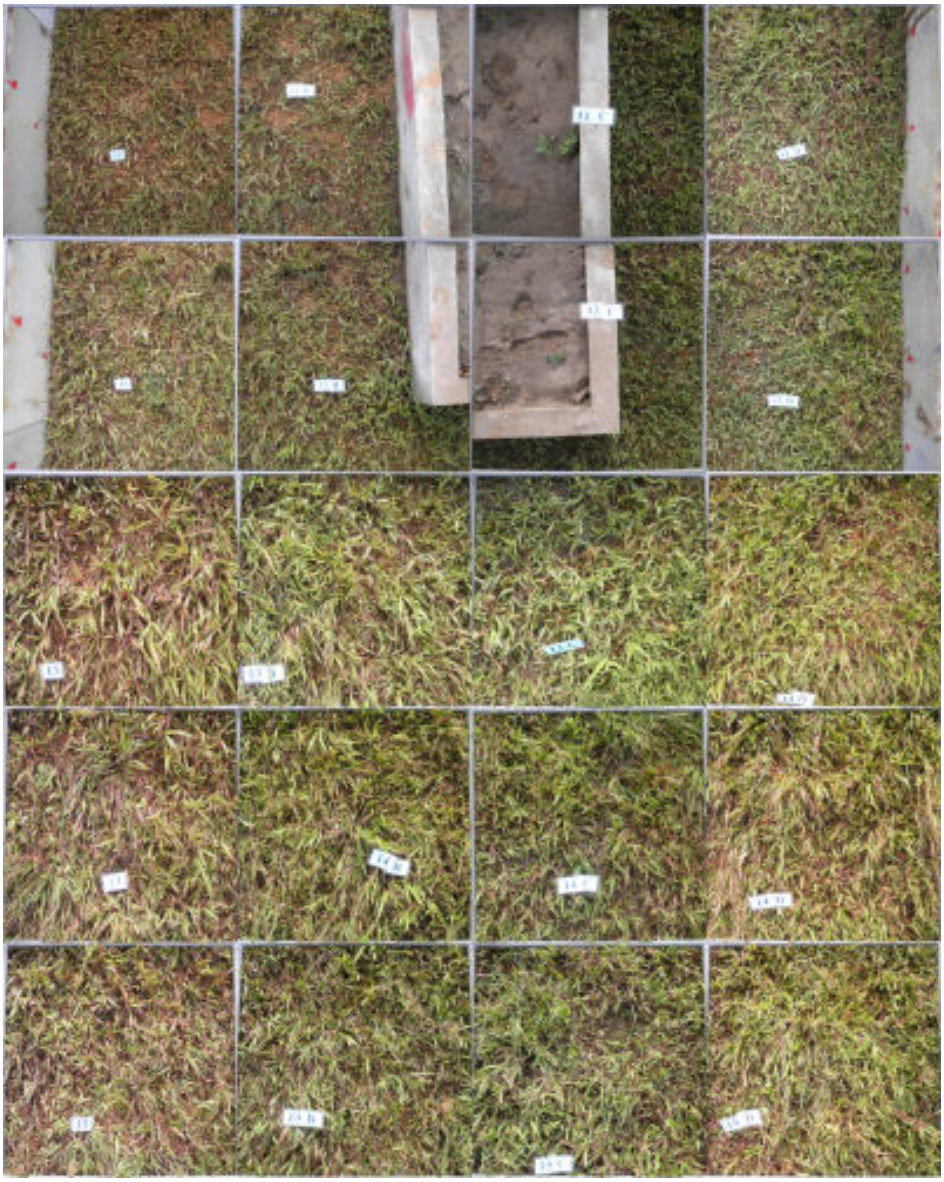

Figure B.46: 0x0, 11 to 15 m from the dike crest, section YB4.

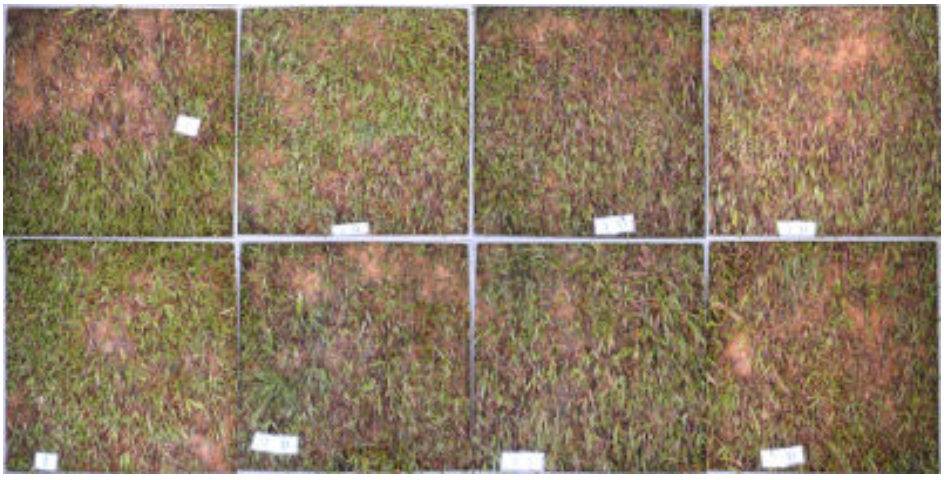

Figure B.47: 40x2 + 60x6 + 80x4, 1 to 2 m from the dike crest, section YB4.

Figure B.48: 40x2 + 60x6 + 80x4, 10 to 11 m from the dike crest, section YB4.

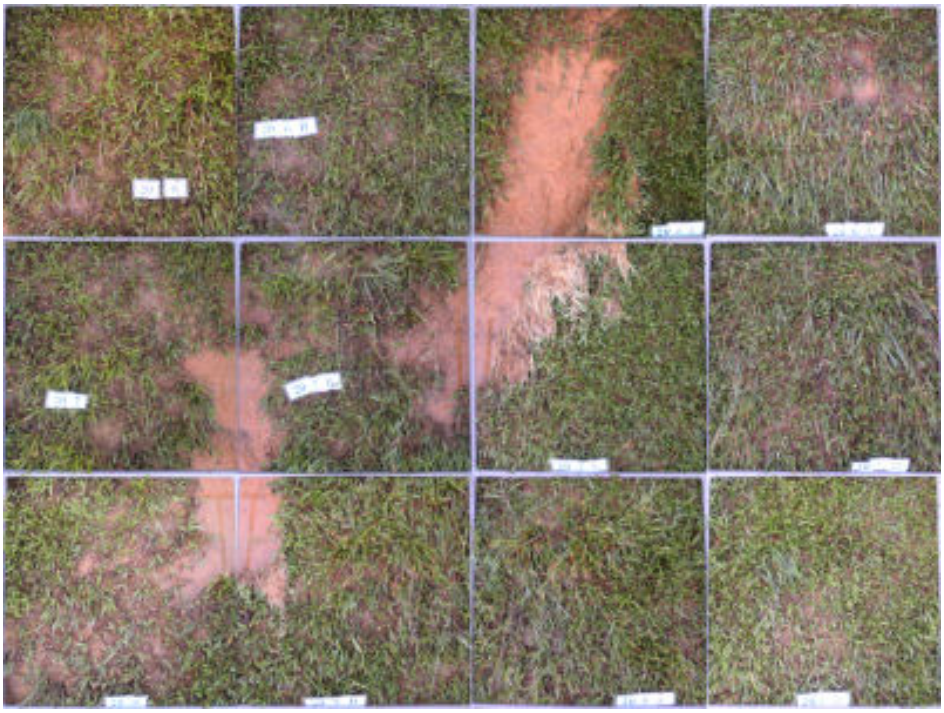

Figure B.49: 40x2 + 60x6 + 80x4, 26 to 28 m from the dike crest, section YB4.

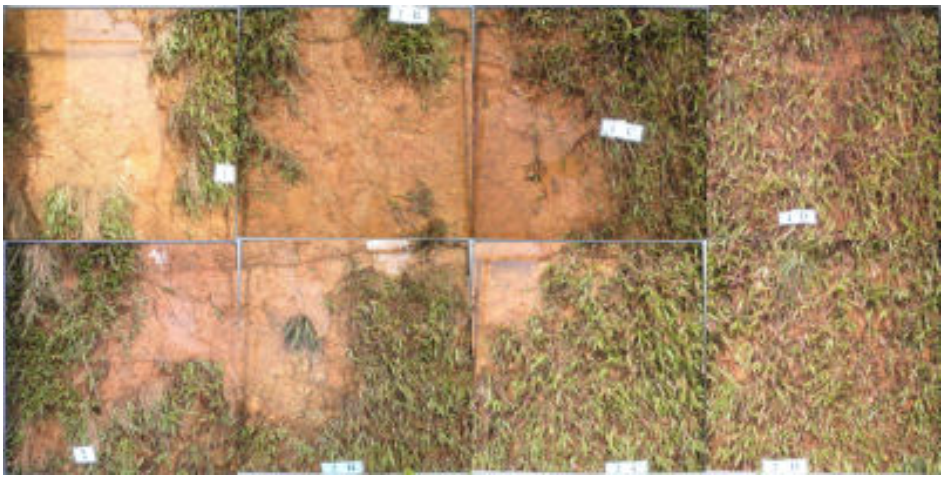

Figure B.50: 40x2 + 60x6 + 80x4 + 100x1, 1 to 2 m from the dike crest, section YB4.

Figure B.51: 40x2 + 60x6 + 80x4 + 100x1, 10 to 11 m from the dike crest, section YB4.

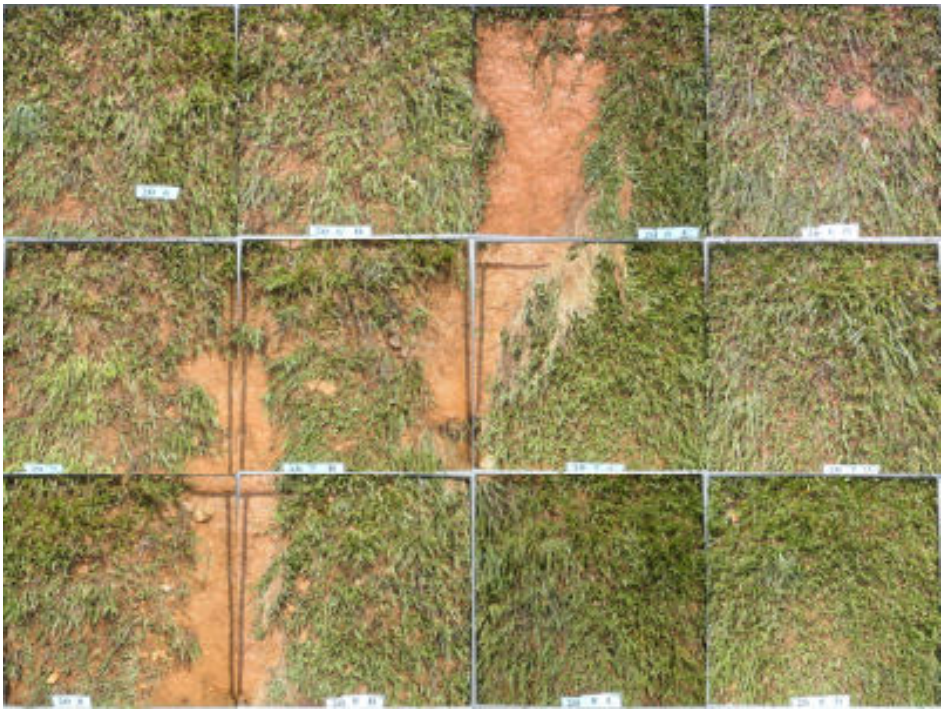

Figure B.52: 40x2 + 60x6 + 80x4 + 100x1, 26 to 28 m from the dike crest, section YB4.

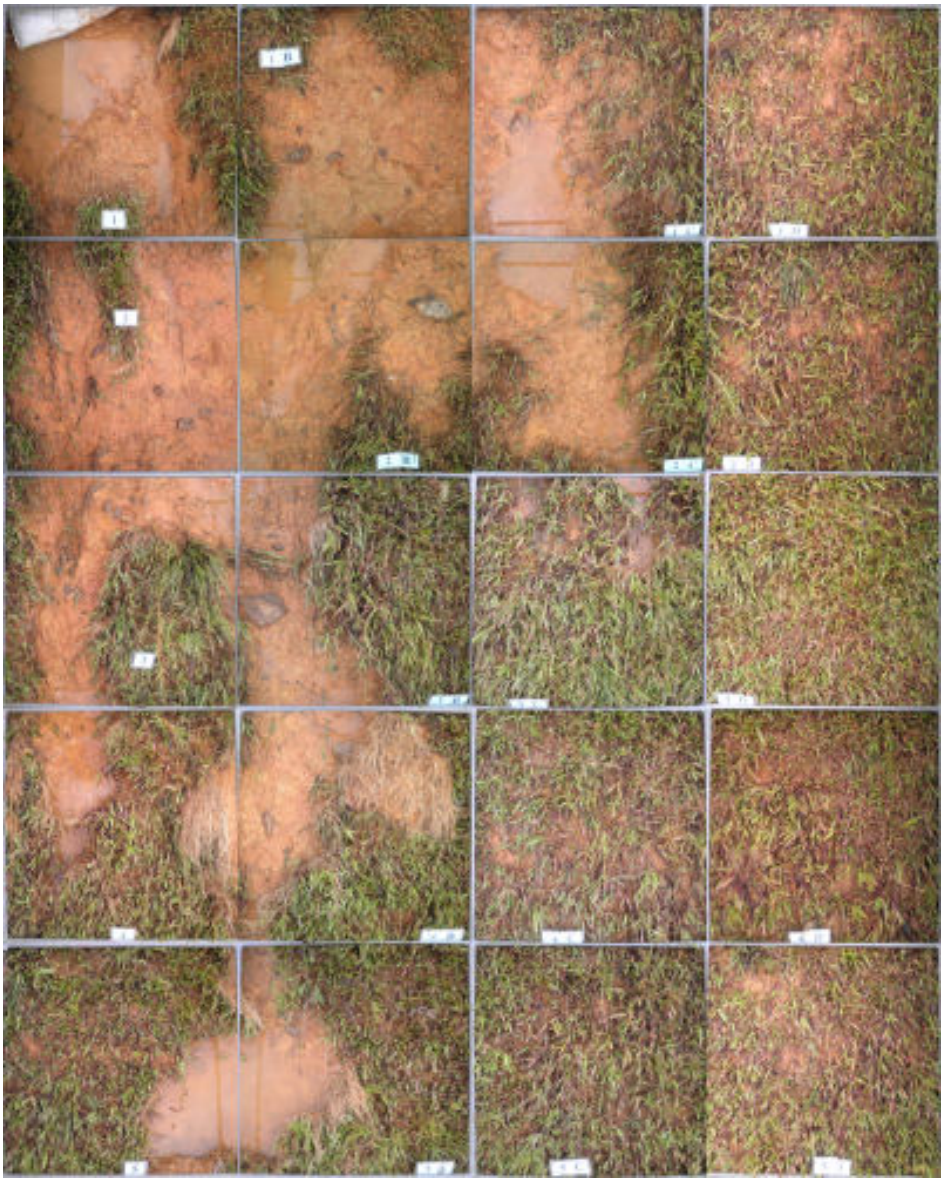

Figure B.53: 40x2 + 60x6 + 80x4 + 100x2, 1 to 5 m from the dike crest, section YB4.

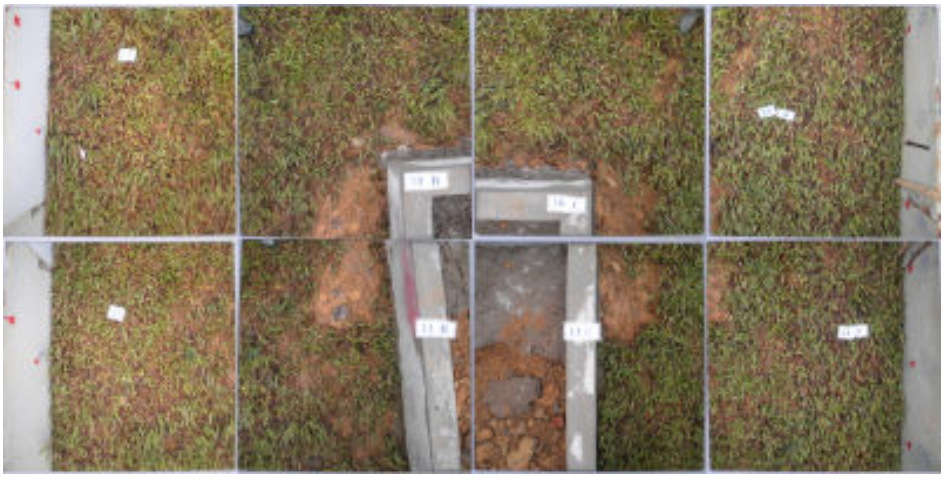

Figure B.54: 40x2 + 60x6 + 80x4 + 100x2, 10 to 11 m from the dike crest, section YB4.

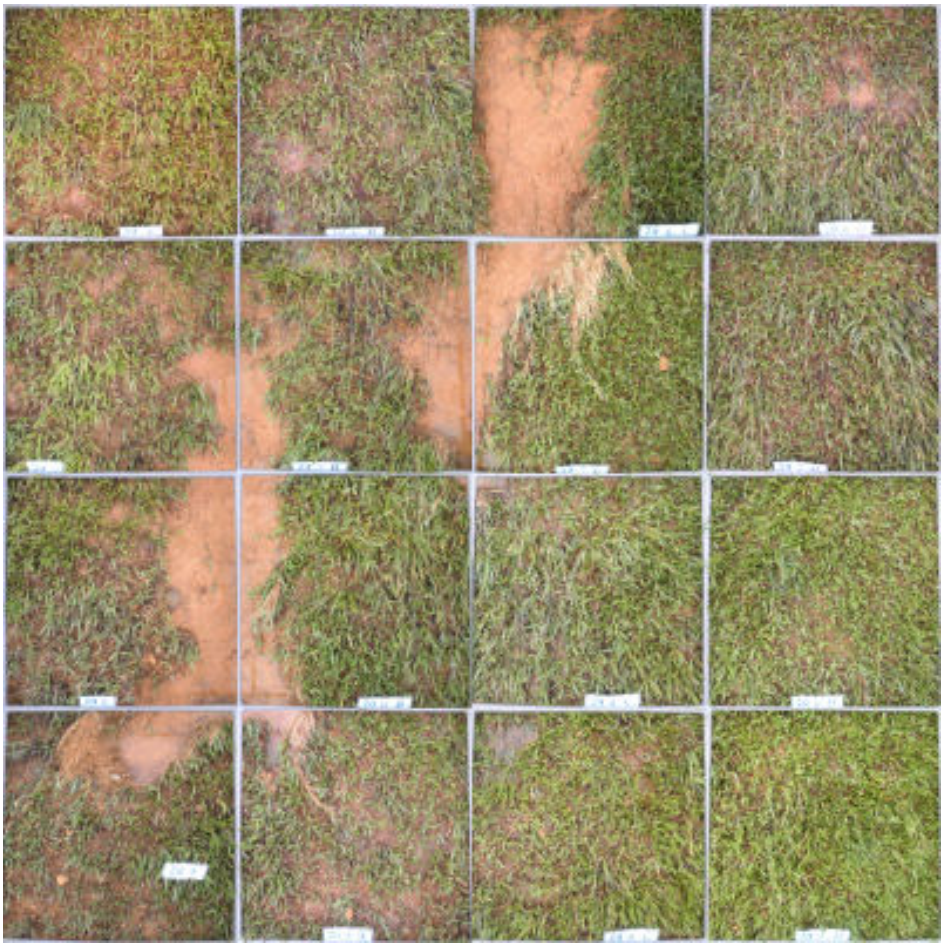

Figure B.55: 40x2 + 60x6 + 80x4 + 100x2, 26 to 29 m from the dike crest, section YB4.

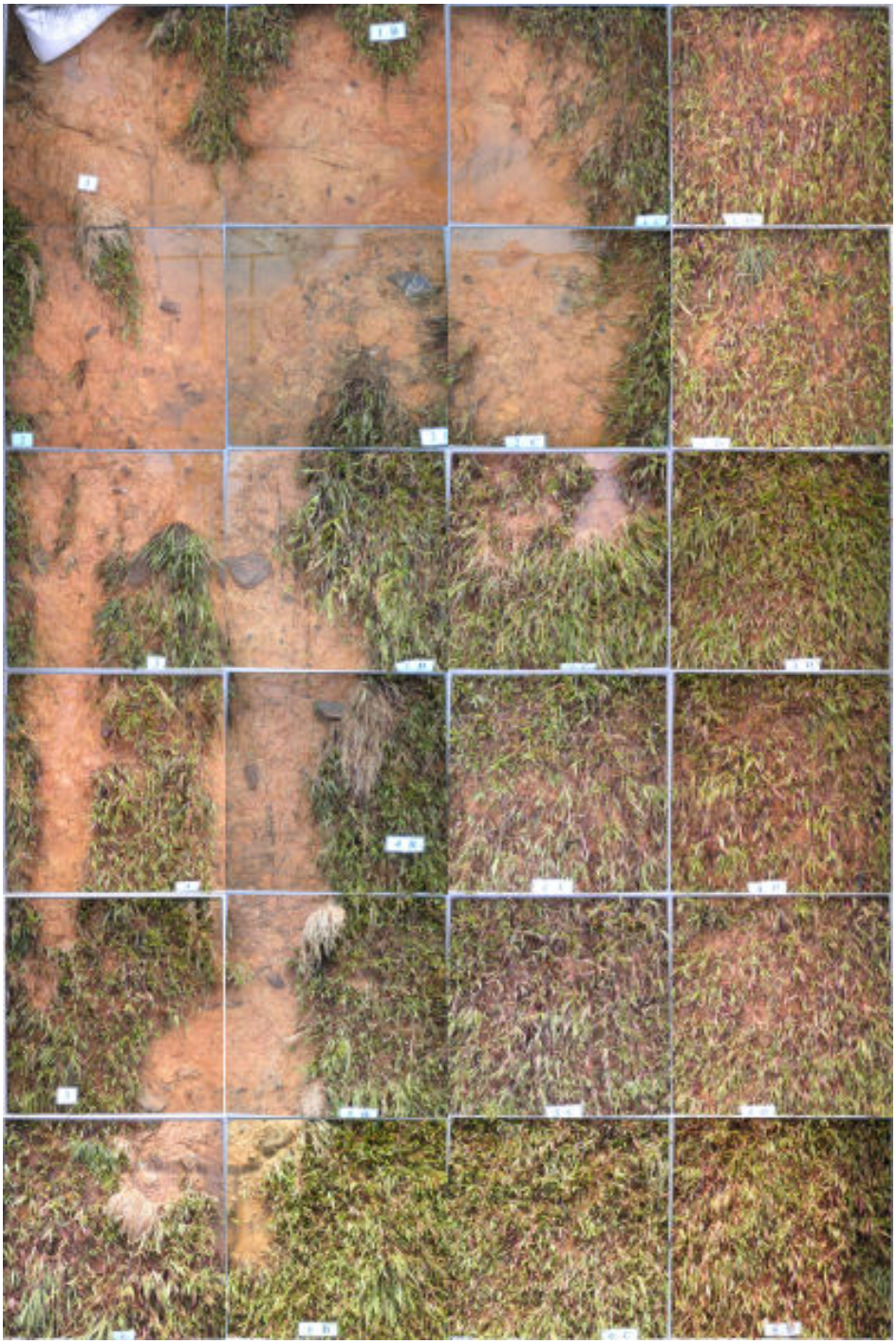

Figure B.56: 40x2 + 60x6 + 80x4 + 100x3, 1 to 6 m from the dike crest, section YB4.

Figure B.57: 40x2 + 60x6 + 80x4 + 100x3, 10 to 11 m from the dike crest, section YB4.

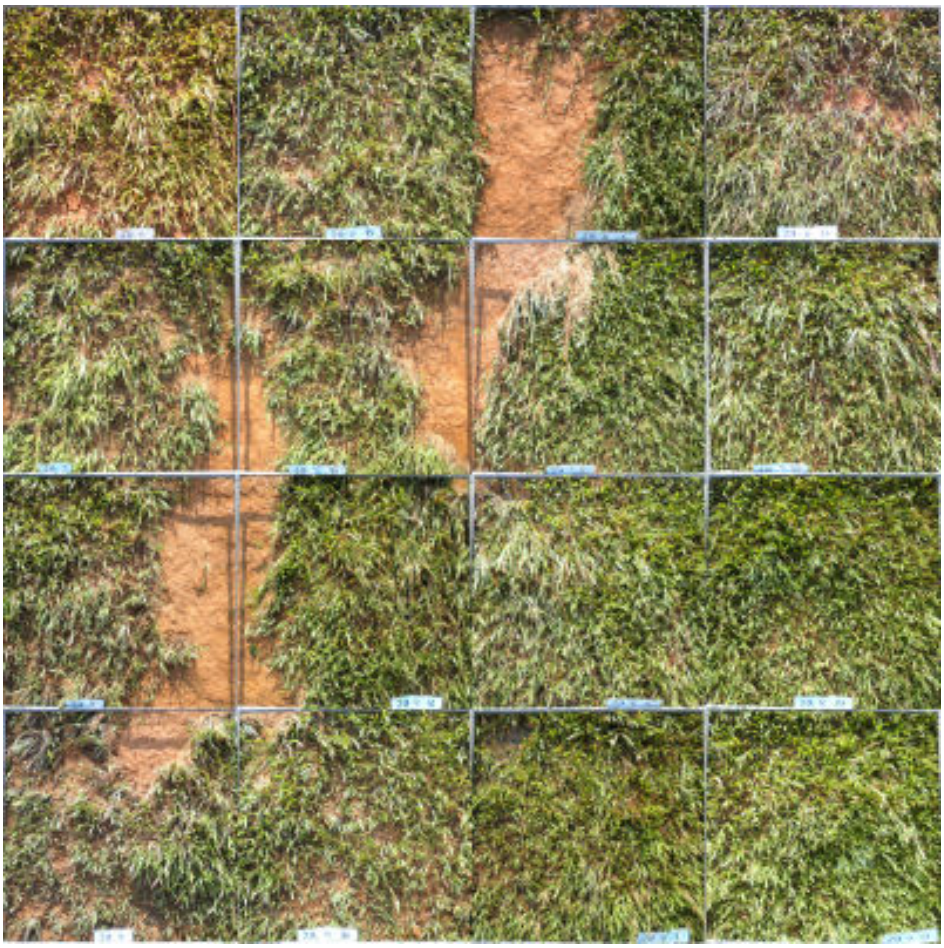

Figure B.58: 40x2 + 60x6 + 80x4 + 100x3, 26 to 29 m from the dike crest, section YB4.

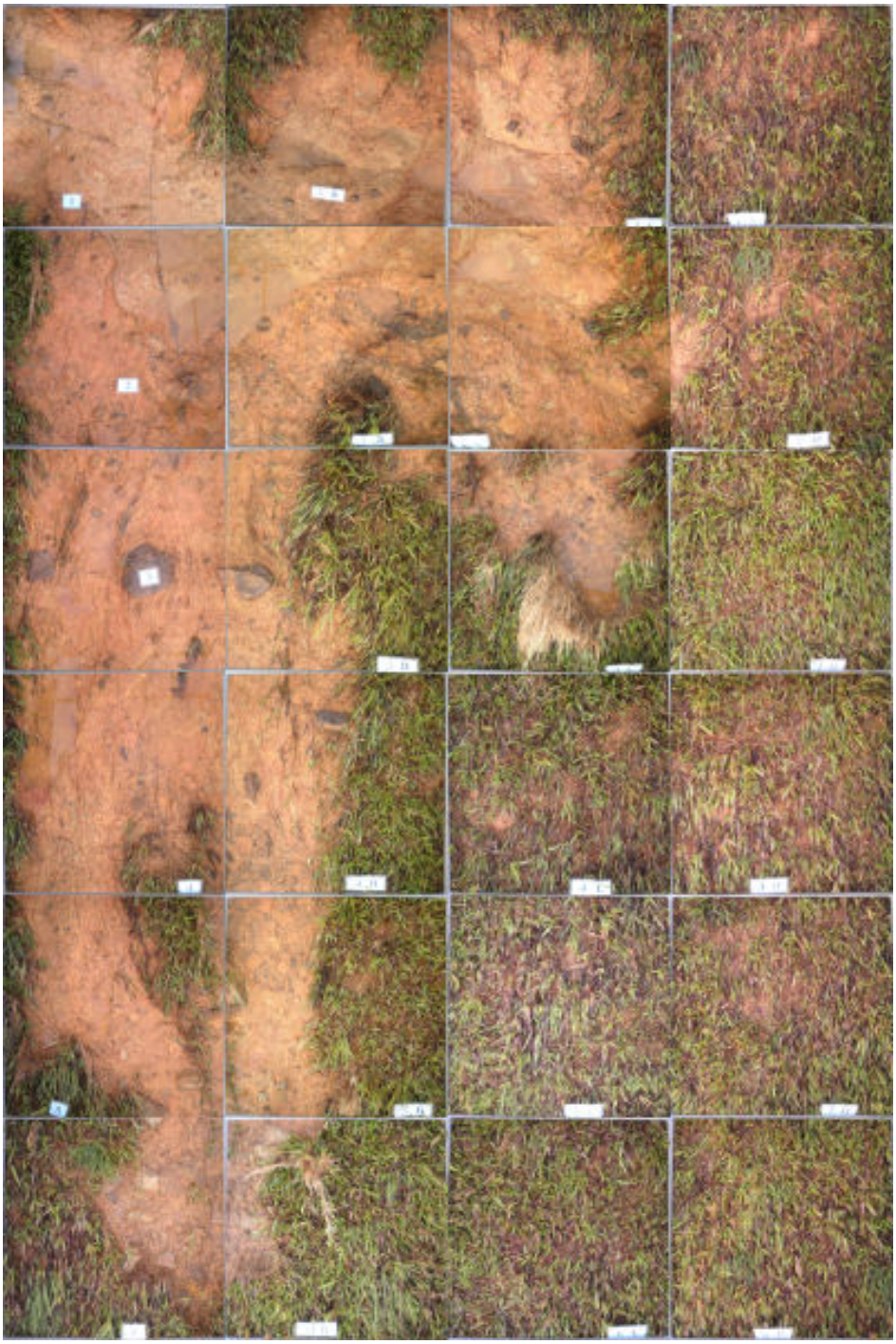

Figure B.59: 40x2 + 60x6 + 80x4 + 100x6, 1 to 6 m from the dike crest, section YB4.

Figure B.60: 40x2 + 60x6 + 80x4 + 100x6, 10 to 11 m from the dike crest, section YB4.

Figure B.61: 40x2 + 60x6 + 80x4 + 100x6, 26 to 29 m from the dike crest, section YB4.

Appendix C

Soil properties

Four soil sample taken from the super dike body were analysed to determine soil types and associated characteristics. Soil particle size distributions were determined by sieve analysis and sedigraph analysis and are shown in Figure C.1 to C.4. The super dike soil are classified clay with sand content of less than 40 %. In which, sand contents of grains with size smaller than 2 mm and larger than 0.05 mm with regard to the current guidelines in Viet Nam [Vie]. In comparison, a range varying between 0.063 and 2 mm is used for grain size of sand in TAW [1996]. According to TAW [1996], the erosion resistance of this soil is little when all result points are lower than the A-line (see Figure C.5).

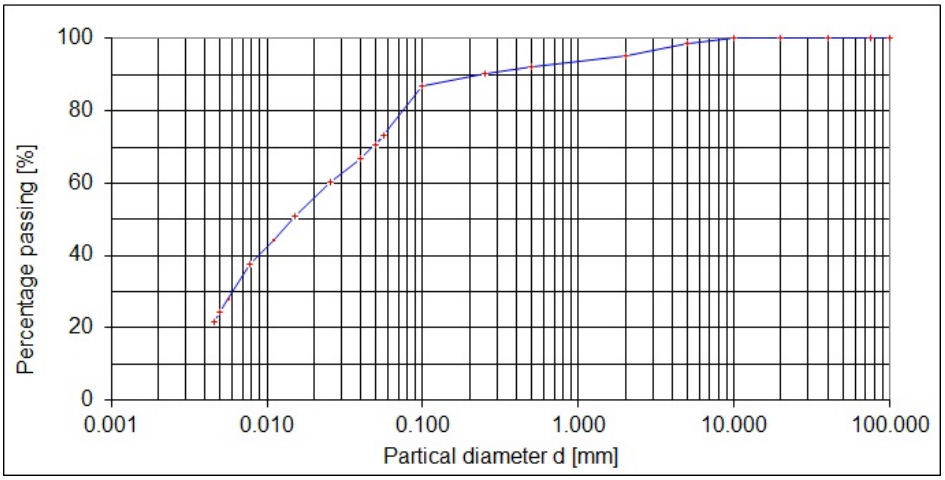

Figure C.1: Soil particle size distribution of the YB1 sample, sand content of 28.55 %.

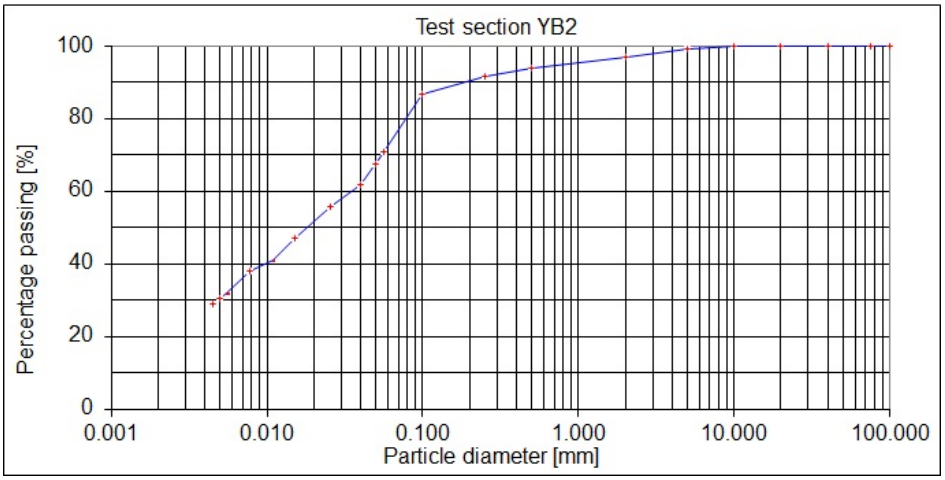

Figure C.2: Soil particle size distribution of the YB2 sample, sand content of 35.11 %.

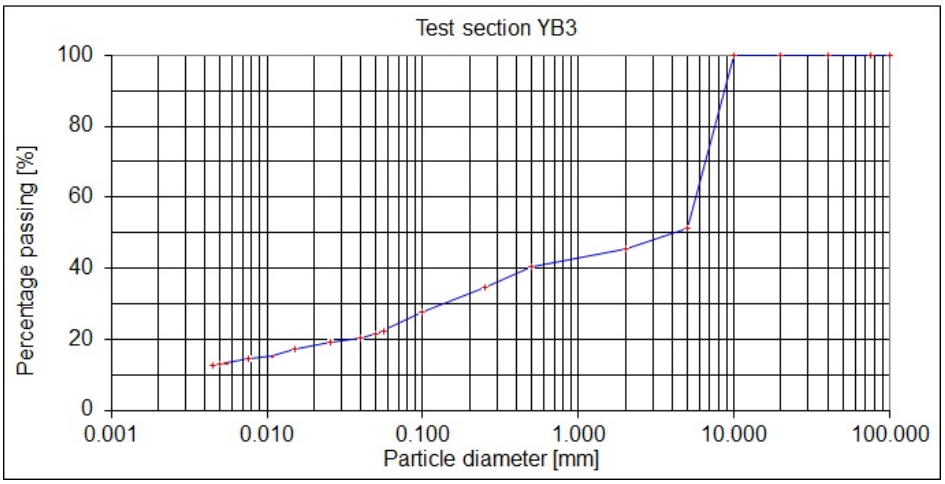

Figure C.3: Soil particle size distribution of the YB3 sample, sand content of 25.10 %.

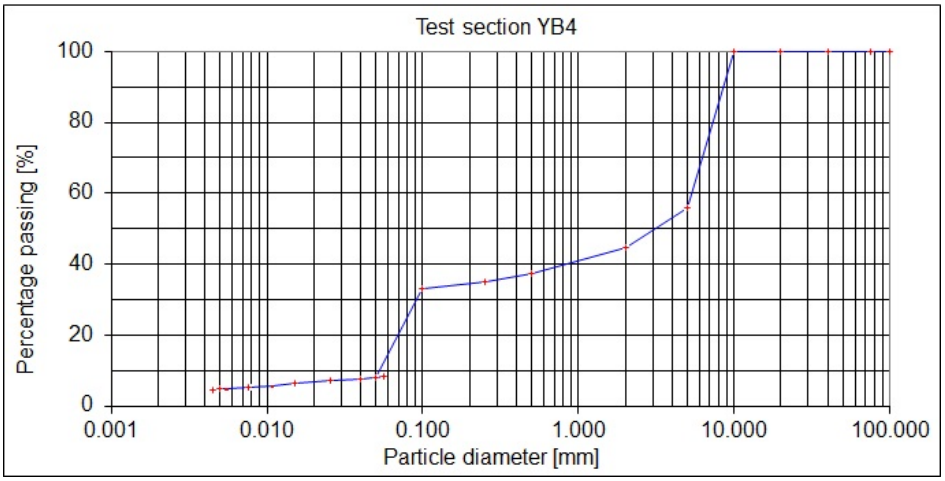

Figure C.4: Soil particle size distribution of the YB4 sample, sand content of 37.24 %.

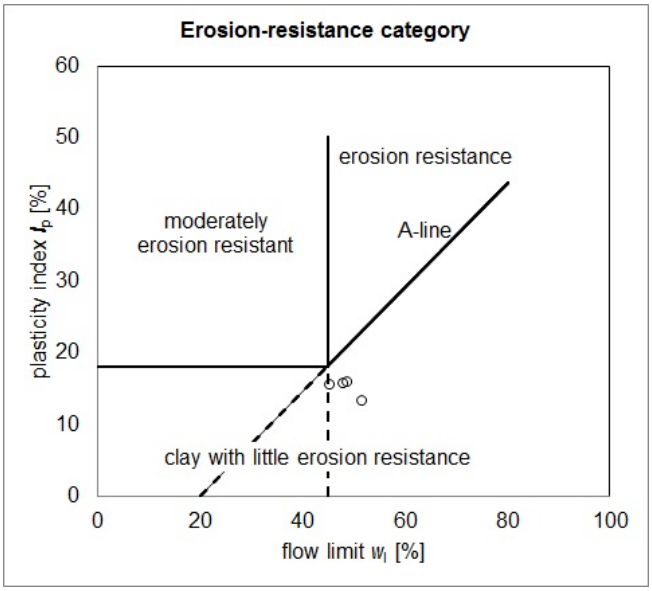

Figure C.5: Erosion resistance category based on flow limit and plasticity [TAW, 1996], round dots are soil samples taken from the super dike body.

Table C.1: Summary of soil testing results.

																			Atterberg			
	Sieve size										Moisture content	Specific gravity	Density	Dry density	Saturation	Porosity	Void Ratio	Liquid limit	Plasticity limit	Plasticity index	Liquidity index	Cohesion	Angle of internal friction
	> 5.0	5.0 to 2.0	2.0 to 1.0	1.0 to 0.5	0.5 to 0.25	0.25 to 0.1	0.1 to 0.05	0.05 to 0.01	0.01 to 0.005	< 0.005	w	γ_s	ρ	ρ_d	S	n	e_o	w_l	w_p	I_p	LI	C	φ
Sample	mm										%	g/cm^3	g/cm^3	g/cm^3	%	%	-	%	%	%	-	kG/cm^2	-
YB1	1.383	3.250	1.383	1.902	1.727	3.492	20.043	29.094	13.611	24.115	39.860	2.690	1.739	1.240	91.722	53.900	1.169	48.540	32.430	16.110	0.461	0.333	20^o18 ’
YB2	0.952	2.068	0.820	2.100	2.268	5.234	24.689	23.946	7.586	30.338	36.630	2.690	1.743	1.280	89.414	52.430	1.102	45.130	29.460	15.670	0.458	0.432	14^o31 ’
YB3	48.636	5.982	1.423	3.382	5.821	7.036	7.440	5.887	1.420	12.974	38.790	2.690	1.762	1.270	93.332	52.790	1.118	51.230	37.760	13.470	0.076	0.342	17^o29 ’
YB4	43.971	11.254	3.717	3.758	2.335	2.033	25.396	2.188	0.528	4.821	31.400	2.690	1.775	1.350	85.061	49.820	0.993	47.600	31.690	15.910	< 0	0.357	16^o17 ’